UNIVERSITÀ DEGLI STUDI DI PADOVA

DIPARTIMENTO DI SCIENZE CHIMICHE

CORSO DI LAUREA MAGISTRALE IN CHIMICA

Crystallographic Characterization of the Interaction between Protein Transthyretin and Small-Molecule Ligands

RELATORE: Prof. Roberto Battistutta

CORRELATORE: Chiar.mo Prof. Giuseppe Zanotti

CONTRORELATORE: Dott.ssa Marilena Di Valentin

LAUREANDO: Riccardo Pederzoli

ANNO ACCADEMICO 2014/2015

Almost all aspects of life are engineered at the molecular level, and without understanding molecules we can only have a sketchy understanding of life itself.

Francis Crick (1988), *What Mad Pursuit: A Personal View of Scientific Discovery*, p. 61

INDEX

Abbreviations and symbols (alphabetical order):

Å: Angstrom

A. thaliana: *Arabidopsis thaliana*

Abs: Absorption

AD: Alzheimer's Disease

ALS: Amyotrophic Lateral Sclerosis

ATP: Adenosine Tri-Phosphate

Bam HI: *Bacillus amyloliquefaciens* type II restriction endonuclease

BLASTp: Basic Local Alignment Search Tool-protein

Cα: alpha carbon

CagA: Cytotoxin-associated gene A

CDS: CoDing Sequences

CDT: Cytolethal Distending Toxin

Cj: *Campylobacter jejuni*

CNSA: Central Nervous System Selective Amyloidosis

Coot: Crystallographic Object-Oriented Toolkit

COX: Cyclooxygenase

Da: Dalton

DegP: Degradation of Periplasmic Proteins

DNA: Deoxyribonucleic Acid

DTT: Dithiothreitol

E. coli: *Escherichia coli*

EDTA: Ethylenediaminetetraacetic acid

eLBOW: electronic Ligand Builder and Optimisation Workbench

EP: Extracellular Polysaccharide

FAC: Familial Amyloid Cardiomyopathy

FAP: Familial Amyloid Polyneuropathy

FPLC: Fast Protein Liquid Chromatography

FT: Flow-Through

GBS: Guillain-Barré Syndrome

GSH: Glutathione

GST: Glutathione-S-Transferase

HBP: Halogen Binding Pocket

His_6-tag: Hexahistidine-tag

Hp: *Helicobacter pylori*

HtrA: High temperature requirement A

hTTR: human Transthyretin

IgG: Immunoglobulin G

IPTG: Isopropyl-β-D-1-ThioGalactopyranoside

LB: Luria-Bertani

LOS: Lipooligosaccharide

LPS: Lipopolysaccharide

MAD: Multi-wavelength Anomalous Dispersion

MCS: Multi Cloning Site

MD: Molecular Dynamics

MR: Molecular Replacement

Mtb: *Mycobacterium tubercolosis*

MW: Molecular Weight

NSAID: NonSteroidal Anti-Inflammatory Drug

OD: Optical Density

OMV: Outer Membrane Vesicles

PAI: PAthogenicity Island

PBS: Phosphate Buffered Saline

PCR: Polymerase Chain Reaction

PDB: Protein Data Bank

PDZ: Postsynaptic density of 95 kDa (PSD-95), discs large (DLG1), and zonula occludens 1 (ZO-1)

PHENIX: Python-based Hierarchical ENvironment for Integrated Xtallography

Phyre2: Protein Homology/analogY Recognition Engine V2.0

PMSF: PhenylMethaneSulfonylFluoride

RBP: Retinol Binding Protein

resv: Resveratrol

r.m.s.d.: Root Mean Square Deviation

RNA: Ribonucleic Acid

SAD: Single-wavelength Anomalous Dispersion

SB: Sample Buffer

SDS: Sodium Dodecyl Sulphate

SDS-PAGE: Sodium Dodecyl Sulphate-PolyAcrylamide Gel Electrophoresis

SeMet: Selenomethionine

SSA: Senile Systemic Amyloidosis

T_4: Thyroxine

TB: Terrific Broth

TBG: Thyroxine-Binding Globuline

TBS: Tris-Buffered Saline

TLS: Translation/Libration/Screw

Tris: Tris(hydroxymethyl)aminomethane

TTBS: Tris Tween-Buffered Saline

TTR: Transthyretin

Ure: Urease

VacA: Vacuolating cytotoxin A

wt: wild type

XDS: X-ray Detector/Diffraction Software

XmaI: *Xanthomonas malvacearum* restriction endonuclease

SUMMARY

This Thesis work describes mainly Synchrotron X-rays Diffraction Studies on complexes between Transthyretin (TTR) and various ligands. TTR is a naturally-occurring protein in humans that performs different and relevant biological and physiological functions, such as the transport of Vitamin A and Thyroid Hormones, particularly T_4. Nevertheless, in humans the onset of TTR point mutations can lead, in most cases, to deleterious effects for the organism. This is because such mutations induce the dissociation of TTR, which in its native state is a tetramer, and this leads to amyloid fibrils formation: these protein aggregates are the *conditio sine qua non* for the development of important and serious forms of amyloidosis in different organs. Liver transplantation was the first therapeutic solution to amyloidosis caused by TTR mutants: however, over the years, it became necessary to find alternatives, less invasive and easier to implement and, to date, the most promising treatment is the use of small molecules able to kinetically stabilize the TTR tetramer preventing, consequently, the dissociation. The understanding, at the molecular and structural level, of the interaction between these drugs and the specific binding sites on TTR is also an indispensable condition for a more rational design of these dissociation inhibitors, in order to obtain molecules more effective, specific and selective. The relative ease with which the TTR·ligand complexes co-crystallize, joined to the continuous advancement and progress made in the field of X-ray Diffraction with Synchrotron sources, allow to obtain three-dimensional models able to sketch out with sufficient accuracy the details of the interaction, placing the groundwork for an optimized search of most powerful candidates in the treatment of TTR amyloidosis. In addition, the structural study of complexes between TTR and various ligands has allowed not only the acquisition of more information useful for the rational design of new drugs but, at the same time, they have placed new and fascinating questions of interest not only to the community of Crystallographers. For example, it remains unclear how it is possible that the two binding sites on TTR, despite the fact that they are related by a rotation axis of order 2 (both crystallographic and molecular), are not equivalent with respect to their binding capacity, being characterized by two different affinity constants. As often happens, the answer to a question generates many others: after all, isn't this the major driving force of Scientific Research and, more generally, of the Search of Knowledge and Truth?

A large part of the Thesis work involves computational processing of experimental diffraction data obtained through Synchrotron X-rays, their use in structural determination, refinement of the model and its interpretation. Among the ligands involved in the study there are thyroxine, as well as other small molecules of proven therapeutic efficacy, one of which is already on the market as commercial drug for the treatment of TTR amyloidosis. Although the structure for most of the complexes was already solved, for some of them it was possible to refine the PDB model through the analysis of crystals able to diffract to a better resolution, while, for

others, it was possible to obtain for the first time the structural model. In all cases, relatively to the known structures, it has been verified that the ligands bind as already reported in the literature, with a singular exception in which the binding mode has proved to be the opposite to what was expected: for this case, two possible explanations have been advanced to justify the discrepancy between the two models.

Finally, this Thesis work is also concerned with the expression and purification of another totally different protein, unrelated to TTR, the HtrA protease from *Campylobacter jejuni* (*Cj*). The goal in this case was its crystallization and structure determination through X-ray Diffraction. *Cj* shares several common features with microorganisms of the genus *Helicobacter*, among which the best known is, without any doubt, *Helicobacter pylori* (*Hp*): both are responsible for colonization of the digestive tract of most humans and for the ability, under certain conditions, to cause gastrointestinal diseases such as ulcers, gastritis and gastric cancer. In recent decades, many efforts were made to identify the factors responsible for the virulence of pathogenic strains of *Campylobacter*, *Helicobacter* and many others: however, to understand the underlying mechanism of virulence it was necessary to clarify the crystal structure of these factors and in this context the X-ray diffraction has been, and indeed still holds, the record in terms of accuracy and reliability of the information obtained through it. In the case of *Hp*, one of the demonstrated causes of its virulence is the HtrA protease, which plays a similar role in many other prokaryotic microorganisms. Attempts to isolate, purify and crystallize such protease, however, have proved unsuccessful because of its intrinsic instability: given the similarity with the strains of *Campylobacter* and the common mechanism of action of HtrA of different bacteria, it has been suggested to infer the *Hp*-HtrA structure from that of *Cj*-HtrA. Being able to obtain crystals of the latter makes possible to obtain the structure of it through SeMet isomorphous derivatives using SAD/MAD (Single- and Multi-wavelength Anomalous Diffraction) techniques or, possibly, through Molecular Replacement (MR) owing to the high sequence homology with other known HtrA. This was confirmed through Bioinformatics analysis, which has also established a high degree of homology with the amino acid sequence of the *Hp*-HtrA: this could be the starting point for the resolution of the *Hp*-HtrA structure, together with a 3D Modelling proving a good structural similarity between the two proteins. The possibility of solving, through MR, the structure of *Cj*-HtrA is also reinforced by the results of two independent modelling, based on the same principle, which lead to identify, in the PDB, the same structure (an HtrA from *E. coli*) as the most similar. The final part of the Thesis focuses on the use of Molecular Biology techniques for expression and purification of *Cj*-HtrA. These attempts have proven to be hard: during the different trials, it has been shown that *Cj*-HtrA is susceptible to degradation, through a series of intermediate fragments, and this even by adopting all the possible experimental attentions. In light of this, it was decided to continue the study on a *Cj*-HtrA protease having a single specific mutation in the active site, in order to reduce its proteolytic activity, increase its stability and improve, therefore, its expression.

The thesis is divided into two parts: in the first chapter, the main part of the project is emphasized. In this regard, an introduction to transthyretin is presented, highlighting its biological roles, the information known about its structure and that of its complexes, its implication in various amyloidosis and the central role played by X-ray Diffraction in the search of new therapeutic molecules. Afterwards, the results obtained from processing of experimental diffraction data are presented and discussed. The second part of the work on *Cj*-HtrA protease is presented in Part II: after an introduction on the main bacterial strains that use it for their virulence, its functions in various organisms and structures solved to date, the results obtained after various expression and purification trials are shown and critically analyzed.

The entire Thesis work was carried out in the Laboratory of Structural Biology directed by Prof. Giuseppe Zanotti at the Department of Biomedical Sciences of the University of Padua.

SOMMARIO

Il presente elaborato di Tesi Magistrale concerne principalmente gli studi di Diffrazione di Raggi X prodotti da sorgente di Sincrotrone di complessi fra la proteina Transtiretina **(**TTR) e diversi suoi leganti. La Transtiretina è naturalmente presente nell'organismo umano (e non solo) dove assolve importanti funzioni fisiologiche e biologiche, fra le quali si annoverano il trasporto della Vitamina A e degli ormoni tiroidei, particolarmente T_4. Tuttavia, diverse sono le cause che, nell'uomo, possono determinare l'insorgenza di mutazioni puntiformi della TTR e che, abbastanza spesso, si rivelano deleterie per l'organismo. Questo avviene perché le mutazioni inducono la dissociazione della TTR, che allo stato nativo è un tetramero, a formare fibrille amiloidi le quali rappresentano la *conditio sine qua non* per lo sviluppo di importanti e gravi forme di amiloidosi a carico di diversi organi. Il trapianto di fegato ha rappresentato la prima soluzione terapeutica alle amiloidosi causate da mutanti della TTR: tuttavia, nel corso degli anni si è reso necessario trovare alternative meno invasive e di più facile attuazione e, ad oggi, il trattamento più promettente riguarda l'uso di piccole molecole in grado di stabilizzare cineticamente il tetramero della TTR, prevenendone di conseguenza la dissociazione. La comprensione, a livello molecolare e strutturale, dell'interazione fra questi farmaci e i siti di legame specifici sulla TTR rappresenta anch'essa una condizione indispensabile per un disegno più mirato e razionale di tali inibitori della dissociazione, al fine di ottenere molecole sempre più efficaci, specifiche e selettive. La possibilità di co-cristallizzare la TTR insieme a diversi leganti, congiuntamente ai continui avanzamenti e progressi ottenuti nel campo della Diffrazione di Raggi X con sorgente di Sincrotrone, permette di ottenere modelli tridimensionali capaci di delineare con sufficiente accuratezza i dettagli dell'interazione, ponendo così le basi per una ricerca ottimizzata di candidati più potenti nel trattamento delle amiloidosi da TTR. In aggiunta, lo studio strutturale dei complessi fra la TTR e vari leganti ha permesso non solo di acquisire maggiori informazioni utili per il design razionale di nuovi farmaci ma ha, nel contempo, posto nuovi ed affascinanti interrogativi d'interesse non solo alla comunità dei Cristallografi. Ad esempio, rimane ancora da chiarire come sia possibile che i due siti di legame della TTR, nonostante il fatto che siano correlati da un asse di rotazione di ordine 2 (sia cristallografico che molecolare), non siano però equivalenti rispetto alla loro capacità di legame, in quanto caratterizzati da due differenti costanti di affinità. Come sempre accade, rispondere a una domanda ne genera molte altre: del resto, non è forse questo il motore della Ricerca Scientifica e, più in generale, della Ricerca della Conoscenza e della Verità?

Larga parte del presente lavoro di Tesi riguarda l'elaborazione computazionale di dati provenienti dall'analisi di cristalli di complessi TTR·legante attraverso Raggi X ottenuti da Sincrotrone, il loro utilizzo nella determinazione strutturale, affinamento del modello e sua relativa interpretazione. Fra i leganti coinvolti nello studio, si

annovera il legante naturale T_4, così come altre piccole molecole di comprovata efficacia terapeutica, una delle quali già sul mercato come farmaco commerciale per il trattamento delle amiloidosi da TTR. Nonostante di parte dei complessi fosse già nota la struttura, per alcuni di essi si è stati in grado di perfezionare il modello precedente attraverso l'analisi di cristalli capaci di diffrangere ad una migliore risoluzione, mentre per altri è stato ottenuto per la prima volta il modello strutturale. In tutti i casi, relativamente alle strutture note, è stato verificato dai dati sperimentalmente ottenuti che il legante si lega come già riportato in letteratura, con una singolare eccezione nella quale la modalità di binding si è rivelata essere opposta a quanto atteso: per questo caso, due soluzioni in grado di spiegare l'incongruenza fra i due modelli strutturali sono state avanzate.

Infine, il presente lavoro di Tesi ha riguardato anche l'espressione e la purificazione della proteasi HtrA da *Campylobacter jejuni* (*Cj*), con l'intento di riuscire a cristallizzarla e poterne determinare la struttura attraverso la diffrazione di raggi X. *Cj* condivide diverse caratteristiche con i microorganismi del genere *Helicobacter* di cui il più noto è, con tutta probabilità, *Helicobacter pylori* (*Hp*): con esso condivide, ad esempio, la colonizzazione dell'apparato digerente della maggior parte degli esseri umani (e non solo) e la capacità, in determinate condizioni, di determinare l'insorgenza di patologie gastrointestinali di varia natura fra cui ulcere, gastriti e neoplasie gastriche. Negli ultimi decenni, molti sforzi sono stati profusi nell'identificare i fattori di virulenza responsabili per la patogenicità dei ceppi di *Campylobacter*, *Helicobacter* e molti altri: per comprendere, però, il meccanismo alla base della loro virulenza è stato necessario chiarire la struttura di tali fattori, e in questo contesto la Diffrazione di Raggi X ha avuto, e del resto detiene ancora, il primato in termini di accuratezza ed attendibilità delle informazioni ottenibili attraverso essa. Nel caso di *Hp*, una delle cause dimostrate della sua virulenza è da imputare alla proteasi HtrA, che gioca un ruolo analogo in molti altri organismi procarioti. Tentativi di isolare, purificare e cristallizzare tale proteasi si sono però rivelati vani a causa della sua instabilità: data la similitudine con i ceppi di *Campylobacter* ed il comune meccanismo di azione delle HtrA dei diversi batteri, è stata avanzata l'ipotesi di inferire la struttura dell'HtrA di *Hp* da quella della HtrA di *Cj*. Riuscire ad ottenere i cristalli di quest'ultima permetterebbe di ottenerne la struttura attraverso i SeMet derivati isomorfi sfruttando le tecniche SAD/MAD o, come si ritiene più probabile, attraverso Molecular Replacement (MR) data l'alta omologia di sequenza con altre HtrA note. Ciò è stato confermato attraverso un'analisi Bioinformatica, la quale ha oltremodo sancito un'elevata omologia della sequenza amino acidica anche con la proteasi HtrA di *Hp*: questo potrebbe essere il punto di partenza per la risoluzione (con metodi *ab initio* o attraverso Molecular Dynamics) della struttura della HtrA di *Hp*, insieme ad un Modelling 3D che comprovi una buona somiglianza strutturale fra le due proteine. La possibilità di risolvere, attraverso MR, la struttura della HtrA di *Cj* è rafforzata anche dal risultato di due Modelling indipendenti, ma basati sullo stesso principio, che portano ad

identificare, nel PDB, la stessa struttura (una HtrA di *E. coli*) come la più affine dal punto di vista strutturale.

La parte sperimentale della Tesi ha riguardato l'utilizzo degli strumenti della Biologia Molecolare per l'espressione e la purificazione dell'HtrA di *Cj*. Tali tentativi si sono tuttavia rivelati ardui: durante le diverse prove, è stato infatti dimostrato che la proteasi HtrA da *Cj* è suscettibile a facile degradazione, attraverso una serie di frammenti intermedi, e questo anche adottando le maggiori accortezze sperimentali. Alla luce di ciò, è stato deciso di proseguire lo studio su una proteasi HtrA da *Cj* avente una mutazione specifica nel sito attivo, in modo tale da ridurne l'attività proteolitica, aumentarne la stabilità e migliorare, quindi, la sua espressione, purificazione e cristallizzazione.

La Tesi è suddivisa in due parti: nel primo capitolo viene dato risalto alla parte principale del Progetto. A tal proposito, si presenta un'introduzione alla Transtiretina, evidenziando i suoi ruoli biologici, le informazioni note riguardo la sua struttura e quella dei suoi complessi, la sua implicazione in diverse amiloidosi ed il ruolo centrale rivestito dalla Diffrazione di Raggi X per la ricerca di nuove molecole terapeutiche. Quindi, sono presentati e discussi i risultati ottenuti dall'elaborazione dei dati sperimentalmente ottenuti. La seconda parte dell'elaborato, invece, concerne la proteasi HtrA da *Cj*: dopo un'introduzione sui principali ceppi batterici che la utilizzano ai fini della loro virulenza, sulle sue funzioni in vari organismi e sulle strutture ad oggi risolte, vengono mostrati e analizzati criticamente i risultati ottenuti a seguito delle diverse prove di espressione e purificazione effettuate.

L'intero lavoro di Tesi è stato svolto presso il Laboratorio di Biocristallografia del Prof. Giuseppe Zanotti, Dipartimento di Scienze Biomediche dell'Università di Padova.

1 INTRODUCTION

The first Chapter introduces Transthyretin outlining the key aspects regarding its biological functions, structure (alone and with different ligands) and the implication of different mutants in TTR amyloidosis. Furthermore, the molecular bases of amyloidogenesis, along with past and current therapeutic treatments, are discussed. In particular, emphasis is given to the treatment with small molecules as drugs and to the role of X-ray Diffraction in the understanding of the interaction between TTR and such ligands.

1.1 General considerations on TTR

Transthyretin (TTR) is a protein present in the extracellular fluids, mainly serum and cerebrospinal fluid (CSF) [1], of different vertebrate species. Crystal structures are available for TTR from mammals [2] [3] [4], chicken [5] and fish [6] [7]. Its localization in the organism has been confirmed, among the various techniques, also by detection of TTR mRNA [8] [9] [10]. TTR derives its first name, prealbumin, from the fact that, on electrophoresis gels, it run faster than albumin; however, the actual name reflects its biological and physiological role since the acronym stays for **Trans**porter of **Thy**roxine and **Retin**ol molecule. Human transthyretin (hTTR) was first crystallized in 1966 by Haupt & Heide and, in the following decade, the complete amino acid sequence [11] and the crystal structure were determined. Combined, these data provided important structural information about TTR and, in subsequent years, more defined crystal structures [12] [13] [14], near to atomic resolution [4], revealed new insights crucial in explaining its functions. To date, over 200 crystal structures are deposited in the Protein Data Bank (PDB) and there is an urgent need to summarize and explain this large amount of information with the purpose of comprising biological functions and improving actual therapeutic treatments for diseases associated with TTR [15].

1.2 Biological functions

It is believed that TTRs probably evolved in a prevertebrate species by a duplication event involving the gene that encodes the enzyme 5-hydroxyisourate hydrolase (5-HIU) [16] [17]. This enzyme belongs to the transthyretin-related protein (TRP) family, which comprises proteins that share with TTRs essentially the same tertiary and quaternary structures and that are present in a wider range of species (bacteria, plants and animals). Moreover, TRPs are unable to recognize thyroid hormones. They are involved in purine catabolism, particularly in the hydrolysis of 5-HIU [18] [19] [20] [21] [22] [23] [24] [25]: so, TTR and 5-hydroxyisourate hydrolase (HIUase) are closely related phylogenetically and structurally, although performing different functions, and a hypothesis to explain the drastic evolution of the function (from enzyme to binding protein) has been advanced [26]. TTR (at least in humans) is present already at the embryonic stage and its production continues throughout the entire life span; liver and brain (choroid plexus) are engaged in its synthesis and reverse TTR in the bloodstream and in the CSF, respectively. Here, TTR acts as an important carrier of thyroid hormones (THs), T_4 in particular, and vitamin A in complex with retinol binding protein (RBP) [27]. THs are extremely lipophilic and this is the reason why TTRs are indispensable for an adequate distribution of these molecules in the body. Nature has developed three main proteins with this aim that are, in order of decreasing affinity towards THs: thyroxine-binding globuline (TBG), TTR and albumin. In human blood, 99.98% of T_4 and 99.8% of T_3 are bound to one or more of these carriers; nevertheless, it is worth noting that a percentage smaller than 3% of TTR binds and transports T_4 in blood plasma (major ligands are albumin

and TBG) but almost 50% of the TTR binds to RBP in complex with retinol (*holo*-RBP) [28] [29] [30] [31] [32]. To investigate further the roles of TTR in the organism, diverse knockout mice studies were carried out, although their results were in contrast: some TTR knockout mice display normal life span, whereas others reveal depressed levels of retinol, RBP and T_4 in the blood, suggesting that the protein is important in maintaining normal concentrations of this metabolites. However, knockout animals are phenotypically normal and fertile [33]. Furthermore, other investigations show implications of TTR in the nervous system physiology [34] [35] [36] and as a protective agent capable of binding the β-peptide implicated in the Alzheimer's disease, preventing the onset of neurodegeneration [37] [38] [39]. Some studies also report on a possible cryptic protease activity of TTR after the identification of different substrates, despite the lack of a real proteasic domain [36] [40]. Anyway, the main interest about TTR derives from several point mutations (more than hundred have been identified) that, in most cases, are the origin of different amyloidosis.

1.3 Pathogenesis of TTR amyloidosis

In 1978 the first study in which the authors suggested the existence of a link between TTR and familial amyloid polyneuropathy (FAP) was published, particularly in the presence of TTR mutations [41]. To date, more than hundred of these mutations have been reported and only a small portion of them are apparently non-amyloidogenic. A regularly updated list of mutations together with their primary citations is available on the website http://amyloidosismutations.com/mut-attr.php. Amyloidosis is a rare disease characterized by an abnormal deposition and accumulation of a protein as amyloid fibrils. The most notorious is, probably, Alzheimer's disease (AD) and the related Aβ peptide [42]. Even though peptides and proteins implicated in amyloidosis are disease-specific, the amyloid fibrils share the same morphology, irrespective of sequence homology, native structure and functions. More than a decade ago it was first proposed the amyloid hypothesis, which states that the accumulation of Aβ in brain tissue is the primary driver of AD-related pathogenesis. Amyloid hypothesis is currently lacking in detail and certain observations do not fit easily with the simplest version of it: at present, there are more recent and broadly supported variations of this hypothesis [43] [44] [45]. TTR amyloid fibrils are responsible not only for FAP, but also for senile systemic amyloidosis (SSA), familial amyloid cardiomyopathy (FAC) and central nervous system selective amyloidosis (CNSA) [46] [47] [48]. Principal deposition sites are peripheral nerves and/or the heart. Most of the FAC/FAP mutations are conservative, that means no important modifications in the overall structure of TTR, but a number of mutations (such as V30M, L55P and V122I) modify the kinetic and thermodynamic stability of TTR that is a homotetramer in the native form. Such kind of mutations alter the tetrameric form and lead to the dissociation that, in turn, is responsible for the onset of the amyloidosis [49].

Dissociation of the tetramer alone is not sufficient for amyloid fibril formation because the native monomers originated in this way are not aggregation-competent: its partial denaturation is necessary to form an amyloidogenic intermediate that is proposed to be a partially unfolded monomer [50].

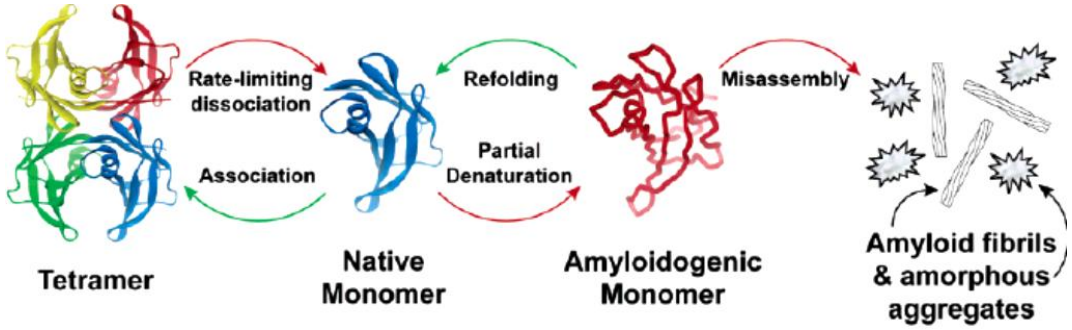

Figure 1.1: Hypothetical TTR amyloidogenesis pathway based on biophysical studies ([51]).

Actually, two different hypotheses have been advanced. The nucleation-dependent amyloid formation hypothesis suggests the formation of oligomeric species that can act as seeds to induce protein misfolding, as happens in classical crystal growth (with an activation energy barrier associated with the process). For the conformational changes hypothesis, there must be the tetramer dissociation in order to induce the build up of amyloid fibrils [49] [52] [53]. Probably, there is a thermodynamic equilibrium between tetramer and native monomers and the latter needs to undergo partial denaturation in order to form amyloid fibrils [54]. Based on biophysical studies, the TTR amyloidogenesis pathway provides for rate-limiting tetramer dissociation (this is true at physiological conditions) that leads to native monomers that can either reassociate or partially unfold. The misfolded monomers can aggregate *via* a downhill polymerization to yield a variety of aggregate morphologies, including amorphous aggregates and amyloid fibrils. Dissociation and aggregation are extremely slow under physiological conditions but a pH reduction, for example in lysosomes [52] [53] [55] [56] [57] [58] [59] or in the presence of metal ions such as Zn^{2+} [60] [61] dramatically increase the rate of the process, favouring amyloidogenesis. These studies show that the rate of fibrils formation is pH dependent and that some TTR mutants - as L55P - can dissociate into amyloidogenic monomers at neutral pH and 37°C, unlike wt-TTR, as a consequence of the reduced activation barrier. L55P is then more sensible toward acidic conditions and it starts to dissociate at pH values at which wt-TTR is still in the tetrameric form. Crystal structure studies can provide deep insights into amyloidogenesis, but the clear influence of pH states the necessity to collect data from crystals grown at pH values low enough: unfortunately, at present, many structures were solved using crystals grown in non amyloidogenic conditions and acidic crystallization conditions will likely become a requirement for future studies [63].

However, among the structures solved to date and obtained from crystals grown in acidic conditions there are few of them that do not show significant conformational changes. This is probably due to the tendency of TTR to select, during crystal growth stages, only symmetric conformations. Taking into account the possibility of having, in solution, an equilibrium between native TTR and the same protein in which some conformational changes occurred, it can be speculated that the system selects only TTR molecules non altered by the lowering in pH. This, in turn, is probably caused by the specific crystal packing (*i.e.*, by the specific orthorhombic point group in which most of the TTR crystals grow easily). No one has made a systematic screening of TTR crystal forms in acidic conditions but it is likely that this will shed light on this still open question.

1.4 Structure of wt-TTR

When Colin Blake solved, for the first time in 1971, the structure of TTR at a resolution of about 6Å [62] he noticed that, among the different proteins known at the time of the discovery, TTR was unique owing to the high content in β-sheets characterizing its secondary structure. TTR is a homotetramer of 55kDa in which each of the four subunits (named A, B, C and D) is composed of 127 amino acids.

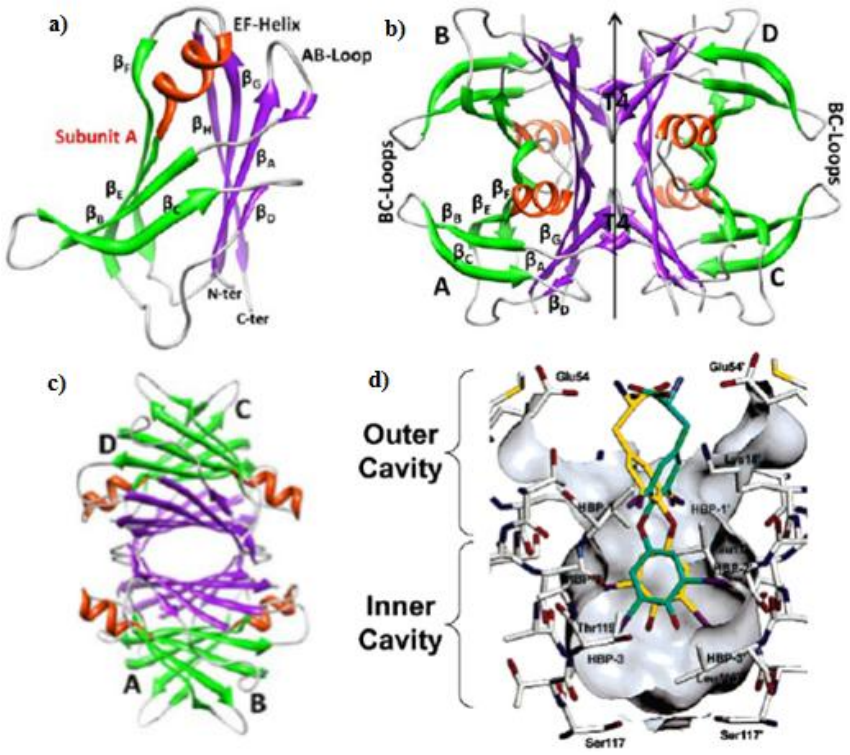

Figure 1.2: ***a)*** Ribbon representation of subunit A of TTR tetramer, showing secondary structural elements; ***b)*** Ribbon representation of TTR tetramer with the T_4 hormone binding sites and the C_2 axis that relates dimers AB (the content of the asymmetric unit) and CD; ***c)*** View of the TTR tetramer rotated 90° to show the central channel and ***d)*** View of one T_4 binding site with T_4 shown in both the symmetry-related conformations ([49], [60]).

To date, 14 wt-TTR structures are deposited in the PDB: they usually crystallized in the same orthorhombic space group $P2_12_12$ and they have approximate lattice dimensions: a = 43Å, b = 85Å and c = 64Å. The asymmetric unit of the crystal contains the AB dimer (subunits A and B), while the CD dimer is generate through the crystallographic two-fold axis, corresponding to one of the C_2 symmetry axis present in the protein. Often, monomers C and D are also named A' and B', respectively (this denomination will be used later in the text). Each subunit contains 2 antiparallel β-sheets formed by the strands A-D and E-H arranged in a β-barrel topology, with a short α-helix (EF helix) localized between strands E and F. In TTR, there are 2 different dimer/dimer interfaces: the more strong AC/BD interface, stabilized by interstrand hydrogen bonds, and the weaker AB/CD interface, which consists of hydrophobic interactions. The latter are responsible for the presence of two funnel-shaped hydrophobic T_4 binding sites that passes through the C_2 axis. In each binding site there are two types of cavities, the narrow Inner cavity and the larger Outer cavity with three pairs of depressions named Halogen Binding Pockets (HBPs) in which the iodine atoms of the natural ligand thyroxine are localized. Despite two different affinity constants were determined for the binding of this ligand to the binding sites on TTR, whose order of magnitudes are 10^6 and 10^8 M^{-1} at physiological pH [29] [64] [65] [66], crystal structures reveal the presence of T_4 in all of them. Two diverse association constants imply that the two binding sites are not equal, despite their formal equivalence due to the presence of a 2-fold rotation axis. This also means that T_4 binds with a negative cooperativity mechanism, as demonstrated in solution [65] [66]. It is likely that the binding event of the first T_4 molecule causes conformational changes in TTR, rendering the second site less suitable for binding. Inspections of the electron density, molecular dynamics simulations and other evidences seems to confirm this hypothesis and, probably, this arises from a certain degree of flexibility of some portions of TTR [67] [68] [69]. Recent neutron diffraction studies on perdeuterated TTR, able to visualize and locate with more accuracy hydrogen (D-substituted) atoms with respect to X-ray diffraction, yield new structural information [70]. The authors found a single water molecule in the channel (interacting with Ser117A and Ser117A'), present only at the A/A' interface (site A): as a result, the entry to the binding pocket is wider for the B than for the A pocket and this would be responsible for the different measured affinities.

1.5 Molecular basis of amyloidogenesis

In a paper published in 2000, some authors investigated 23 different structures, comprehensive of wt-TTRs, amyloidogenic and non amyloidogenic mutants and different TTR·ligand complexes [4]. They concluded that the differences considered of importance in the amyloidogenesis were insignificant; others studies [14] [71] also concluded that lowering the pH does not induce any significant conformational changes in wt-TTR crystal structures.

Only in 2008 the first evidence of a conformational changes in the structure of wt-TTR at pH 4.0 and 3.5 was presented [72]. In particular, at pH 4.0 in the subunit B, the EF-helix-loop composed of the EF-helix, the EF-loop and part of β-strands E and F, display significant conformational flexibility that increases at pH 3.5, acting as possible initiation mechanism for TTR amyloidogenesis. Lowering the pH induces the protonation of some residues of the EF-helix-loop region suggesting a possible origin for the conformational changes. Some metal ions, such as Zn^{2+}, causes similar changes in a manner comparable to that shown by protons; already at physiological conditions and if present in sufficiently high concentrations, zinc ions induced amyloid fibrils formation perturbing the EF-helix-loop region [60] [61]. However, the effect its greatest at acidic pH: this was also seen in a study on the complex TTR F87M/L110M:Zn^{2+}. It was clearly demonstrated that Zn^{2+} binding near the EF-helix-loop region perturbs it, inducing a significant conformational change that raises the flexibility, particularly at low pH values [60]. The crystal structure determination of another mutant, TTR G53S/E54D/L55S, reveals another type of conformational change, called β-slip, because of a dramatic shift in the positioning of β-strand D [73]. This β-shift involved three residues because it places Leu58 at the position normally occupied by Leu55 that is mutated to serine: the effect has consequences on protein-protein interactions and on the crystal packing, leading to a new model for amyloidogenesis. Presently, the comprehension of amyloidogenesis is based on the movements of EF-helix-loop region upon acidification and/or the presence of metal ions and on the β-slip induced by some mutations. Finally, there are two possible explanations for the apparent absence of significant conformational changes in different crystal structures: *i)* in low pH crystallization drops a heterogeneous ensemble of TTR molecules in equilibrium is present such as partially denatured tetramers and native tetramers, but the crystal selects only the conformation of the predominant species; or, *ii)* TTR has a natural propensity in packing itself as a symmetric tetramer, hindering the determination of misfolded and/or unfolded monomers.

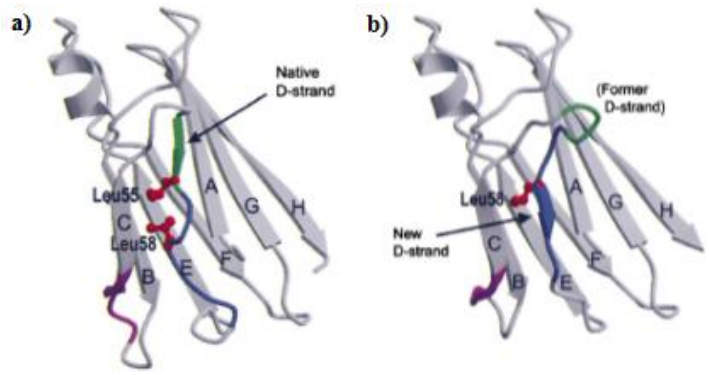

Figure 1.3: ***a)*** Monomer A in native TTR (the position of the triple mutation is shown in green) and ***b)*** Monomer B from TTR G53S/E54D/L55S ([73]).

1.6 Molecular basis for the treatment of TTR amyloidosis

Until a few years ago, the general treatment for TTR amyloidosis was liver transplantation, which enables the substitution of the mutant TTR with the wild type TTR. However, this strategy has to deal with some drawbacks (shortage of donors, the need to resort to surgery for both donor and recipient and high costs) and different strategies are being studied. The onset of amyloidosis has as first stage tetramer dissociation and, as a consequence, whatever molecule able to inhibit this step is a potential candidate in TTR amyloidosis treatment. So, a promising therapy consists in using small molecules capable of binding to TTR and, through kinetic stabilization, to block the protein in its tetrameric form, preventing deleterious dissociation. Besides these treatments, other possibilities are currently under study such as gene therapy, plasma exchange, immune therapy [74] and others [75]. Regarding the former, different solutions are possible and they span from ribozymes, catalytic RNA molecules used to inhibit gene expression cleaving specifically the mRNA derived from the transcription of the defective gene [76] [77], to antisense oligonucleotides, which act on the same target (mRNA) taking advantage of the complementarity between the two nucleic acid sequences [78]. Single stranded oligonucleotides [79] and RNA interference [80] are also under study. The gene therapy also emerges as a possible treatment in heterozygote patients which present an amyloidogenic mutation like V30M on one allele and a stabilizing mutation on the other (for example, T119M) [55]. The association of these two mutations seems to protect his carriers from the severe form of the disease: *trans*-suppression refers to the concept that a T119M TTR subunit has the ability to significantly stabilize the V30M-comprised TTR tetramer against dissociation and misfolding [81]. The T119M suppressor subunit could be incorporated post-secretion into the quaternary structure of TTR using a subunit-exchange strategy, or during biosynthesis using the aforementioned gene therapy approach before secretion [82]. Lastly, immune therapy consists in the immunization through an amyloidogenic mutant TTR: this entails the production of a specific antibody that reacts with amyloid deposits determining a reduction/inhibition of TTR deposition, as demonstrated for Y78F TTR [83]. Nonetheless, the use of small drugs is the most conservative therapeutic strategy because it prevents the process of amyloidogenesis from the beginning.

1.7 Using small drugs in the treatment of TTR amyloidosis

Using small drugs are currently under investigation in the treatment not only of TTR amyloidosis but also for other amyloidosis as ALS (Amyotrophic Lateral Sclerosis), in which SOD aggregation plays an important role [84], or in lysozyme amyloidosis where variants of lysozyme render the protein amyloidogenic [85] [86]. However, pharmacologic treatment of TTR amyloidosis must take into account the structure of TTR, in other words the dimensions and binding affinities of the two binding sites for thyroxine. Most of the molecules with a demonstrated activity against tetramer dissociation, briefly called “inhibitor”, bind to TTR with a negative cooperativity

mechanism. Such molecules are typically composed of two aromatic rings, linked directly or by means of linkers with different chemical nature [51]. Generally, one aromatic ring is substituted with polar groups, while the other ring displays halogen atoms, alkyl groups or a combination of both. Polar substituents (i.e., carboxylates or phenolates) are complementary to positive charges on side chains of Lys15 or Glu54 in the outer binding site, whereas the other groups are compatible with the hydrophobicity of the inner binding cavity, occupying some HBPs. There exist two different binding modes exhibited by ligands: in the so called forward binding mode, the aromatic ring bearing the anionic substituent is oriented towards the outer binding pocket, thanks to favourable electrostatic interactions. On the contrary, in the reverse binding mode the carboxylate bearing the aryl ring prefers the inner binding pocket (but this usually does not happen). As proved *in vitro*, the natural ligand T_4 binds to TTR preventing amyloid fibrils formation and does so by stabilizing the tetramer against dissociation: the binding of small molecules to TTR raises the activation energy barrier necessary for tetramer dissociation, preventing amyloidosis [87]. Is also emphasizes the fact that more than 99% of T_4 sites on human TTR are unoccupied and, as a consequence, they are eligible targets for small drugs; these molecules bind in a forward or in a reverse binding mode depending on polarity and dimensions of the substituents to the aromatic rings. Among such bi-aryl systems, some non steroidal anti-inflammatory drugs (NSAIDs) like the approved flufenamic acid (Flu), Diflunisal (Diflu) and Diclofenac show good complementarity with the hormone binding sites on TTR; they are effective inhibitors owing to their structure and not because their NSAIDs activity. Even natural compounds with bi-aryl scaffold, such as resveratrol, were crystallized in complex with TTR and tested, unveiling very promising percentages of inhibition over fibrils formation in acidic conditions [88]. Due to their efficacy, several structures of TTR:NSAIDs inhibitor complexes were solved [89] [90] and some information were used to develop new drugs like iodo-Diflu and analogues, that showed an improved inhibitory effect thanks to additional iodine atoms mimicking those found in thyroxine [91]. These structures suggest, also, other effective molecules based on a tryciclic ring system [81] [83], in particular Tafamidis, a benzoxazole derivative approved and marketed for the amelioration of FAP [74] [92]. However, some compounds show a few drawbacks: for example, the main defect of NSAIDs is that they inhibit not only the mutant TTR, but also COX enzymes, resulting in a series of different collateral effects [67]; in addition, TTR circulates in high concentrations in the serum and the drug might be delivered in high doses to be effective. Last but not least, inhibitors circulating in the bloodstream should bind selectively only TTR and not all the other proteins present (~4000 additional proteins in plasma). These are the reasons for which drug design must keep in consideration the potency of a compound as inhibitor but, also, side and off-target effects. Some of the co-crystal structures previously mentioned suggest that it is possible to design a single molecule that occupies, simultaneously, both binding sites on TTR: these molecules were named

bivalent inhibitors and they might overcome problems such as negative cooperativity and affinity towards COX-1 and COX-2.

1.8 Structures of TTR complexed with main ligands

1.8.1 Structure of TTR with T_4

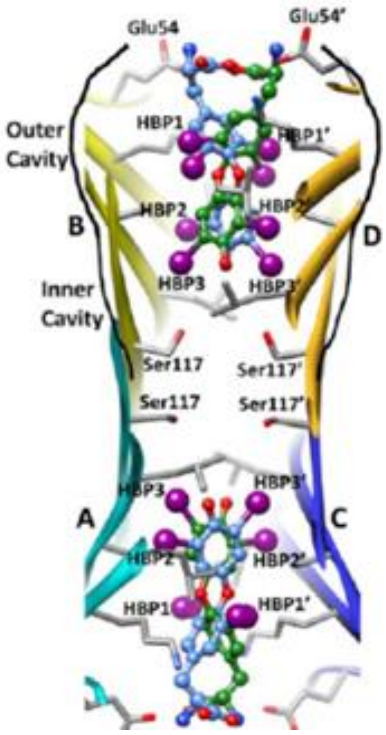

Figure 1.4: Interaction of T_4 with one of the T_4 binding site on TTR. The ligand is shown in both of its symmetry-related conformations (green and blue), in the forward binding mode ([63]).

Blake *et al.* solved the crystal structure of TTR in complex with T_4 and then investigated its mechanism of binding: they found that T_4 binds in the two symmetry equivalent sites, deeply buried along the central channel; since the electron density was not very clear, both for the relatively low resolution and for symmetry reasons (see below), they tryed to locate the iodine substituents of the ligand [12]. In the ensuing years, other structures were solved, confirming that the crystals are orthorhombic, belonging to the same space group of TTR, $P2_12_12$, with two monomers in the asymmetric unit [93]. In consequence of the intrinsic 2-fold symmetry, T_4 binds in two symmetry-related conformations with 50% occupancy, but to distinguish the two is a challenge also at high resolution. T_4 fully lock into the central channel making favourable bonding interactions and stabilizing TTR in its native tetrameric form. As already described, each T_4 site is composed of two different (inner and outer) pockets and is equipped with three pairs of HBPs: the number and the nature of the aminoacids exposed by these cavities determine the affinity and the binding mode of T_4 and T_4 analogues. The hormone Iodine atoms protrude towards the halogen binding pockets: in particular, in the inner cavity the 3' and 5' iodine atoms are linked to the HBP2/2' and HBP3/3' pockets and the 4' hydroxyl group establish water-mediated hydrogen bond interactions with the same groups of Ser117/117' and Thr119/119'. Depending on whether the carboxylate bearing aryl ring of T_4 orients towards the outer or the inner binding pocket, the ligand displays the forward or the reverse binding mode, respectively. It is interesting to note the remarkable capability of TTR to accommodate various ligands in different conformations: this open the possibility to design small drugs as inhibitors of amyloid fibrils formation but, on the other hand, the great capacity to bind several molecules make a challenge finding a selective and specific inhibitor.

1.8.2 Structures of the TTR·*holo*-RBP complexes

Trans-retinol, one of the various forms of animal vitamin A, is a small diterpenoid molecule implicated in diverse functions, like cell differentiation, growth and development of embryos, vision and others: inside the organism, it is transported as a complex with retinol binding proteins (RBPs), a family of proteins that act as carriers of the different forms of vitamin A in the blood. They are small proteins (about 21kDa) belonging to the lipocalin superfamily, composed of a single polypeptide chain organized in eight antiparallel β-sheets forming a β-barrel with an internal cavity well suited for retinol. The stability of the TTR:RBP complex is significantly affected by the presence of retinol as a ligand of RBP. On RBP, the residues on the loops at the entrance of the β-barrel are the main responsible for complex formation: binding of retinol is crucial for the stabilization of RBP loops and in turn for the TTR:RBP complex formation. As demonstrated, TTR is unable to bind to *apo*-RBP (without retinol) [94] [95]. Different structures of TTR·*holo*-RBP complexes are deposited, comprising some TTR mutants [30] [31] [96], and are well reviewed [97]; despite the presence of four equivalent binding sites on TTR, only two of them can bind to RBP as a consequence of steric hindrance. Two different quaternary structures were observed for the complex, namely the same and the opposite dimer model: in the former, the two RBP molecules interacts with the same TTR dimer (AB or CD), whereas in the latter they interacts with subunits on different dimers (AC or BD). *Holo*-RBP interacts with specific regions on three different TTR subunits (A, B and D) and because of the presence, at the interface, of the EF-helix-loop region (highly flexible in acidic conditions or in the presence of Zn^{2+}), many studies attempt to investigate the role of some residues in this region in the TTR:RBP complex formation.

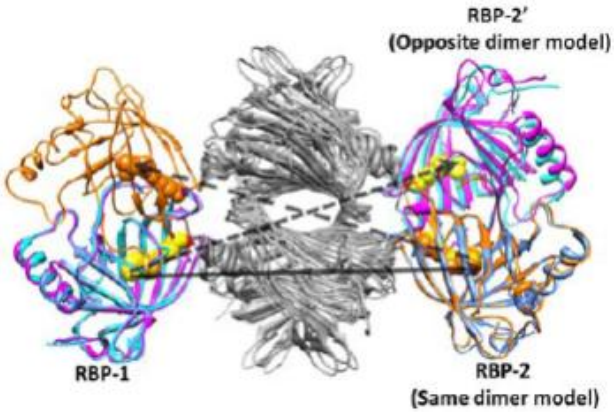

Figure 1.5: Representation of the two possible binding modes of *holo*-RBPs to TTR (same dimer model indicated by solid arrow and opposite dimer model indicated by dotted arrow) ([63]).

1.8.3 Structure of the complex TTR·resv

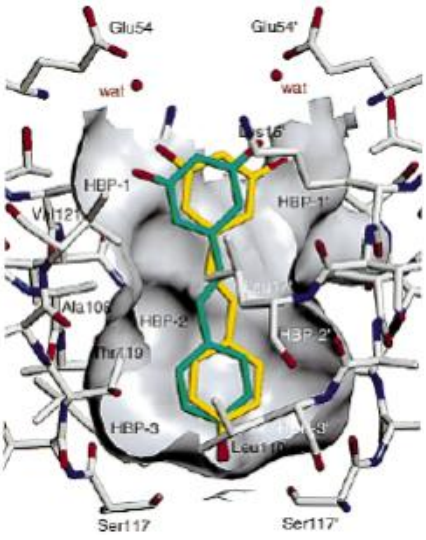

Figure 1.6: One of the two hormone binding of TTR with resv bound in two symmetry-related binding modes (shown in yellow and green) ([88]).

The structure of TTR:resv complex was determined, in view of the promising inhibitory activity of the phenolic compound resveratrol (resv) [88]. The structure shows that resv fits well into the two T_4 binding sites; because of the intrinsic 2-fold symmetry, resv, as all the other ligands, binds in two possible orientations related by a rotation of 180° along the channel. Interactions between TTR and resv are mediated by the stilbene moiety through non polar contacts. Two main factors contribute to the potency of resv, that is specific hydrogen bonds and favourable entropic contributions. The *p*- hydroxyl group is bound deeply in the cavity and is involved in hydrogen bond interactions with the hydroxyl group of Ser117 and Ser117'. Furthermore, the other two hydroxyl groups, present at the entry of the cavity, forms hydrogen bonds with some ordered water molecules. Favourable entropic contributions derive from the release of such ordered water molecules (at higher energy inside the cavity) and from the minimal conformational penalty that the system has to pay upon binding of the rigid stilbene moiety.

1.8.4 Structure of TTR·Tafamidis complex

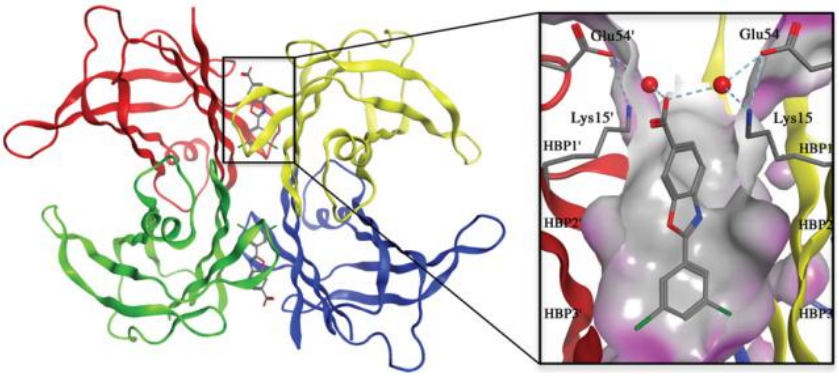

Figure 1.7: Ribbon representation of the TTR tetramer with the Tafamidis bound. Magnified image of Tafamidis in one of the T_4 binding sites ([98]).

The recently solved TTR:Tafamidis complex structure at 1.3Å resolution reveals the molecular and structural basis of TTR tetramer stabilization by Tafamidis, suggesting that the binding stabilizes the weaker dimer/dimer interface against dissociation [98]. The 3,5-dichloro substituents occupy HBP3/3' in the inner binding cavity.

The benzoxazole moiety is inserted in the hydrophobic environment of HBP1/1' and HBP2/2'. In this configuration, the carboxylate substituent is involved in water mediated hydrogen bonds with Lys15/15' and Glu54/54' of TTR. This combination of hydrophobic and electrostatic interactions appears to link adjacent dimers to kinetically stabilize the TTR native tetramer.

1.8.5 Structure of TTR·CHF5074 complex

Crystal structures of wt-TTR·CHF5074 (at pH 7.0) and of I84S TTR·CHF5074 (at pH 4.6) complexes were solved and published in the PDB in 2013, at a resolution of 1.67Å and 1.69Å, respectively [99]. CHF5074 is a fibrillogenesis inhibitor [100] [101] [102] and represents a chlorinated derivative of Flurbiprofen [103]; moreover, it possesses high binding affinity for wt-TTR. It binds to TTR in the forward binding mode and its position in the complex is relatively well defined for both T_4 binding sites. In particular, the di-chloro phenyl ring is deeply buried inside the central channel and the carboxylic moiety protrudes towards the solvent. However, despite a well-defined electron density for the inner and medium rings, the cyclopropane ring and the carboxylate end appear poorly defined. The ligand makes hydrophobic and electrostatic interactions with residues lining the TTR binding cavities. The former are mediated by Leu17/17', Ala108/108', Leu110/110' and Thr119/119', whereas the latter are represented by four polar contacts. From the superimposition with the other available structures it can be inferred that CHF5074 stabilizes the native structure of the TTR I84S tetramer, as it is able to readjust the altered structure of uncomplexed I84S TTR at acidic pH, converting it to that typical of wt-TTR at neutral pH. As in the complex of TTR with Diflunisal, it appears that the structure of TTR in complex with fibrillogenesis inhibitors remains nearly unchanged at both neutral and acidic pH: in other words, the ligand stabilizes the native protein structure mostly filling the central channel, while the protein conformation remains essentially the same.

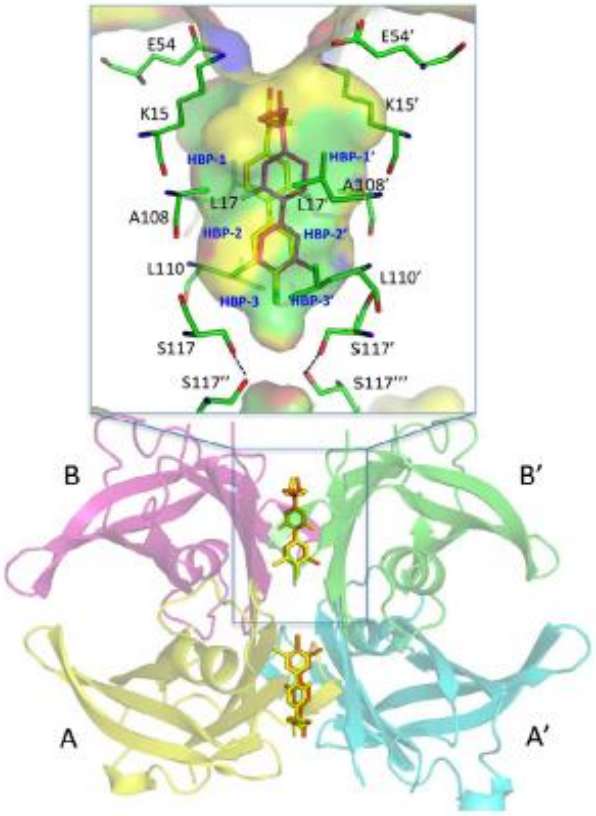

Figure 1.8: Ribbon representation of wt-TTR·CHF5074 complex and close-up view of one binding site [99].

The final effect is the rigidification of the tetramer and, as a consequence, the likelihood of a transition into the altered amyloidogenic conformation (favoured by lowering in pH and particularly for the variant I84S) is reduced.

1.9 Purpose of the Thesis Project

As discussed in the previous paragraphs, despite the significant difference between the two binding constants measured in solution for most of the TTR ligands, the two binding sites are very similar in the crystal structures of these complexes, and both appear occupied. Only very recently important and robust observations coming from X-ray and neutron diffraction and Molecular Dynamics Simulations shed light (in part) on the small, though significant, differences between sites A and B that are responsible for different geometries for the two hormone binding sites.

In the present Thesis work the problem is considered from a "crystallographic" point of view through the use of the tools offered by X-ray Crystallography. In particular the ability of this technique to provide details about the occupation of the sites by selected ligands is exploited. Although the ligands used in the present study have already been crystallized in complex with TTR and their structures solved, other aspects remain to be elucidated. For example, the structures so far determined were obtained by soaking the TTR protein crystals with an excess of ligand. The preparation of the complexes in solution and the use of a controlled stoichiometry ratio can reveal new insights into the mechanism of asymmetric ligand binding; the same can be said for mixed complexes, *i.e.* for complexes between TTR and (at least) two different ligands. With the aim of clarifying the ligand preference of TTR, attention has been focused either on different complexes with 1:1 stoichiometry ratio between protein Transthyretin and small-molecule ligands and on a single mixed complex. The question is of interest not only from a theoretical point of view, but it could have important therapeutic implications in the use of mixed ligands for the treatment of TTR amyloidosis.

2. MATERIALS & METHODS

In this Chapter are described the procedures with which co-crystals of the complexes were obtained, together with the protocol used to determine the crystal structure of TTR·ligand complexes.

2.1 Crystal structure refinement of TTR complexes

2.1.1 Crystallization

Crystals of TTR·ligand complexes suitable for X-ray diffraction studies were obtained in the Group of Prof. Rodolfo Berni at the University of Parma. Recombinant human wild type TTR was prepared as described previously in literature [71]. Crystals of TTR·ligand complexes were obtained at room temperature in about one week by co-crystallization, using the hanging-drop vapour diffusion method. Regarding all the 1:1 complexes, the protein (5 mg/ml), in 20 mM sodium phosphate at pH 7, was incubated for a few hours with an equimolar quantity of ligands solubilized in DMSO. For TTR·ligand excess, the same conditions have been used, but the protein was incubated for a few hours with a fourfold molar excess of ligands solubilized in DMSO. Drops were formed by mixing equal volumes of the solution containing TTR·ligand complexes and of the reservoir/precipitant solution (2.0 M ammonium sulfate, 0.1 M KCl, 0.05 M sodium phosphate, pH 7.0).

2.1.2 Data collection and structural determination

The crystals were directly flash cooled at 77K after fishing from the crystallization drops. The datasets concerning the different TTR·ligand complexes were collected at the PXIII Beamline of Swiss Light Source synchrotron radiation facility (Villigen, Switzerland).

Datasets were processed with the software XDS [104] and scaled with Scala [105] contained within the CCP4 suite [106]. The structures of the TTR·ligand complexes were refined starting from the atomic coordinates of the hTTR dimer as a template (PDB ID code: 1F41 ([4])). Atomic coordinates of the ligand molecules and restraints were obtained through the PRODRG server [107] [108] or the function eLBOW implemented in Penix.refine. The models were refined using the package Phenix (PHENIX version 1.9-1692) [109] with a maximum likelihood target function. After each series of refinements, map visualization and manual adjustment of the models were performed using the Coot graphic interface [110]. Water molecules were added automatically to the model and were revised and eventually adjusted manually using Coot. In the last cycles, TLS refinement was applied.

Inspection of the electron density in the channel for TTR·ligand complexes indicated the presence of the ligands bound in one or both of the TTR binding sites. Crystals of hTTR in complex with the various ligands diffracted to a maximum resolution between 1.38Å and 1.73Å: this allowed to define, in most cases, details of the T_4 binding sites and to refine quite carefully the occupancies of the ligands in the TTR molecule. All the structures are isomorphous to wild type hTTR: in all cases, the crystal lattice is orthorhombic, space group $P2_12_12$ (Appendix A) and the cell parameters are quite similar for all crystals.

Data collection and refinement statistics are summarized in Table 2.1.

Table 2.1: Data collection and refinement statistics. Data were measured at PXIII beamline of Synchrotron Light Source, Villigen, Switzerland.

Data set	TTR·resv 1:1	TTR·resv excess	TTR·resv·T_4	TTR·T_4 1:1	TTR·Tafamidis 1:1	TTR·CHF5074 1:1
Wavelenght	1.00	1.00	1.00	1.00	1.00	1.00
Cell dimensions						
a, *b*, *c* (Å)	42.44, 85.61, 63.64	42.94, 85.35, 63.91	42.54, 85.63, 63.83	42.56, 85.75, 63.93	42.42, 85.37, 63.60	42.43, 85.07, 64.11
Resolution (Å)	42.80-1.39 (1.46-1.39)*	42.94-1.38 (1.46-1.38)	42.82-1.54 (1.63-1.54)	42.88-1.38 (1.46-1.38)	42.69-1.73 (1.82-1.73)	42.53-1.38 (1.46-1.38)
R_{merg}	0.032 (0.744)	0.058 (1.275)	0.041 (0.298)	0.052 (0.884)	0.057 (0.324)	0.045 (0.521)
R_{pim}	0.015 (0.349)	0.031 (0.605)	0.019 (0.143)	0.026 (0.443)	0.029 (0.171)	0.023 (0.248)
$\langle I/\sigma(I) \rangle$	24.7 (2.3)	14.6 (1.1)	21.3 (4.9)	14.8 (1.6)	17.4 (3.1)	19.3 (3.2)
Completeness (%)	99.5 (97.3)	97.4 (92.9)	99.5 (97.3)	99.1 (95.6)	97.7 (88.9)	99.3 (97.9)
Redundancy	6.4 (6.1)	6.0 (5.9)	6.2 (6.1)	6.0 (5.7)	5.9 (5.1)	6.0 (5.8)
Refinement						
No. reflections	89471	80196	65091	89075	43322	87717
R_{work} / R_{free}	0.168/0.191	0.237/0.266	0.166/0.193	0.170/0.213	0.204/0.262	0.182/0.233
No. atoms	1975	2107	1966	2013	3740	2068
Protein	1804	1810	1793	1841	1833	1835
Solvent/Ligands	171/17	297/17	173/41	172/48	159/40	233/42

R.m.s. deviations						
Bond lenghts (Å)	0.009	0.011	0.010	0.012	0.012	0.011
Bond angles (°)	1.334	1.362	1.287	1.478	1.392	1.345
Ramachandran plot (%)**						
Favored	98.25	97.83	98.26	97.83	96.52	97.34
Allowed	1.31	1.74	1.30	1.74	3.48	2.17
Outliers	0.44	0.43	0.43	0.43	0	0.43
Rotamer outliers (%)	1.54	0.51	0.52	1.53	1.53	1.53
Cβ deviations	1	0	0	2	0	1

* Numbers in parentheses refer to the last resolution shell.

** MolProbity statistics.

R_{sym} defined as: $R_{sym} = \frac{\sum_{hkl}\sum_j |I_j - \langle I \rangle|}{\sum_{hkl}\sum_j I_j}$ where *I* is the intensity of a reflection and <*I*> is the mean intensity of all symmetry related reflections *j*.

$R_{p.i.m.}$ defined as: $R_{p.i.m.} = \frac{\sum_{hkl}\left\{\left[\frac{1}{N-1}\right]\sum_j |I_j - \langle I \rangle|\right\}^{1/2}}{\sum_{hkl}\sum_j I_j}$ where *I* is the intensity of a reflection, <*I*> is the mean intensity of all symmetry related reflections *j* and *N* is the multiplicity.

3. RESULTS & DISCUSSION

In this Chapter, results obtained from the refinement process of the six complexes studied will be illustrated. The results will be presented discussing the overall quality of the model obtained after the refinement process, possibly comparing them with those previously reported in the literature and, in some cases, analyzing the interactions between the ligand and the specific amino acids in the cavities. The molecules involved in the complex with the transthyretin are its natural ligand thyroxine (T_4), the phenolic compound resveratrol, the drug already approved and marketed Tafamidis and the promising candidate (involved in the late-phase of clinical trials) CHF5074:

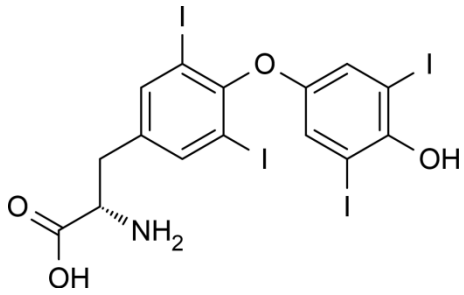

Figure 3.1: Thyroxine.

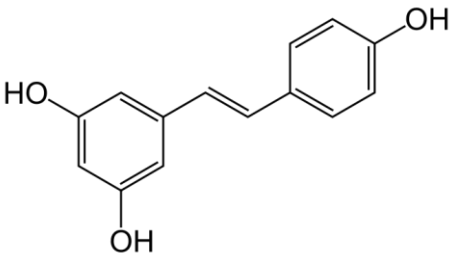

Figure 3.2: Resveratrol.

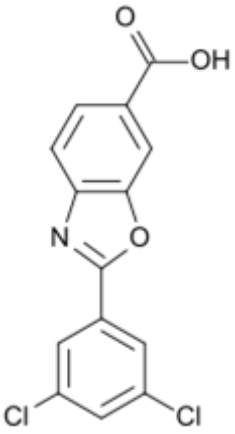

Figure 3.3: Tafamidis (Vyndaqel).

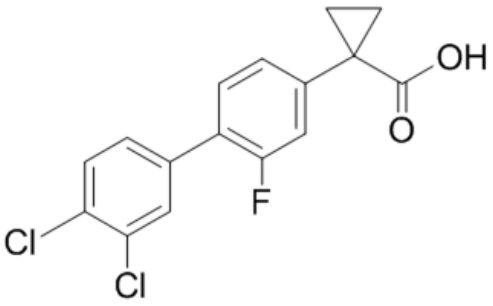

Figure 3.4: CHF5074 (CSP-1103).

3.1 Crystal structure refinement of TTR complexes

3.1.1 Structure of TTR·CHF5074 1:1 complex

As reported for the wt-TTR·CHF5074 complex at 1.67Å, whose crystals were obtained with a fourfold molar excess of CHF5074 [99], also with an equimolar mixture two molecules of ligand are present in both the sites on the protein, despite with different occupancy (Fig. 3.7). The good resolution of the structure (1.38Å) is reflected in the quality of the electron density map, into which the model of the three-dimensional protein structure is built (a higher resolution of the data means higher resolution of the electron density maps, which in turn means higher accuracy of the positions of the atoms in the structure). In Fig. 3.5 is reported a selected trait from Chain A of the TTR·CHF5074 complex, testifying the quality of the electron density map.

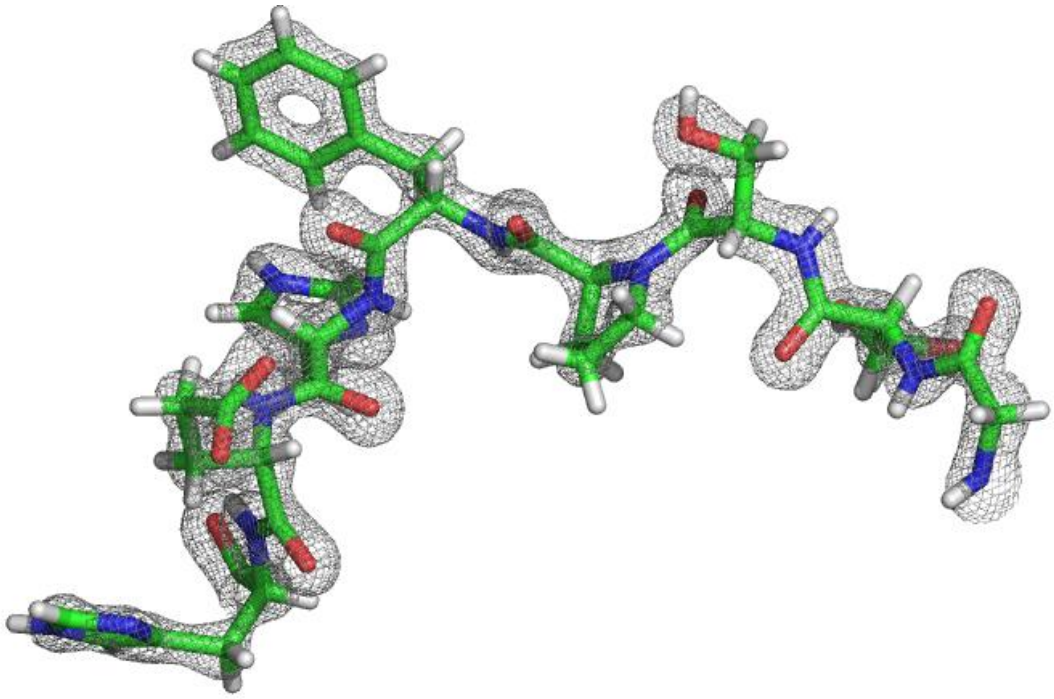

Figure 3.5: View of the electron density map in chicken-wire representation only for residues from 83 to 90, chain A, corresponding to a β-sheet trait, from TTR·CHF5074 complex. The map has been calculated with coefficients $2|F_o| - |F_c|$ and contoured at 2.0σ level. This electron density map, along with all the others in the text, have been produces using the phenix.maps tool with final model and reflection files as input and after graphical visualization and adjustments in MacPyMOL.

In particular, the electron density of the ligand is clearly visible from the first stages of refinement and this facilitates its placement in the cavity. However, it is worth noting that the presence of a crystallographic and molecular twofold axis through the cavity in which the ligand is hosted implies the presence of two possible orientations of the molecule: this is responsible for an intrinsic disorder in the observed electron

density. From Fig. 3.6, it is possible to note that the electron density map is sufficiently defined to show both conformations of the ligand inside the cavities.

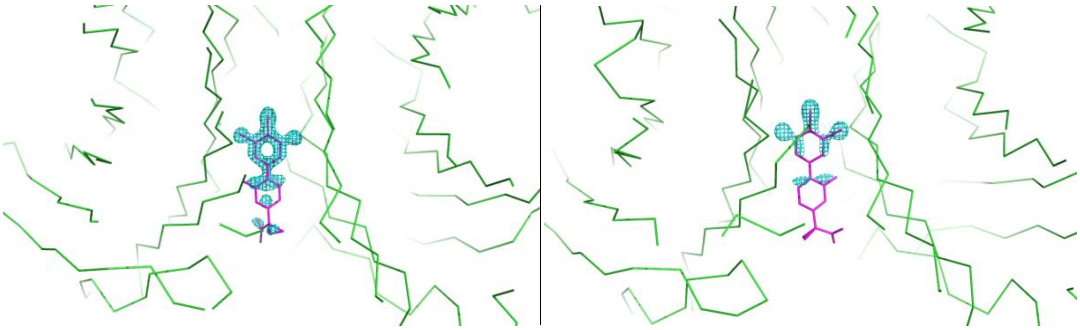

Figure 3.6: View of the electron density map in chicken-wire representation, calculated with coefficients $2|F_o| - |F_c|$ and contoured at 2.0σ level only around the ligand (*on the left* in site B, *on the right* in site A), for CHF5074 bound to wt-TTR. Only one of the two symmetry-related conformations is shown in magenta.

From the same Figure, the electron density associated with the two phenyl rings appears well defined, whilst the ligand portion comprising the cyclopropane ring and the carboxylic group is, in fact, not visible, owing to the flexible nature and the reduced interaction of this ligand moiety with some residues. Indeed, when some parts of the structure are not so well ordered (due to flexibility), this results in high temperature factors (or *B*-factors) and poor electron density maps. Looking at the *B*-factors for the inhibitor molecules in both binding sites (hereinafter referred to as site A and site B, because the former is lined by monomers A and A' and the latter by monomers B and B'), it is possible to make two observations. First, in agreement with what was said before, the atoms that are part of the cyclopropane ring and of the carboxylate end group show higher *B*-factor values compared to all the other atoms of the ligand. Second, apart from one exception, all the atoms of the ligand inside site A display a *B*-factor higher than that of the atoms of the ligand in site B and this is so because of the exponential relation that links together occupancy and the temperature factor (refining the structure fixing the B values and allowing the occupancy to adjust itself show, in fact, that ligand atoms in site A have an average occupancy lower than the atoms in site B). Another feature in common with previous results obtained for the complex concerns the binding mode of the ligand inside the cavities of the TTR tetramer: the inhibitor is bound in the so called forward binding mode, with the di-chloro phenyl ring embedded inside the cavity and the flexible portion protruding outward.

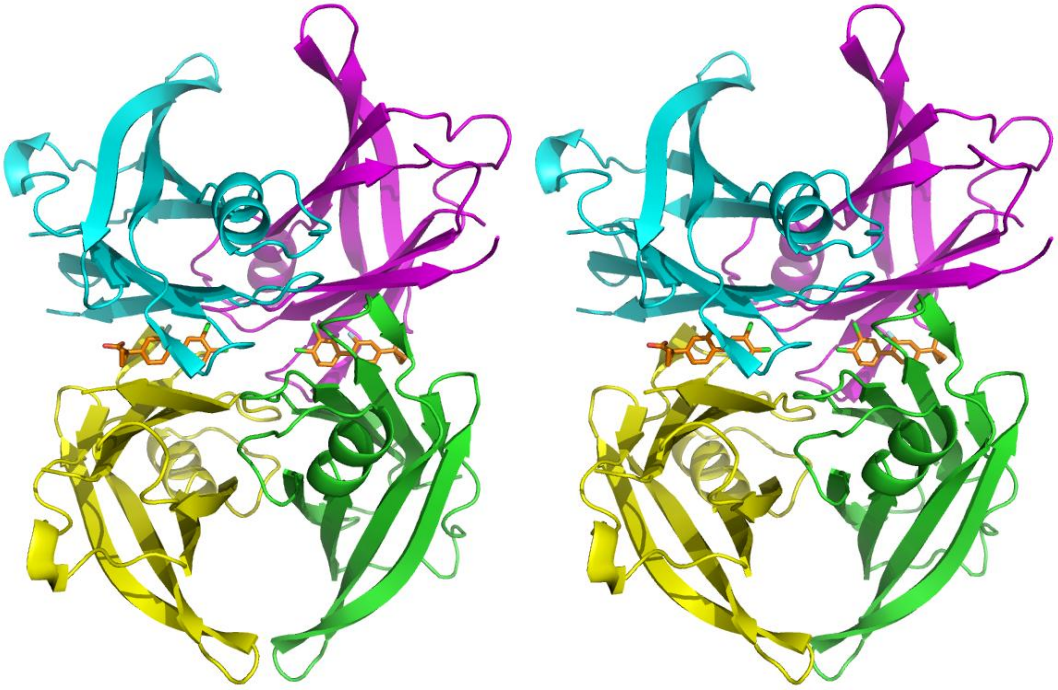

Figure 3.7: Stereo view of the TTR·CHF5074 complex in cartoon representation with the secondary structure elements, showing the four monomers with different colours (yellow, green, magenta and cyan) and the ligands in the hormone binding sites as stick model (for clarity, only one of the two conformations is shown for each ligand). Water molecules are omitted. This figure, along with all the others (excluded electron density images), have been produces using software MacPyMOL (DeLano, 2007, MacPyMOL: A PyMOL-based Molecular Graphics Application for Mac OS X. DeLano Scientific LLC, Palo Alto, CA.)

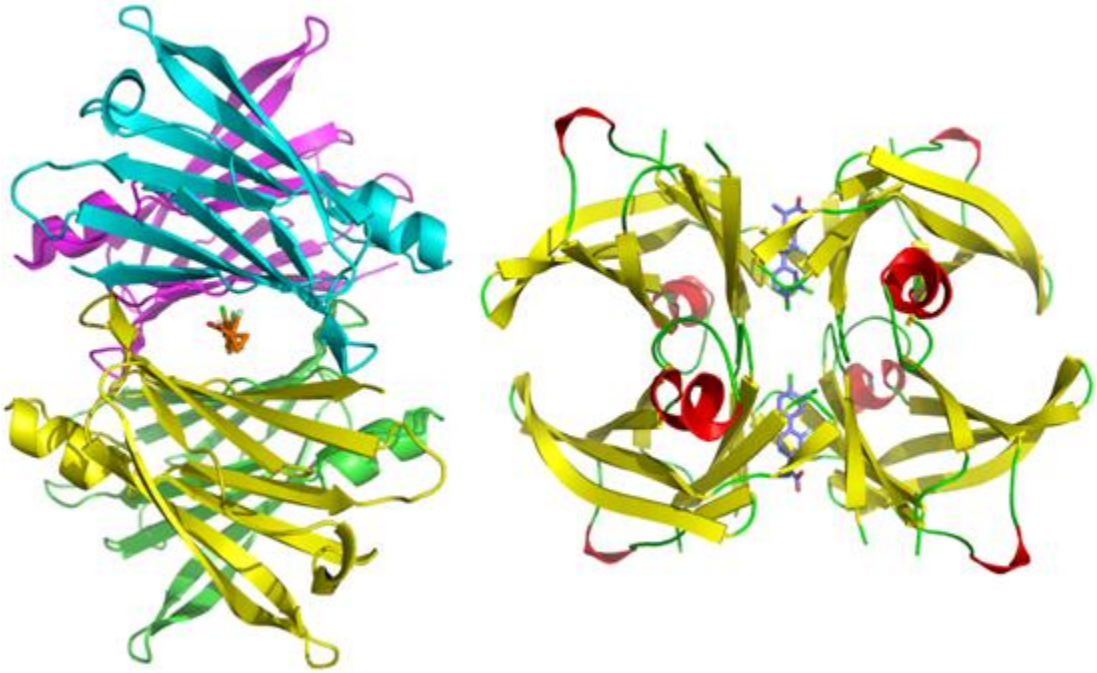

Figure 3.8: *On the left*, view of the TTR·CHF5074 complex along the central hormone binding channel with the two ligands shown. *On the right*, ribbon representation of the same complex coloured on the base of the secondary structure elements (helix in red, sheet in yellow and loop in green) with the CHF5074 molecules in the T_4 hormone binding sites formed between two dimers.

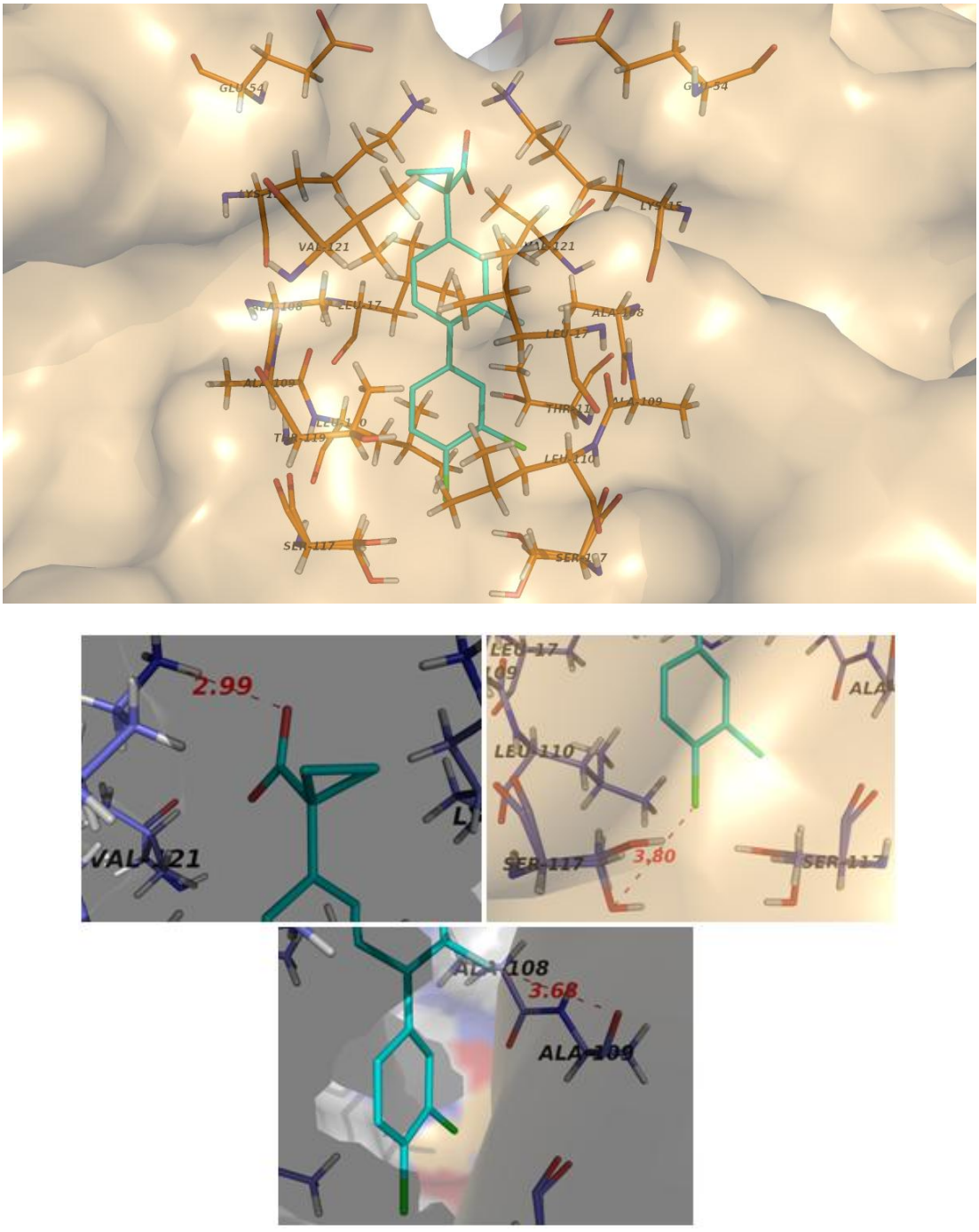

Figure 3.9: *At the top*: hormone binding site structure of the TTR·CHF5074 1:1 complex, showing the relevant residues involved in the interaction with the ligand. The representation confirms the model previously solved [99]. *At the bottom*: three magnifications showing the main electrostatic interactions inside the cavity, with the measured distances (Å) .

As shown in Fig. 3.9, to visualize the main residues involved in the interaction with the ligand inside the cavity a detailed view was created and compared to what was already reported in literature [99]. In Fig. 3.9 have been evidenced amino acids Lys15 and Leu17 (HBP 1 and 1'), Ser117, Leu110, and Ala108 (HBP3 and 3') and residues Leu17, Ala108, Ala109 and Leu110 (HBP2 and 2').

As introduced in Paragraph 1.8.5, both TTR-bound CHF5074 molecules make hydrophobic and electrostatic interactions with some amino acids in the cavities: the latter are mediated by four polar contacts: the –COOH group of the ligand is close to the ε-amino group of Lys15 (2.48-3.15Å); the *p*-Cl atom of the di-chloro phenyl ring is close to the –OH group of Ser117 (3.8Å); the *m*-Cl atom interacts in a similar way and the fluorine atom interacts with the carbonyl oxygen of Ala109 (3.52Å). Measured distances are in agreement with values reported in literature. In addition, it is important to note that Ser117 and 117' of B and B' subunits interacts with the same residues of A and A' subunits through hydrogen bond, stabilizing further tetrameric TTR.

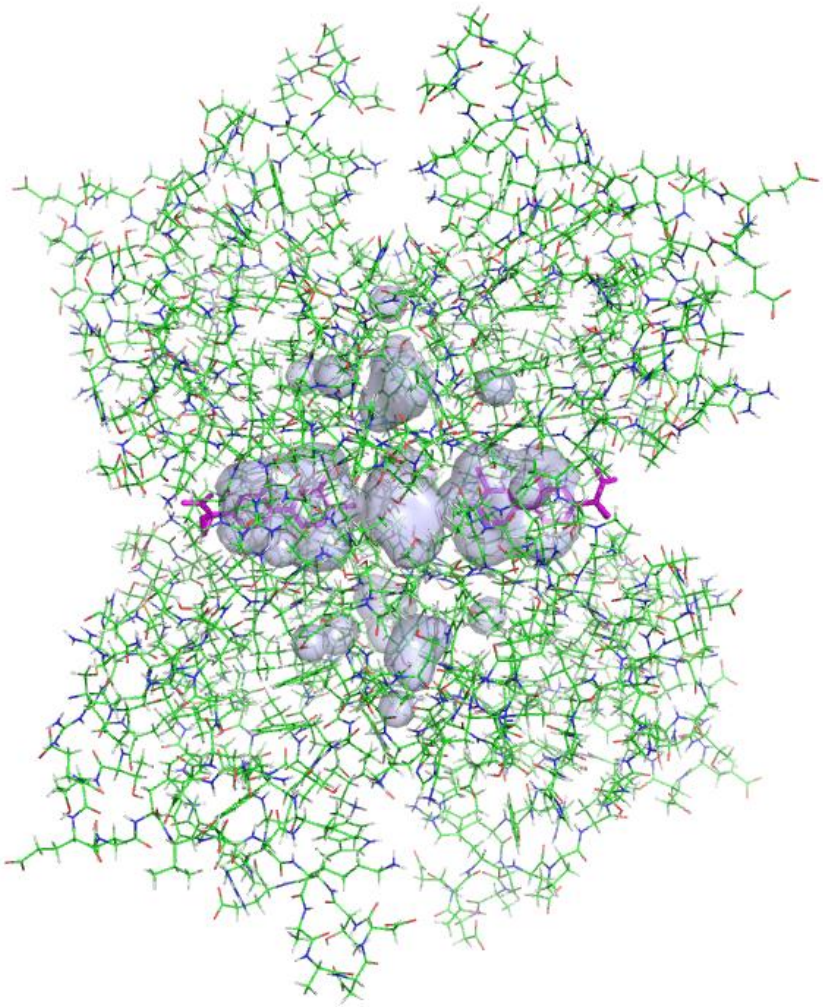

Figure 3.10: Surfaces (in lightblue) of the tetrameric TTR, comprising the two cavities in which ligand molecules (in stick model representation, coloured in magenta) are inserted.

3.1.2 Structure of TTR·Tafamidis 1:1 complex

By screening a library of 2-arylbenzoxazoles, several potent and highly selective amyloidogenesis inhibitors were identified and, after obtaining high resolution crystal structures (1.3-1.5Å), structures of the various complexes were solved [111]. Tafamidis represents one of the most important benzoxazole derivatives: it was discovered by Kelly's laboratory and developed by FoldRx Pharmaceuticals (acquired by Pfizer in 2010) [92]. It was demonstrated its capacity to slow the progression of FAP and, owing to this, it became the first drug to be approved for the treatment of FAP in 2011 [112].

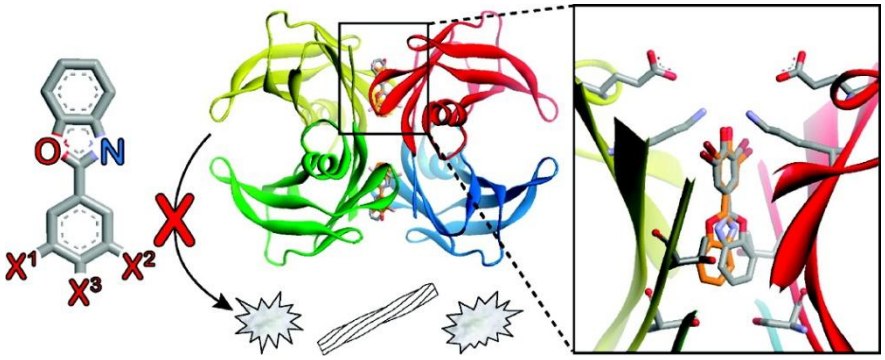

Figure 3.11: Schematic depiction of the inhibitor activity of a generic arylbenzoxazole derivative (stabilization of the TTR homotetramer, preventing amyloid fibrils formation) and magnification of the same inhibitor inside one of the two cavity, representing the X-ray crystallographic structure of the complex [111].

To date, TTR·Tafamidis complex is the highest-resolution structure solved (1.30Å) among the TTR·(ligand)$_2$ structures [98]. In the context of the present work, the structure of the complex at 1.73Å was obtained from an equimolar mixture of protein and inhibitor, and not with a fivefold molar excess of Tafamidis as described by Bulawa *et al.* [98]. However, regardless of the stoichiometry ratio, Tafamidis was found in both the T_4 binding sites and the good quality electron density map allowed for the unambiguous placement of the inhibitor in the cavities. As shown in Fig. 3.12, there is no electron density corresponding to the carboxylate substituent, indicating that this part of the molecule is disordered in the crystal. Instead, the electron density associated with the more rigid benzoxazole moiety and the di-chloro phenyl ring is well defined. It is possible to confirm the binding mode by which the ligand enter the cavity: the benzoxazole ring and the 3,5-dichloro substituent of Tafamidis are located deep in the cavity and they establish interactions with all the HBPs, whereas the carboxylate end group is positioned at the entry port of the T_4 binding pocket. This results in water-mediated hydrogen bonds with Lys15/15' and Glu54/54'.

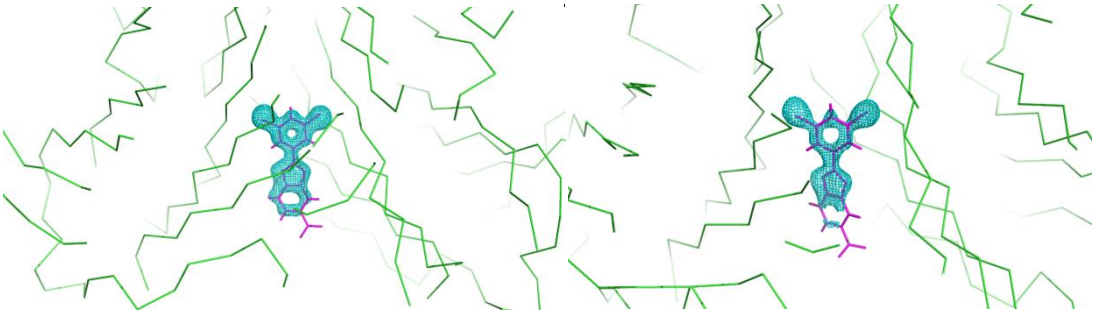

Figure 3.12: View of the electron density map calculated with coefficients $2|\boldsymbol{F_o}| - |\boldsymbol{F_c}|$ and contoured at 2.0σ level only around the ligand (*on the left* in site B, *on the right* in site A), for Tafamidis bound to wt-TTR.

As suggested by Bulawa *et al.* [98], because these low *B*-value waters are not conserved either in TTR and TTR·(ligand)$_2$ complexes and because these hydrogen bonds are solvated, it appears unlikely that they represent the driving force for Tafamidis binding to TTR.

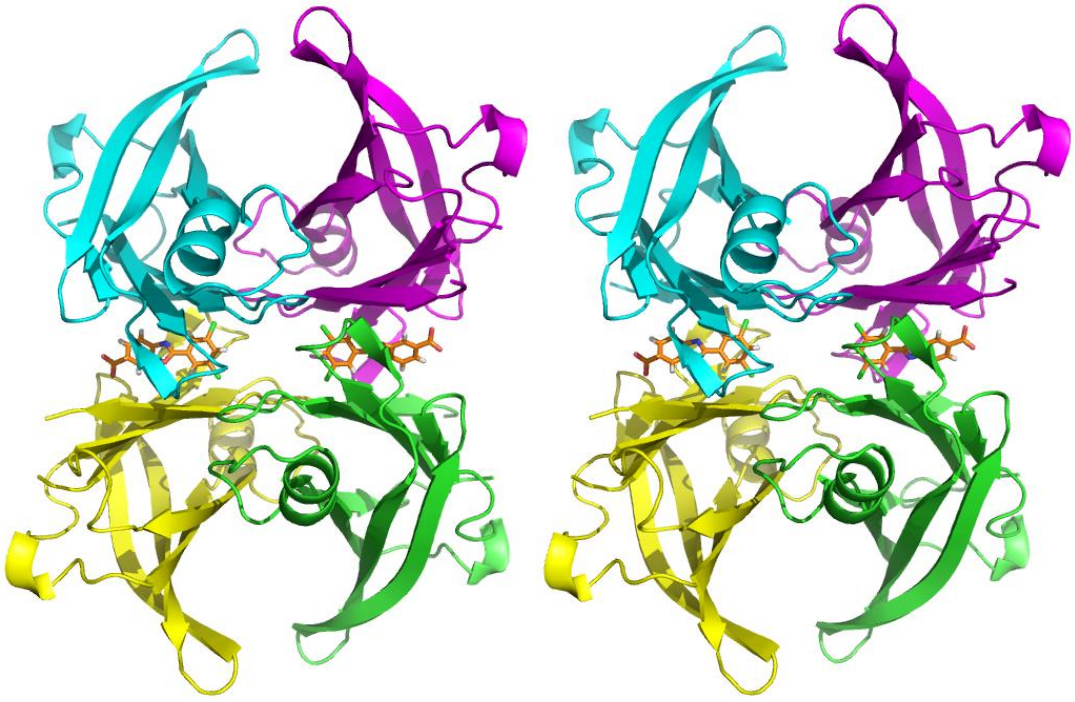

Figure 3.13: Stereo view of the TTR·Tafamidis 1:1 complex showing the two Tafamidis molecules occupying both the hormone binding sites.

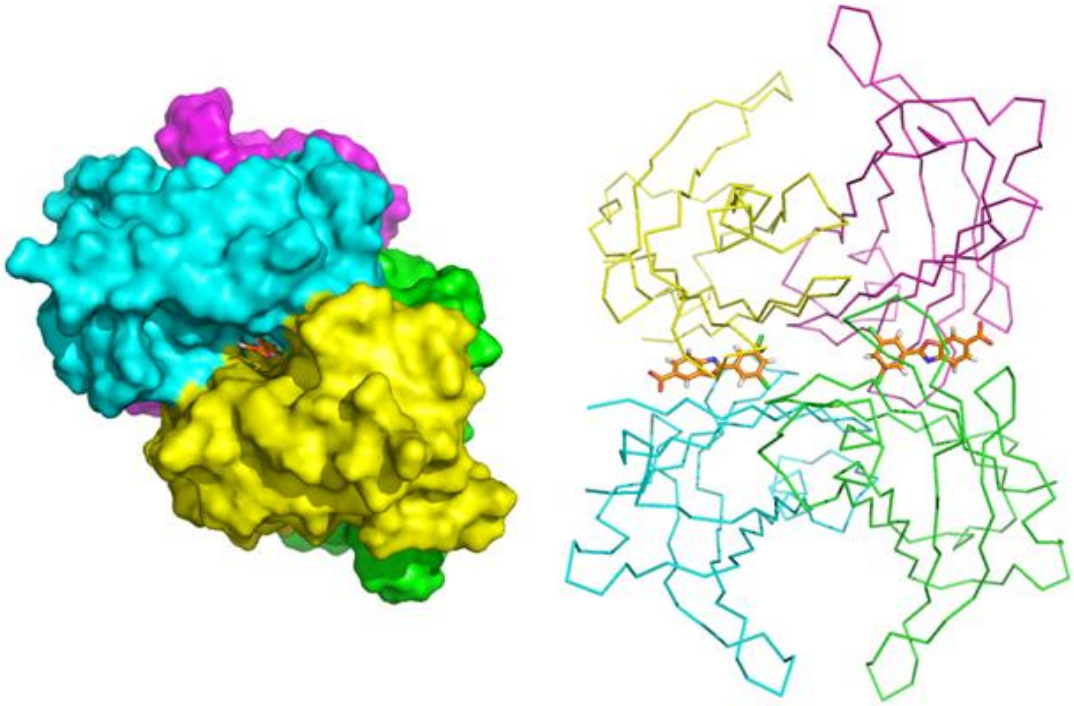

Figure 3.14: *On the left*, surface representation of the TTR·Tafamidis 1:1 complex, showing an overall view of the surface and one hormone binding site with the ligand inside it. *On the right*, Cα chain trace of TTR and the two Tafamidis molecules.

3.1.3 Structures of TTR·resv complexes

The huge interest for resveratrol (3,5,4'-trihydroxy-*trans*-stilbene), a natural stilbenoid particularly found in berries, red wine and grape's juice, is due to its beneficial effects on human health (at least on some heart diseases, cancers and metabolism). In addition, resveratrol (resv) significantly reduces TTR fibril formation and this is the reason why the stilbene derivative represents an excellent lead compound for the development of a new class of drugs against TTR amyloid diseases. In the present work, the structures of TTR·resv complexes were obtained either from an equimolar mixture and with a fourfold excess of the ligand. Moreover, the crystals used for data collection diffracted to a maximum resolution of 1.38Å and 1.39Å and the structures attained from these crystals are the highest-resolution structures so far obtained. This has also allowed to define more details of the T_4 binding sites and to refine quite carefully the structure.

Figure 3.15: Cartoon representation of the TTR·resv 1:1 complex showing the presence of the ligand only in one of the T_4 binding sites (site B).

With respect to the TTR·resv 1:1 complex, interpreting the electron density map is made easy thanks to the medium-high resolution and also the positioning of the ligand appears simple and unambiguous.

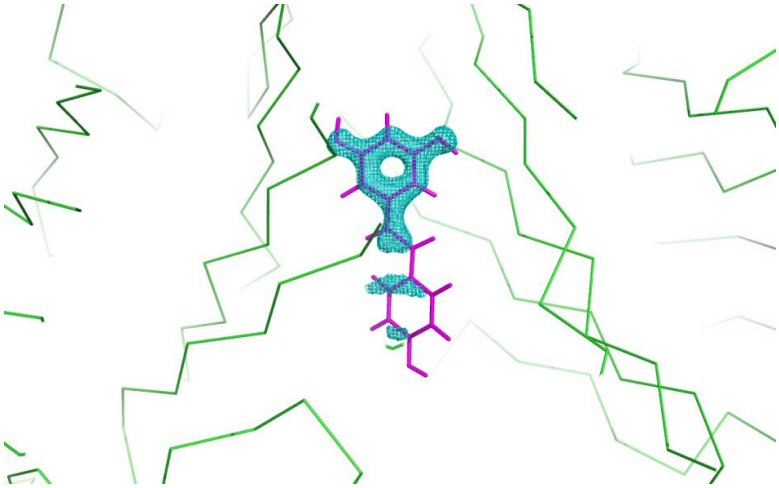

Figure 3.16: View of the electron density map of resveratrol in site B with coefficients $2|\boldsymbol{F_o}| - |\boldsymbol{F_c}|$ and contoured at 2.0σ level.

In particular, only in the site B the electron density of the ligand is clearly visible from the first stages of the refinement and, consequently, the structure was refined with a single resveratrol molecule. Slightly different appears the case of the TTR·resv complex obtained in the presence of an excess of the ligand: here, a well defined electron density of the ligand is visible in the site B but a less defined electron density can be noted in site A after several cycles of refinement. Including the second molecule of resveratrol in site A and performing a refinement shows that ligand atoms in site A are characterized by higher *B*-factors and lower occupancy, as expected. Both structures, however, show the same binding mode for the ligand: the *p*-hydroxyl group is positioned at the entry port of the T_4 binding pocket, whereas the other two –OH groups are located deep in the cavity.

Nevertheless, comparing this result with the structure reported in 2000 by Klabunde *et al*. [88] revealed an exactly opposite binding mode (Fig. 3.17).

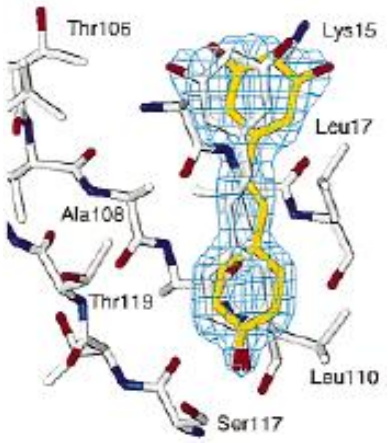

Figure 3.17: Stick model of the resv bound to the hormone binding site. Electron density map is shown in cyan chicken wire around both the conformations of the ligand (in yellow and white) [88].

These two conflicting results may have at least two explanations: *in primis*, the structure reported in the article quoted above was obtained at a lower resolution (1.9Å) and it is possible that there has been, during refinement procedure, a wrong positioning of resveratrol in the cavity, due to lower definition of the electron density map. In fact, the electron density in Figure 3.17 represents the result of several cycles of refinement and so it contains a bias due to the original position of the model, because during the optimization procedure phases (hopefully) gradually improve and this is reflected in the quality of the electron density map, which also improves. In any case, there is probably a combined effect taking into account a second explanation: unlike the crystals obtained for the present study, Klabunde and co-workers have prepared the crystals by soaking. Growing crystals from a mixed solution is clearly different from soaking, in which a pre-existing crystal of TTR is placed in a solution containing the ligand at a precise concentration (Klabunde *et al.* used a tenfold molar excess of resveratrol to ensure full saturation of both binding sites). When transthyretin is in solution, it has more degrees of freedom and it is characterized by a greater flexibility: as a consequence, when an hypothetical ligand molecule approaches one of the cavity cannot only enter inside it but can also sit in the best conformation, eventually after a series of structural adjustments in order to find the minimum energy conformation. With the soaking method, the molecules of TTR are already packaged inside the crystal lattice in a rigid manner and the entry of the ligand, obviously, is not as free as in the previous case because of additional restraints imposed by the lattice forces. In other words, in solution the structure of the uncomplexed TTR is unaffected by the interaction of symmetry-related molecules present in the crystal lattice.

Fig. 3.18 is a representation of the main residues involved in the interaction between resveratrol in site B. In spite of the opposite findings [88], some features remains probably unaffected: also with an opposite binding mode, ligand-protein interactions remain likely dominated by non-polar contacts mediated by the stilbene moiety, which is stacked between the hydrophobic side chains of Lys15, Leu17, Ala108, Leu110, Ser117, Thr119 and Val121. It is expected that changes in the interaction between resveratrol and the residues lining the cavity involve the hydroxyl groups of the ligand and the amino acids that are present deep in the cavity and at the entry of it. As already discussed, Klabunde *et al*. reported the structure of the complex in which the *p*–OH of the distal phenyl ring is deeply bound in the cavity and they argued that this causes the displacement of water molecules positioned in HBP3 of the *apo*-form. This, in turn, is responsible for the formation of a tight hydrogen bond between the *p*–OH of resv and the Oγ atom of Ser117 (2.6Å). With an opposite binding mode, it is possible that hydrogen bond interactions are strengthened: this is because in the new situation there are two hydroxyl groups involved and the measured distances ranges from 1.8Å to 3.5Å. The hydrogen bonds are not too long and remain sufficient strong to justify the high affinity of resv.

Secondly, they reported a structure in which the two hydroxyl groups on the second phenyl ring are located at the entry of the binding cavity and they also stated the formation of hydrogen bonds with ordered water molecules. There are no reasons why this should change with an opposite binding mode; however, it has also to be considered that the *p*–OH can establish (weak) hydrogen bonding interactions with the side chain carboxylic groups of Glu54 and 54'.

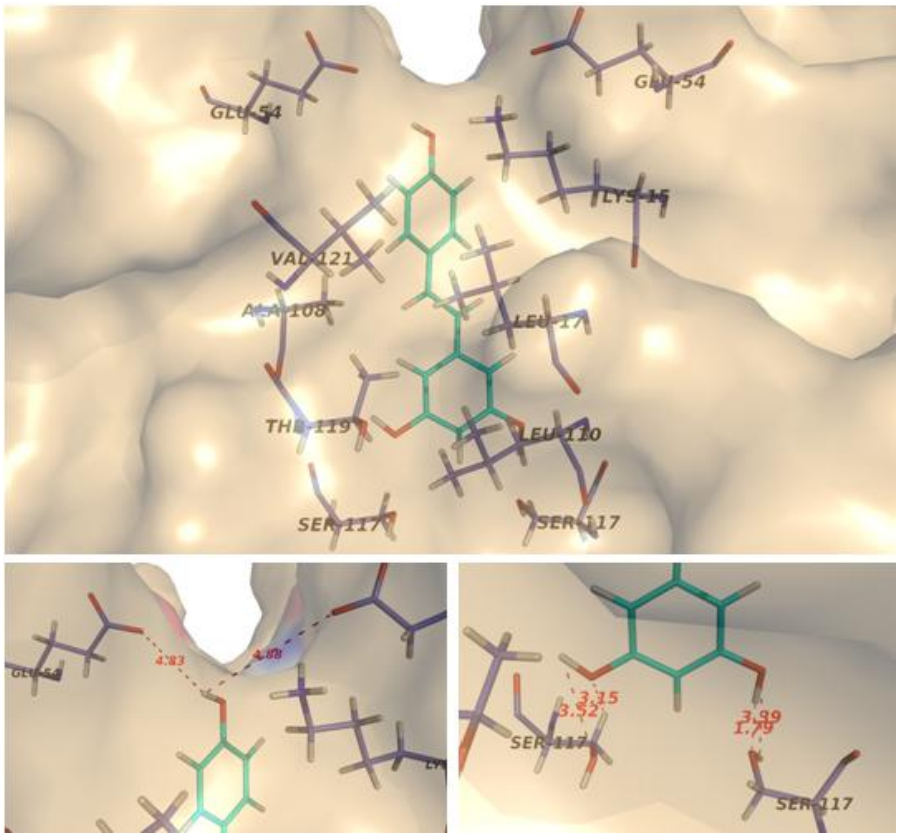

Figure 3.18: *At the top*: hormone binding site structure of the TTR·resv 1:1 complex, showing the relevant residues involved in the interaction with the ligand (the ligand shows Van der Waals interactions with several side chain residues). The stilbene scaffold is sandwiched between two adjacent protein subunits filling the central parts of the channel. *At the bottom*: detailed views of some relevant interactions involving the hydroxyl groups of resv with Ser and Glu residues inside the cavity.

3.1.4 Structures of TTR·T_4 1:1 and mixed TTR·T_4·resv complexes

All structures published so far and relative to the TTR·T_4 complex were obtained from crystals grown in the presence of an excess (usually a 10-fold molar excess) of thyroxine and, in these cases, it was observed that both the binding pockets are saturated with T_4. In this context, it is useful wondering if the T_4 binding sites remain fully saturated even in the presence of an equimolar quantity of the ligand and, to answer this question, crystals of the complex TTR·T_4 1:1 were prepared.

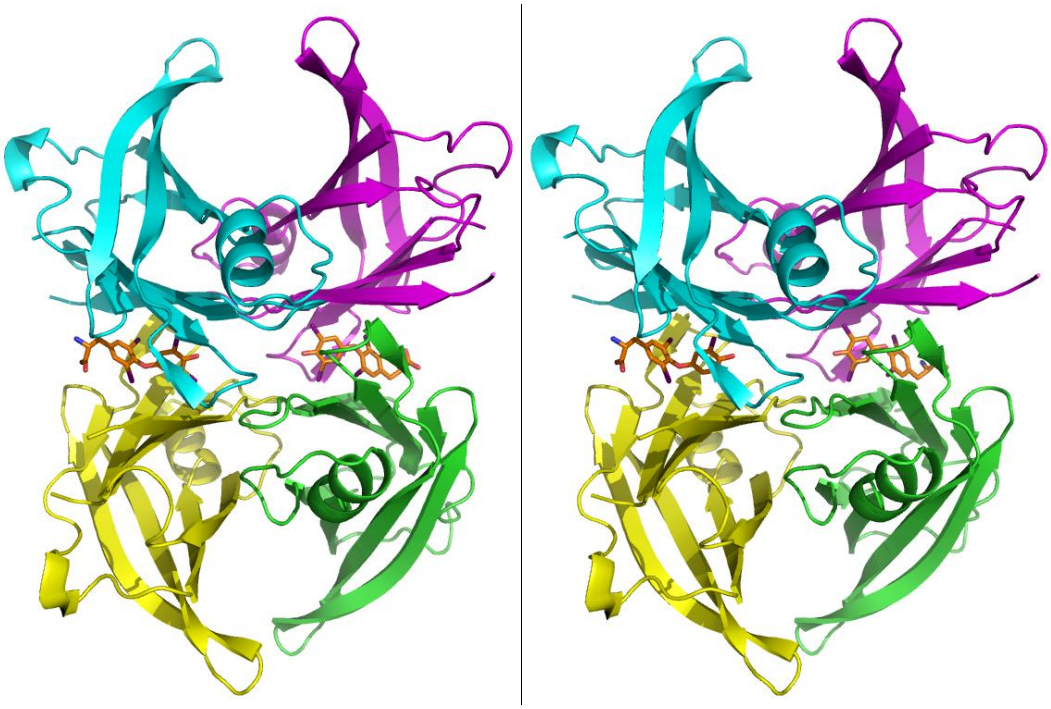

Figure 3.19: Stereo view of the TTR·T_4 1:1 complex showing the two thyroxine molecules occupying both the hormone binding sites.

The subsequent structure refinement revealed that, also in this case, thyroxine occupies both sites on the TTR tetramer: however, positioning it in the two cavities does not appear an easy task. This is so because of the absence of electron density relative to the ligand and exploiting anomalous scattering originated by the four iodine atoms is the only way to try to correctly locate the T_4 molecules in the structure. For this purpose, starting from the anomalous Bijvoet pair structure factors F^+ and F^- as input data, the map coefficients were generated and the related anomalous difference map. This map was used to localize the dispersive iodine atoms and what emerges is that the anomalous signal is present in both the sites. In particular, up to 12σ for site B and up to 14σ for site A, all the iodine atoms are visible: above this level, only half of the dispersive atoms appear in the anomalous difference map.

In agreement with the structures already solved, the ligand interact with the cavities in the so called forward binding mode, that is the α-carboxylate and the α-amino groups of T_4 occupy the outer binding pocket.

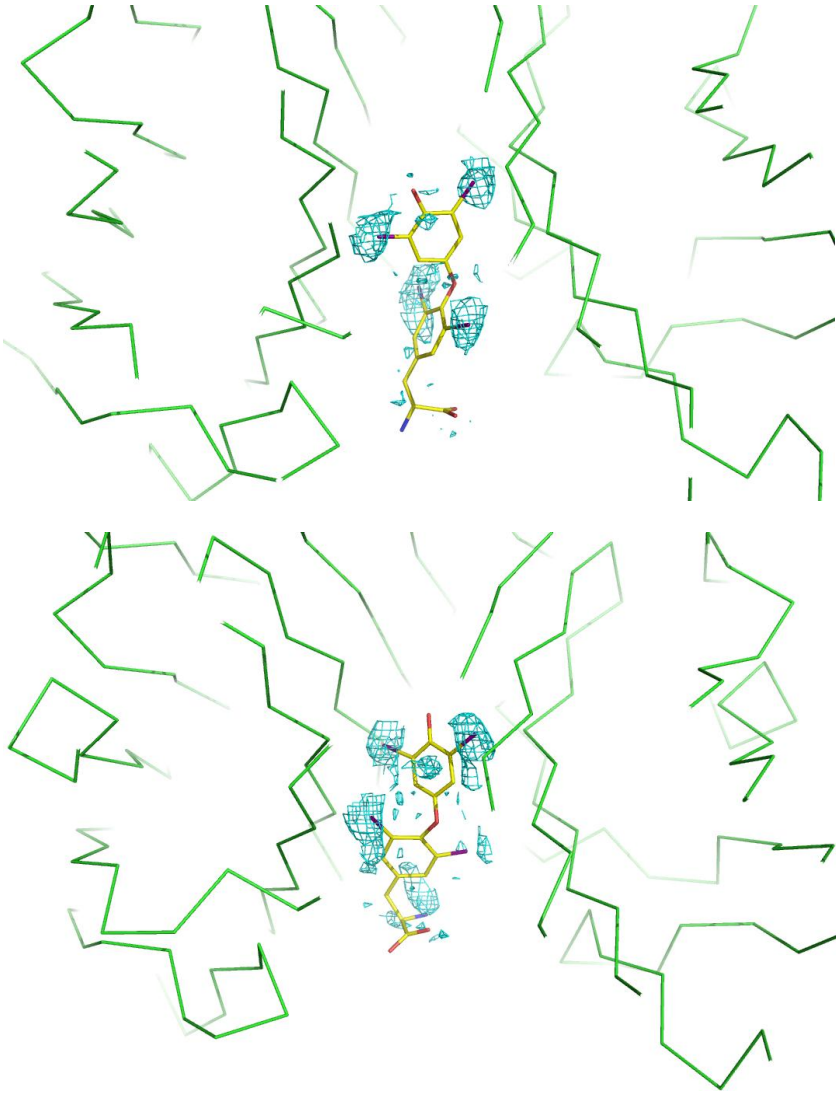

Figure 3.20: View of the anomalous difference map around the ligand with coefficients $2|\boldsymbol{F_o}| - |\boldsymbol{F_c}|$ and contoured at 2.0σ level (*on the top* in site B, *on the bottom* in site A), for TTR·T_4 1:1.

Until now, structures of complexes between TTR and different small molecules were obtained by co-crystallization with a single ligand: however, it is interesting to investigate what happens when transthyretin is crystallized in the presence of, at least, two different molecules. For this aim, TTR was crystallized in the presence of either resveratrol and T_4 and the structure of the relative complex TTR·T_4·resv was obtained. Inspection of the structure so obtained reveals that both the ligands are present in the two binding sites but with different occupancy values: it is worth noting that the crystallographic model reflects the average structure of all unit cells

during the experiment time. This means that if there are different subpopulations of TTR molecules (over the total ensemble) that are bound only to resv, or only to T_4, or both, or anything else, the final crystal structure reflects this heterogeneity. In other words, in the case (and this is it) that not all unit cells in the crystal are perfectly identical (in terms of chemical composition, relative orientation of the molecules *etc*.) the crystal structure is a spatial average, and not a snapshot of a single and arbitrarily subpopulation. Looking at the electron density map, and making use of the anomalous difference map, resveratrol was found mainly in site B whilst T_4 particularly in site A. In site A, all the four iodine atoms are visible up to 9σ: above this level of r.m.s.d., only half of the atoms remain visible (and disappear at 18σ, whereas in site B the anomalous signal vanish at 12σ).

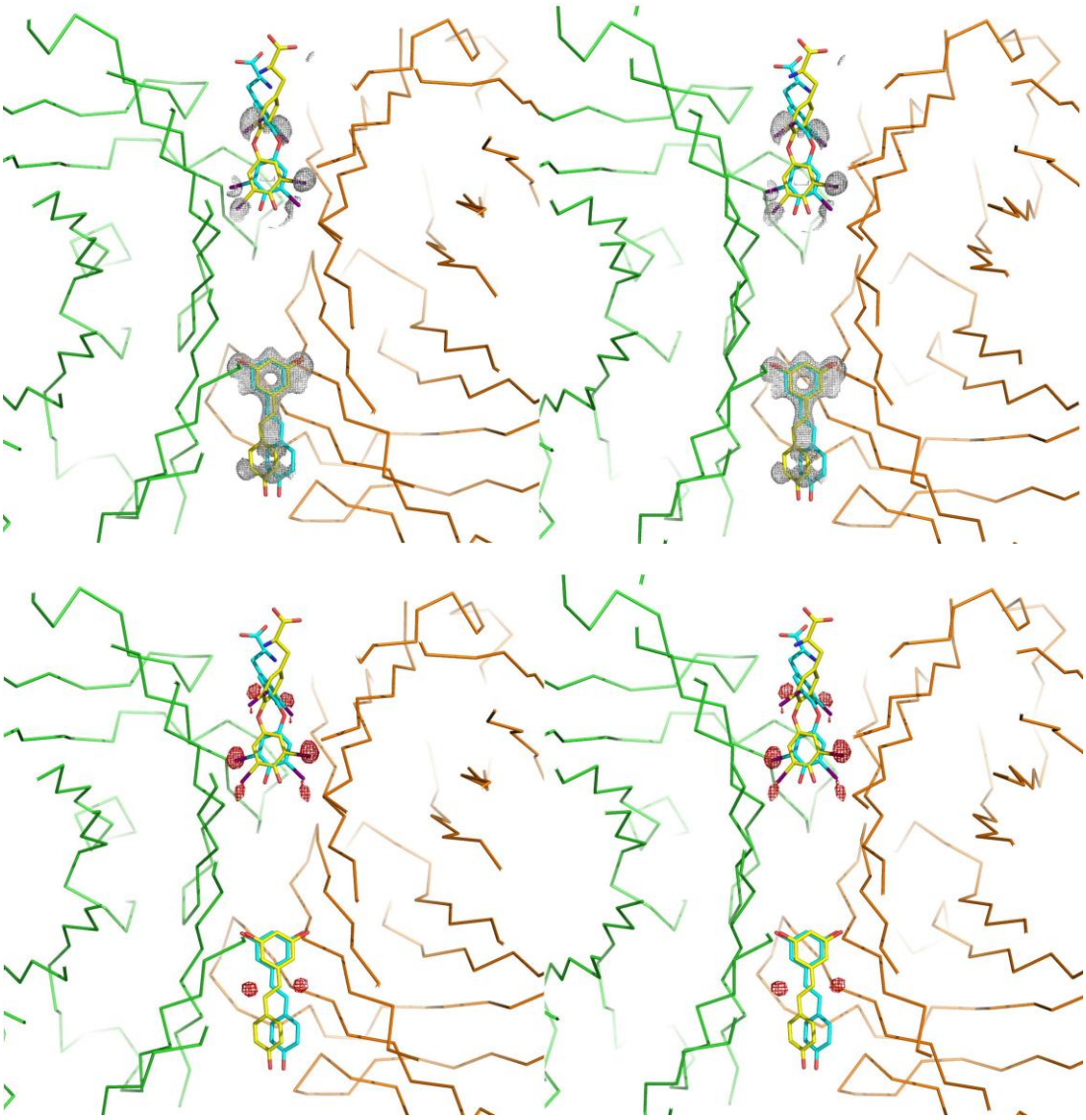

Figure 3.21: *On the top*, stereo view of the electron density maps (in grey) with coefficients $2|\boldsymbol{F_o}| - |\boldsymbol{F_c}|$ and contoured at 2.0σ level around resveratrol in site B and T_4 in site A. *On the bottom*, stereo view of the anomalous difference maps (in red) with coefficients $2|\boldsymbol{F_o}| - |\boldsymbol{F_c}|$ and contoured at 2.0σ level either in site A and B. Both figures are relative to the TTR·T_4·resv complex. Both representations depict TTR ligands as they are bound in the two symmetry-related binding modes.

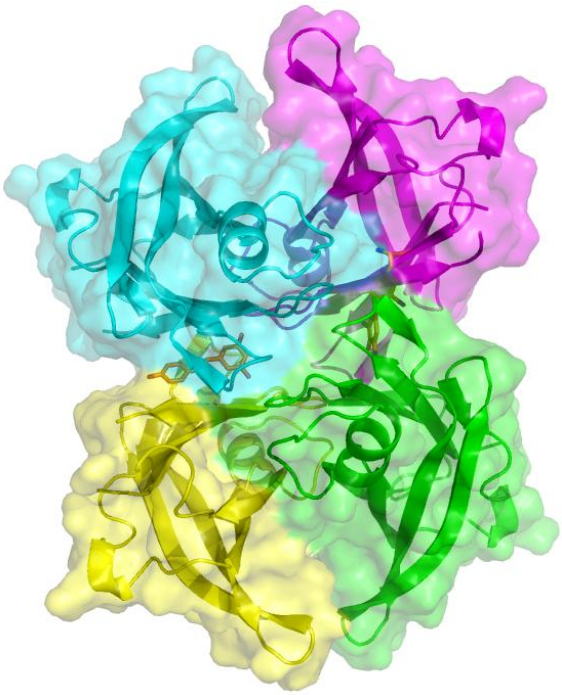

Figure 3.22: Overall view of the surface of the TTR·T_4·resv complex, along with cartoon representation of the monomers, with resveratrol and T_4 occupying the hormone binding sites.

3.1.5 Superposition Analysis

There are several cases in which the binding event of a molecule to a protein is responsible for large conformational changes in the overall structure of the macromolecule: in nature, for example, large conformational modifications of receptors caused by binding of substrates, inhibitors or activators determines the functional state of the receptor and is one of the way to induce signal transmission. This principle represents also the mechanisms of action of many drugs that, upon binding to the target receptor, are able to produce a biological and physiological response. With this premise, it is useful and interesting to evaluate the impact that TTR ligands have on the overall structure of the protein after they have entered the hormone binding site(s). The alpha-carbon superposition of the structure of wt-TTR with the structures of all the six complexes was carried out using the structural alignment tool implemented in MacPyMOL. It performs a sequence alignment followed by a structural superposition, and then carries out some cycles of refinement in order to reject structural outliers found during the fit. In the attempt to align the two structures it minimize the r.m.s.d. for the corresponding coordinates of the structurally equivalent alpha carbons. This works very well for homologous structures, as for the alignment of TTR complexed and uncomplexed, and makes use only of the Cα positions for simplicity and efficiency. The output of a structural alignment are a superposition of the atomic coordinate sets and the minimal root mean square deviation between the structures, which indicates their difference.

Evaluation of the overall protein movements in the TTR tetramer induced by ligand binding showed no significant changes in the hormone binding sites, with an r.m.s.d. ranging from 0.103Å to 0.244Å (see Table 3.1). For instance, in Fig. 3.23 is reported the Cα superposition between wt-TTR and TTR·CHF5074 1:1 complex from which it can be observed the minimal differences in the Cα positions after ligand binding.

Table 3.1: R.m.s.d. values obtained from Cα superposition between wt-TTR and the six complexes.

TTR·ligand complex	r.m.s.d. (Å)
TTR·CHF5074 1:1	0.244
TTR·Tafamidis 1:1	0.206
TTR·resv 1:1	0.125
TTR·resv excess	0.115
TTR·T_4 1:1	0.108
TTR·T_4·resv	0.103

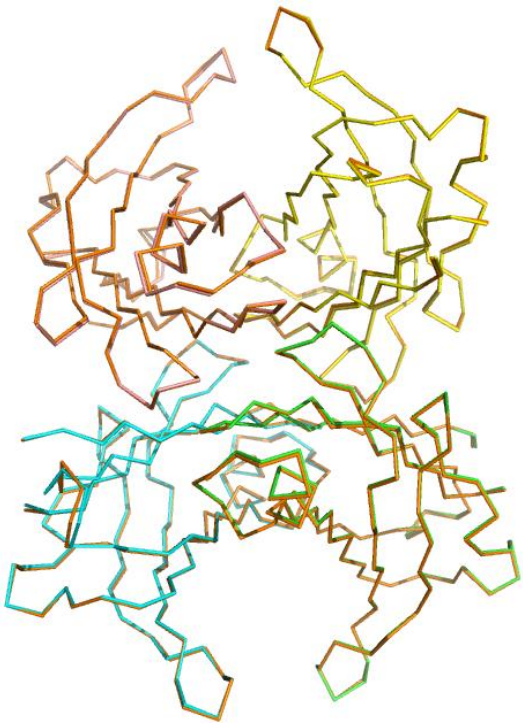

Figure 3.23: Superposition of Cα traces of wt-TTR (orange) and TTR·CHF5074 1:1 complex (coloured by monomers); for this case, r.m.s.d. is 0.244Å.

As anticipated in Paragraph 1.8.5, the same superposition analysis has proven to be a useful tool to assess the effectiveness of the therapeutic strategy based on the use of TTR stabilizers, particularly CHF5074 and Diflunisal [99]. The study focused on the amyloidogenic variant I84S TTR, that undergoes large conformational changes at moderately acidic pH. The superposition of wt-TTR·CHF5074 at neutral pH on the complex I84S TTR·CHF5074 (or with Diflunisal) at acidic pH gives r.m.s.d. of 0.34Å and 0.29Å, respectively. A similar r.m.s.d. was obtained after the superposition with the structure of wt-TTR, whereas the same comparison between I84S TTR and I84S TTR·CHF5074 at low pH provides values of 0.49 and 2.12Å for monomers A and B, respectively. The comparison between these structures showed that the structure of the complex I84S TTR·CHF5074 remains well preserved, even at acidic pH: CHF5074 stabilizes the amyloidogenic TTR mutant converting it to that typical of wt-TTR at neutral pH.

3.1.6 Conclusions

Medium-high resolution data sets were processed and analyzed, allowing to obtain good quality structural models of all the TTR·ligand complexes. All the complexes displayed the presence of the ligand(s) in one or both sites. In the complexes with 1:1 stoichiometry between TTR and CHF5074, Tafamidis and T_4, it was observed that ligands saturate both sites (A and B). In the case of TTR·resv 1:1 complex, resveratrol only occupies site B, whereas for the same complex obtained in the presence of an excess of the ligand even a partial occupancy of site A was noted. For the mixed complex, resveratrol shows a preference for site B and T_4 for site A. From these observations it is possible to state that, in some complexes, ligands exhibit a preference for one binding sites relative to the other. Localization and placement of ligands in the electron density maps was relatively straightforward, with the exception of the complexes of TTR with T_4. In these cases, the exploitation of the anomalous scattering allows the localization of iodine atoms and the ligand has been introduced in the structure based solely on this information. For the other molecules (resveratrol, Tafamidis and CHF5074), the ligand electron density inside the hormone binding sites was good enough from the first refinement cycles to allow the unambiguous positioning inside the cavity. All these molecules have a rigid moiety with some flexible groups: despite the poor (or missing) electron density for the latter, the stiffer aromatic portion shows in good details the contours of the various ligands.

In addition, as introduced before, ligand electron density maps for the complexes involved in the study seems to confirm the preference for resveratrol, T_4 and CHF5074 for one site over the other, *i.e.* the asymmetric ligand binding to transthyretin observed in recent articles. It is worth noting that the crystallization method adopted has a strong influence on the possibility to observe asymmetric ligand binding: relying on what appears recently in literature [69], molecular dynamics simulations suggest a certain degree of flexibility of TTR in solution. The plasticity of some chains causes continuous fluctuations of the protein so that the binding sites became alternatively larger and smaller (compared to the size observed in the crystal structure). In this situation, the first ligand molecule that approaches the protein will enter in the larger cavity and, if present in excess, a second molecule of ligand must fit to the remaining site, temporarily smaller: this explanation can justify the different affinity constants measured for both sites on TTR. However, the simulations provide a realistic picture only if they reflect the behaviour of TTR in solution and the question that arises is whether these differences in ligand preference are already present in solution or not. In the present work, crystal complexes were obtained by co-crystallization, *i.e.* the different complexes were formed in solution and, only when supersaturation was reached, they crystallize: this means that any influence of crystal packing on the formation of the complexes was avoided.

Instead, in the soaking method ligand molecules have to enter in the cavities on TTR when the protein is already embedded in the crystal lattice, locked by lattice forces. In this case, protein has less degrees of freedom and the two binding sites are more similar than in solution, in which TTR can undergoes fluctuations. Indeed, asymmetric ligand binding is not detectable if the complex is obtained by soaking in presence of a ligand excess. After these considerations, it can be only speculated that differences in the preference of some ligands for one site over the other were already present in solution, but further investigations are required in order to fully address this point.

Apart from the complex between TTR and Tafamidis, the co-crystals relative to all the other complexes diffracted to a maximum resolution that is better if compared with the structures so far reported in literature. In addition, the coordinate and the structure factors of some complexes will be deposited in the Protein Data Bank (PDB). In all cases, after an alpha-carbon superposition analysis between wt-TTR and the different complexes, it was established that ligand binding does not alter in any appreciable way the positions of the chains and, as a consequence, the structure of the tetramer. Although until now only TTR complexes with an excess of the ligand have been studied, in the present work also four complexes obtained with an equimolar amount of ligand have been taken into account. This was done in order to study the ligand affinity and the saturation of the T_4 binding sites in the presence of different stoichiometries between TTR and small molecules. Moreover, a novel mixed complex with two different ligands, thyroxine and resveratrol, was crystallized and its structure determined. Such mixed complexes may be promising candidates for an even more effective treatments of TTR amyloidosis: administering a cocktail of two ligands, each of which exhibits a preferential binding to one site relative to the other, it is possible to achieve the full saturation of the TTR tetramer, favouring its stabilization. Moreover, the therapeutic approach based on the use of small molecules in the treatment of TTR amyloidosis has a more general applicability. Indeed, the use of small molecules as drugs is currently under investigation in the treatment of other amyloidosis, as ALS (Amyotrophic Lateral Sclerosis) or in lysozyme amyloidosis.

X-ray crystallography can play a crucial role in this process, as it can provides more insights into the structure of the binding cavities in which the interaction between some key residues and the ligand takes place. Despite the possibility to capture intermediates or end points during protein misfolding, which is a dynamic process, crystal structures determined by X-rays provides static snapshots: as a consequence, biological, biochemical and biophysical studies are also valuable and necessary. With the convergence of all these results, in a not too distant future it will be possible to rationally designed more effective inhibitors for the TTR amyloid diseases.

Part II

HtrA protease

In the following Introduction to Part II, HtrA is described: the main features of prokaryotic and eukaryotic HtrA proteases are outlined, including their structure and biological roles, focusing the attention mainly on the implication for virulence and pathogenesis of *Campylobacter* strains.

2.1 HtrA Proteases

2.1.1 *Helicobacter pylori*

Helicobacter pylori (*Hp*) is a Gram negative bacterium specialized in the colonization of human stomach: it colonizes more than 50% of the human population, but most infected people are asymptomatic and only a minority (15-20%) develop some gastroduodenal pathologies (stomach and duodenal ulcers, adenocarcinomas and stomach lymphomas). To survive in the stomach, it has developed several strategies: firstly, *Hp* synthesizes different ureases to buffer the acidic pH typical of this environment [113]. To do this, *Hp* used several genes, through a seven-gene cluster composed of genes A, B, I, E, F, G, H, corresponding to the respective ureases. These enzymes utilize urea (physiologically present in the stomach) as substrate to produce, by hydrolysis, ammonia and CO_2: in this way, *Hp* can neutralize the acidic pH, even if it is not an acidophile. Urease was the first *Hp* enzyme crystallized, in addition to being the first enzyme shown to contain nickel [114]. It is a dodecamer of six UreA and six UreB subunits and it is a virulence factor with a prominent role in the pathogenesis of *Hp*-associated diseases: *Hp* urease might cause damage to the host cells through the production of cytotoxic ammonia [115] and it was shown that urease defective *Hp* mutants cannot colonize the stomach [116]. In order to survive in the stomach, however, *Hp* elaborates other mechanisms, for example the use of flagella: with these appendages, *Hp* travels across the viscous mucus film and adhere to the host cells. As source of locomotion, flagella are responsible for *Hp* motility and it has been demonstrated that the degree of motility of *Hp* strains correlates with the degree of infectivity [117] [118]. Also its typical helicoidal shape allows *Hp* to cross the thick layer of mucus [113]. Virulence factors other than ureases exist in *Hp*: these molecules contribute to the pathogenicity and the main are: adhesins (three Hop proteins in particular) and outer membrane proteins, VacA and CagA [119] [120]. Many bacterial factors mediate the adhesion of *Hp* to the gastric epithelium (also many polysaccharides), such as the proteins BabA (HopS), OipA (HopH) and SabA (HopP): cell adhesion is an essential requirement in *Hp* colonization and only after this step the pathogen can injects into the host cells different toxins as CagA (for "Cytotoxin-associated gene A"). CagA is a highly immunogenic protein encoded by the *CagA* gene, that is present in approximately 50% to 70% of *Hp* strains and is a marker for the presence of a 40kb genomic Pathogenicity Islands (PAI) that encodes between 27 and 31 proteins. Strains carrying the cagPAI are referred to as $CagA^+$, as they are commonly identified in patients by their potential to induce significant antibody against CagA [120]. In *Hp*, the Cag Type IV secretion apparatus, encoded by cagPAI and composed of a pilus-like structure, can mediate the injection of CagA into the target cells: the translocated CagA proteins will interfere with the physiological signal transduction and cause pathological cellular response (increased cell proliferation, motility, apoptosis and morphological change). In fact, once in the cell, CagA is phosphorylated at Tyr residues in EPIYA motifs by Src family kinases and then interacts with a range of host signalling molecules such as the tyrosine phosphatase

SHP-2, which results in morphological changes in the epithelial cells [121] [122]. The cagPAI also affects the immune response and the interaction between the type IV secretion apparatus and the host cell, resulting in the induction of proinflammatory cytokines. CagA has been associated with severe gastritis and thus with a higher risk for ulcer disease, atrophic gastritis and gastric cancer [123]. After CagA, VacA ("Vacuolating cytotoxin A") is the second most extensively studied *Hp* virulence factor (approximately 50% of all *Hp* strains secrete VacA) with high immunogenicity and with an important role in the pathogenesis of both peptic ulceration and gastric cancer. It induces massive vacuolization in epithelial cells *in vitro* [124] [125]; as other bacterial toxins, it is recognized as a multifunctional protein that can have pleiotropic effects on mammalian cells and tissues. Indeed, it is involved in a series of effects including membrane channel formation, induction of apoptosis, immune modulation and increased transcellular permeability [126].

2.1.2 *Campylobacter jejuni*

As *Hp*, *Campylobacter jejuni* (*Cj*) is a microaerophilic, Gram negative, flagellate bacterium, with a curved or spiral shape [127]. Gram negative bacteria of the genus *Campylobacter* and of related genera, *Cj* in particular, frequently colonize the gastrointestinal tracts of mammals, including humans, and birds [128]. Typical reservoir includes not only wild birds but also insects, poultry (whose intestines are easily colonized with *Cj*), cattle, farm workers, drinking water and many food of animal origin such as milk [129]. *Cj* has been recognized as an important human pathogen, usually causing diarrhoea, fever and abdominal cramps, but other symptoms may occur [130]. Although the cornerstone treatment for *Cj* enteritis consist of maintenance of hydration and electrolyte balance without antibiotics, there are specific clinical circumstances in which antibiotics should be used and local complications can arise [131]. The most important post-infections complication of *Cj* is the Guillain-Barré syndrome (GBS) [132] [133]. Outbreak have been associated with drinking raw milk, contaminated water, consumption of undercooked poultry and mishandling of raw poultry, which constitute major risk factors for human campylobacteriosis [129]. Infection with *Cj* occurs more frequently than do infections caused by *Salmonella* species, *Shigella* species and *E. coli* and, although 14 species of *Campylobacter* have been identified, more than 99% of reported infections with *Campylobacter* in the United States are with *Cj* [131]. During the years, different determinants of *Cj* pathogenicity have been identified, in particular: chemotaxis, motility (*Campylobacter* species are motile by means of unipolar or bipolar flagellae), adhesion, cellular invasion, iron acquisition, epithelial translocation, toxins and lipopolysaccharide (LPS), the latter being a virulence determinant in many species of Gram negative bacteria. Chemotaxis, mobility and flagella are required for attachment and colonization of the gut epithelium. Once colonization occurs, iron acquisition, host cell invasion, toxin production, inflammation and active secretion come into play [127] [129].

However, *Cj* lacks the virulence associated secretion systems, such as type III and type IV secretion systems, possessed by other enteric pathogen: it was demonstrated that, as many bacterial pathogens, *Cj* utilizes outer membrane vesicles (OMVs) for delivery of virulence factors into host cells [134]. Although OMVs from *Cj* were identified nearly 30 years ago, only recently their role in the pathogenesis become clear with the demonstration that the Cytolethal Distending Toxin (CDT) was delivered within OMVs in *Cj* [135]. To understand and clarify the behaviour of *Cj*, in 2000 for the first time the complete genome of *Cj* NCTC11168 has been sequenced [136]:

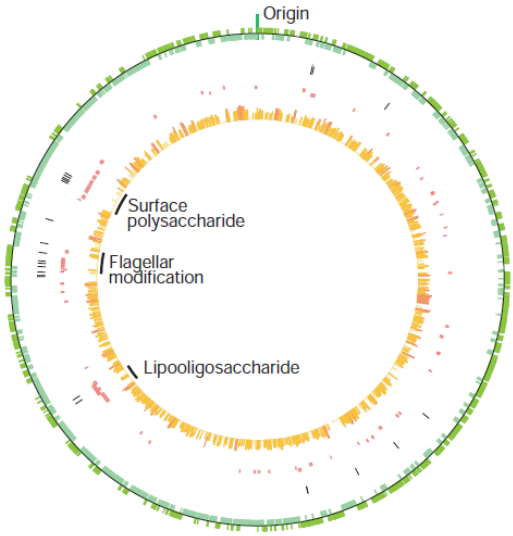

Figure 2.1: Circular representation of the *Cj* genome. Circles in dark and pale green represent coding sequences transcribed in the clockwise and anticlockwise direction, respectively. The black circle shows the positions of hypervariable sequences, while circles in dark (clockwise) and pale red (anticlockwise) show genes involved in the production of surface structures. In orange, the histogram that shows the similarity of each gene to its *Hp* orthologue, where present (height of the bar and intensity of the colours are proportional to the degree of similarity) ([136]).

Cj has a circular chromosome of 1,641,481 bp which is predicted to encode 1654 proteins (referred as coding sequences, CDSs) and 54 stable RNA species: it is characterized by an average gene length of 948bp and because 94.3% of the genome codes for proteins, this is the densest bacterial genome sequenced to date. Functional information could be deduced for 77.8% of the total 1654 CDSs, whereas the remaining matched genes had no database match, revealing an unusually low number of unknowns. Some surprising features emerging from the study are: the almost complete lack of repetitive DNA sequences, the absence of any functional inserted sequence elements, transposons, retrons or prophages in the genome and a little organization of genes into operons or clusters. The most striking finding was the presence of hypervariable sequences, because these tracts might be important in the survival strategy of *Cj*.

Hypervariable sequences were found in genes responsible for lipooligosaccharide (LOS) synthesis, extracellular polysaccharide (EP) synthesis and flagellar modification. Another strangeness is that *Cj* has 3 sets of genes involved in sialic acid biosynthesis: this is an uncommon component of bacterial surface structures and it may be important in GBS. On the other hand, expected results include finding of some toxin genes (such as CDT gene), several type 4 pilus related genes involved in chemotaxis and that the *Cj* genome encodes five major iron acquisition systems. Although *Hp* and *Cj* share many biological properties, there are genes present in *Hp* but absent in *Cj* as urease operon, nickel transport system, vacuolating toxin and the cagPAI, and these features are expected since *Hp* lives in the stomach, a unique niche. Following the same reasoning, that is the presence of *Cj* in a more diverse range of ecological niche than *Hp*, it is not surprising the presence of a broader repertoire of regulatory systems in *Cj* (mainly of the two component regulatory family).

2.1.3 HtrA proteases

The accumulation of damaged proteins (fragmented, misfolded or mislocalized) represents a serious hazard to the cell because it can result in the accumulation/aggregation of proteins, leading to amyloid diseases or, in general, hampering important biological processes. To reduce the amount of unfolded or aggregated proteins, cells have developed a system of proteases and chaperones with the aim to remove hazard polypeptides and to assist the correct folding and assembly of proteins, respectively. Proteases not only are implicated in housecleaning functions by degrading damaged proteins but, particularly in higher organisms, play important roles being involved in cell growth, apoptosis and others [137] [138]. This class of proteins are classified in the MEROPS database (http://merops.sanger.ac.uk/), which include also their substrates and inhibitors. Among these, HtrA is a protein of increasing interest since it is involved in numerous and different physiological processes: it was firstly identified in *E. coli* by Lipinska in 1988 while he was working on *htrA* null mutants. He observed that all mutants do not grow at high temperatures, since the name: **H**igh **t**emperature **r**equirement **A** [139], or in consideration of the null mutant phenotypes it was also referred to as DegP for: **Deg**radation of **p**eriplasmic **p**roteins [140]. However, DegP is not synonymous of HtrA because this acronym indicates only one of the three HtrA in *E. coli*. HtrA represents the first well-studied protein quality control factor that acts in an ATP-indipendent manner; it belongs to the Ser proteases family but it displays both functions, as protease and chaperone. It is widely conserved in single and multicellular organisms [141]: hundreds of different HtrA have been detected in various sequenced genomes, comprising those of microorganisms (both Gram negative and Gram positive bacteria), fungi, plants, frogs, birds, fish and mammals, including *Homo sapiens*.

In addition, in many cases the same organism displays more than one HtrA [138] [142] [143] with different cellular localization and functions: a proof of this comes from the consideration that *E. coli*, cyanobacteria, *Arabidopsis thaliana* and humans have, respectively, three, two to five, sixteen and four HtrAs.

2.1.3.1 Prokaryotic HtrAs

With regard to prokaryotic HtrAs, research has been focused on HtrA homologues from *E. coli*: here, the three family members DegP, DegS and DegQ have been identified as actors in the protein quality control in the periplasmatic space [138]. DegS is a purely regulatory protease and DegQ is highly homologue to DegP and might therefore perform similar functions [144]. Mature DegP from *E. coli* has 448 residues of which His105, Asp135 and Ser210 form the catalytic triad [138]; it combines proteolytic and chaperone activities and, whereas in the resting state it is an hexamer, higher oligomeric structures of 12-, 15-, 18- and 24-mers are observed following activation [145] [146] [147] [148]. Given that the basic building block for all HtrAs is the homotrimer, the transition to protease-active oligomeric forms represents a simple and effective mechanism for controlling access to the proteolytic sites of DegP (and not only). The switching from an inactive, low molecular mass oligomer into a substrate degrading, higher order oligomer allows for precise regulation of protease activity [137]. Evidences for the same mechanism in other HtrA have been suggested, but in certain cases a different regulation of the proteolytic activity was shown [149] [150]. Despite it has both activities, a distinctive properties of DegP is the temperature-dependent switch from chaperone to protease function: the proteolytic activity is negligible below 20°C, but over 30°C it rapidly increases in a non linear fashion. The chaperone function dominates at low temperatures, while the proteolytic activity manifests itself at elevated temperatures: this behaviour, from a protein-folding to a protein-digesting machine, is plausible since at higher temperatures proteins might be too badly damaged to be refolded and have to be removed. At low temperatures, protein repair appears to be more efficient [151]. From the above statements, it is straightforward to infer that DegP is an heat shock protein, that is a protein whose expression is increased in response to exposure to stressful conditions such as temperature, UV light and increased oxidative or osmotic stress: in other words, they counteract protein folding stress. However, unlike other heat shock proteases, the DegP activity is largely independent of cofactors as ATP, pH, reducing agents and divalent cations [138]. It is well established that prokaryotic HtrAs are involved in the heat shock response and contribute to tolerance of harsh conditions [152] [153] [154] [155] [156], but they contribute also to bacterial pathogenicity, *e.g.* supporting biofilm formation [157], secretion of virulence factors [158] and remodelling of the cell-cell contacts within the host organism [159]. In any case, other bacterial proteases also contribute to pathogenesis, revealing a more general trend [160] [161].

It has been demonstrated that HtrAs contribute to virulence in a number of bacterial species [162] [163] [164] [165] [166] [167] [168] [169] [170] [171]. Another example comes from *Hp*, whose HtrA is secreted into the medium to cleave E-cadherin that represents a mammalian cell surface protein that has essential function in cell adhesion. In agreement with recent results [159], this reveals how *Hp* uses HtrA as a bacterial proteases in a coordinate manner with other injected effector proteins, such as CagA. As a consequence of the cleavage, the epithelial barrier is destroyed allowing the persistent colonization, nutrition and pathogenesis. Probably, this finding might unveil a general bacterial strategy and HtrA could therefore be a promising candidate for therapeutic intervention.

2.1.3.2 Eukaryotic HtrAs

Although eukaryotic HtrAs are less well characterized than prokaryotic ones, in the last few years crystal structures of HtrA1 and HtrA2 (also termed Omi) from humans and Deg1 from *A. thaliana* have been solved. Eukaryotic HtrAs displays additional functions to those seen until now for their prokaryotic counterparts because they are also involved in photosynthesis, cell proliferation, apoptosis, cell development and ageing processes; in addition, they contribute to a number of severe medical conditions such as arthritis, cancer, Parkinson and Alzheimer's disease [172]. For example, in *A. thaliana*, five of the 16 HtrAs present (Deg1, Deg2, Deg5, Deg7 and Deg8), are located in chloroplasts [142] [173]: among them, the best characterized is Deg1 that performs the typical dual function, acting as a chaperone in the assembly of PSII and as protease in the degradation of damaged reaction centres [142] [174] [175] [176]. Studies carried out on Deg1 in plants converge towards a model for its function *in vivo*, according to which Deg1 adopts a monomeric resting state in the dark that turns into a proteolitycally active hexamer upon illumination. This is because, in the absence of light, the need for degradation of photosystem components is minimal but, in the presence of strong radiation, the pH of the thylakoid lumen drops and there is an urgent need to remove photosystem proteins damaged by oxidation. So, Deg1 is specifically activated under light-stress conditions and the transition to an higher oligomeric state allows to carry out its function [137] [172]. Despite the important roles that HtrAs cover in plants, human HtrAs (hHtrA) receive most of the attention owing to their involvement in key processes: for example, hHtrA1, the best characterized family members together with hHtrA2 and ubiquitously expressed in all tissues, is implicated in cell proliferation, tumour suppression, processing of numerous secreted proteins, arthritis, cancer, familial ischemic cerebral small-vessel disease, age-related macular degeneration and Alzheimer's disease [177] [178] [179] [180] [181]. In more detail, the loss of HtrA1 correlates with decreased sensitivity to anticancer drugs and increased cell migration [178] [182] [183]; in addition, over-expression of HtrA1 inhibited proliferation *in vitro* and tumour growth *in vivo* [184] suggesting that, in combination with the precedent observations, HtrA1 might function as tumour suppressor.

Another human HtrA, hHtrA2/Omi, promotes cell death, might function as a protein quality control factor in mitochondria similar to prokaryotic HtrAs in the periplasmic space [172] and appears to be implicated in neurodegenerative diseases [185].

2.1.3.3 Structural aspects of HtrA proteins

As seen before, eukaryotic HtrAs display additional set of functions: despite this, HtrA proteins share a common modular domain architecture based on a catalytic protease domain and one or two C-terminal PDZ domains, overall arranged in the same basic oligomerization mode, that is a funnel-shape trimer. The Ser protease domain is structurally well conserved in all HtrAs (average r.m.s.d. ~ 0.6Å) [186] and it displays the canonical trypsin fold (two β-barrel lobes with additional α-helices attached); it forms the central core of the trimer and the catalytic portion is constituted by the triad Ser-His-Asp.

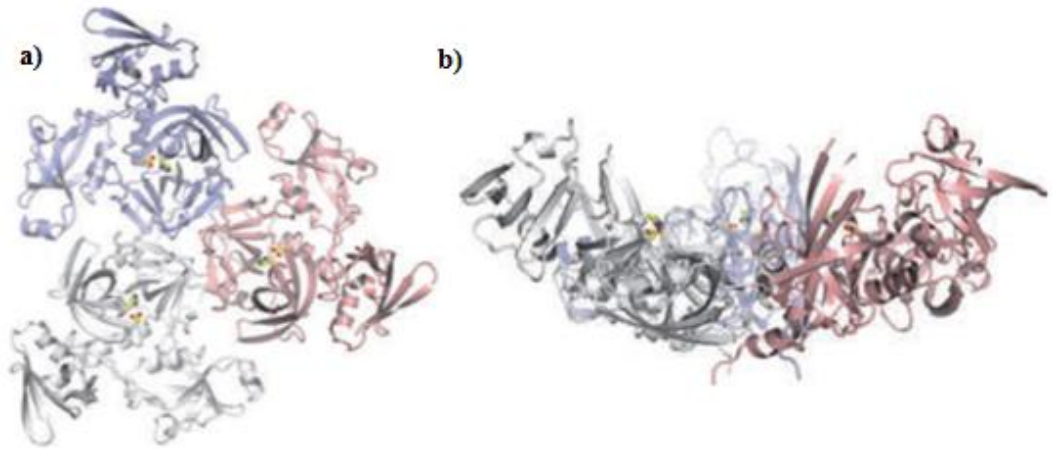

Figure 2.2: ***a)*** Top view of the trimeric building block of HtrA proteases in which the protease domains are located in the centre and the PDZ domains protrude outwards and ***b)*** side view of the same trimer ([137]).

In HtrA proteins, interaction between three protease domains are responsible for the trimer formation; linked to the central core, PDZ domains extend themselves outwards [137] [172]. PDZ domains are highly abundant being present in all kingdoms of life, are composed of 80-100 amino acids and represent one of the most common protein-protein interaction domains in humans. In truth, it was observed that they are scarce in unicellular organisms and this has led to the hypothesis that PDZ domains have evolved to facilitate intercellular signalling in multicellular organisms [187]. The canonical structure consists of five to six β-strands (β1-β6) and two α-helices (α1-α2) [188]. The observed dissociation constants are consistent with their role as malleable protein-protein interaction modules, which can bind to and dissociate from their target ligands on a fast time scale [189]. They often recognize short residues motifs (preferentially three to four residues) at the C-termini of target proteins [137] [190].

Compared to the protease domain, PDZ domains are structurally less conserved (average r.m.s.d. ~ 1.2Å), consistent with the variety of roles that they play in different HtrA family members [172].

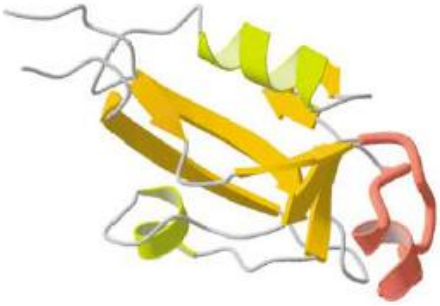

Figure 2.3: PDZ domain: β-strands are coloured orange, α-helices in yellow and the extra segment in red ([138]).

Current research on HtrA proteins, however, could have important implications, for example in protein production: co-overexpression of the protein of interest with an HtrA with dual function can improve the yield of the recombinant product owing to the chaperone activity (that could assist the proper correct folding) and to the protease activity (important in removing misfolded proteins). Another beneficial effect can be derived from the temperature-dependent switch shown by DegP. Furthermore, DegP and DegS could become the target for antimicrobials (thanks to the Human Genome Project, about 14% of human proteases known nowadays are under investigation as potential drug targets) [138] [191]. Also, hHtrA1 and hHtrA2 could be explored as drug targets in osteoarthritis, cancer and aging [138].

2.1.3.4 *Cj* and roles of its HtrA

As all the other Gram-negative bacteria, also cells of *Cj* are composed of a periplasmic space between the Outer and the Inner Membrane. Since the former allows free diffusion of small molecules, periplasmic proteins are more highly exposed to fluctuating and stressful environmental conditions than cytoplasmatic proteins, hence the need to make use of chaperons and proteases. This is exactly what happens in *Cj*, which depends on periplasmic HtrA (and other proteins) to counteract temperature and pH fluctuations, osmotic stress and elevated O_2 tensions during its transmission to human host. In *Cj*, HtrA has at least two functions: it confers tolerance to environmental stress and it is implicated in its virulence. With regard to the first function, initial studies [192] have shown that the tolerance to stressful conditions depends on HtrA, without wondering if this behaviour might depend more on a function that on the other. Successively, several studies have demonstrated that resistance relies mainly on the chaperone activity.

Using a *Cj* mutant lacking only the protease activity of HtrA, it was shown that HtrA chaperone activity is sufficient for growth at high temperatures or under oxidative stress, whereas the HtrA protease activity is essential only under conditions close to the growth limit of *Cj* [193]. In regard to the second function, HtrA displays a role in the virulence of *Cj* through, at least, three mechanisms.

In primis, HtrA of *Cj* is required for efficient binding to the host epithelial cells. By comparing an *htrA* mutant lacking protease activity, but retaining chaperone activity, with a Δ*htrA* mutant and the wt strain, it was seen that binding to epithelial cells was facilitated mainly by HtrA chaperone activity that may be involved in folding of outer membrane adhesins [194]. Other studies, using tissue cultures of human epithelial cells, found that the *htrA* mutant adhered to and invaded human epithelial cells with a decreased frequency compared to the wt strain [192]. Secondly, as seen also for *Hp*, *E. coli* and *Shigella*, the HtrA of *Cj* cleaves E-cadherin on host cells. It was established that HtrA mediated E-cadherin cleavage is a prevalent novel pathogenic mechanism exploited by multiple Gram negative bacteria representing an attractive potential target for therapeutic intervention to tackle bacterial infections [195]. HtrA deletion in *Cj* led to severe defects not only in E-cadherin cleavage but also in other mechanisms such as cellular transmigration (*i.e.* the migration of cells across a barrier, for example a cell layer), representing the third possible mechanism of virulence [196]. However, despite the progress that has been made in recent years in light of potential important applications, there are still open questions concerning the basic aspects of the molecular biology and pathogenicity of *Cj*, including roles of its HtrA [197].

2.2 MATERIALS & METHODS

This section describes the HtrA heterologous over-expression and the purification procedure of the recombinant protein.

2.2.1 *Cj*-HtrA Plasmid Expression Vector Construction

The *Cj*-HtrA plasmid expression vector was prepared in the Laboratory of Microbiology, Department of Biology, directed by Prof. Dr. Steffen Backert at the Friedrich-Alexander Universität Erlangen-Nürnberg, Germany, according to the procedure described by Boehm *et al*. [196]. After amplification of the gene from genomic DNA excluding predicted signal peptides, the *Cj*-HtrA aa 17-472 (GenBank: EAQ72866.1) sequence was cloned: PCR fragments flanked by restriction sites for BamHI/XmaI were cloned into the pGEX-6P-1 (GE Healthcare) vector multi-cloning area to generate the GST (Glutathione-S-Transferase)-fusion protein. The signal peptide from aa 1-16 was cut-off to avoid problems. The vector also carries a recognition sequence located immediately upstream from the multi-cloning site that represents the PreScission Protease site for the removal, if desired, of the GST-tag.

MKKIFLSLSLASALFAASINFNESTATANRVNPAAGNAVLSYHDSIKDAKKSVVNISTSKTI
TRANRPSPLDDFFNDPYFKQFFDFDFPQRKGKNDKEVVSSLGSGVIISKDGYIVTNNHVVDD
ADTITVNLPGSDIEYKAKLIGKDPKTDLAVIKIEANNLSAITFTNSDDLMEGDVVFALGNPF
GVGFSVTSGIISALNKDNIGLNQYENFIQTDASINPGNSGGALVDSRGYLVGINSAILSRGG
GNNGIGFAIPSNMVKDIAKKLIEKGKIDRGFLGVTILALQGDTKKAYKNQEGALITDVQKGS
SADEAGLKRGDLVTKVNNKVIKSPIDLKNYIGTLEIGQKISLSYERDGENKQASFILKGEKE
NPKGVQSDLIDGLSLRNLDPRLKDRLQIPKDVNGVLVDSVKEKSKGKNSGFQEGDIIIGVGQ
SEIKNLKDLEQALKQVNKKEFTKVWVYRNGFATLLVLK

Figure 2.4: Amino acid sequence of the HtrA from *Cj* 81-176 (GenBank: EAQ72866.1), composed of 472aa (51kDa); signal peptide sequence is highlighted in grey.

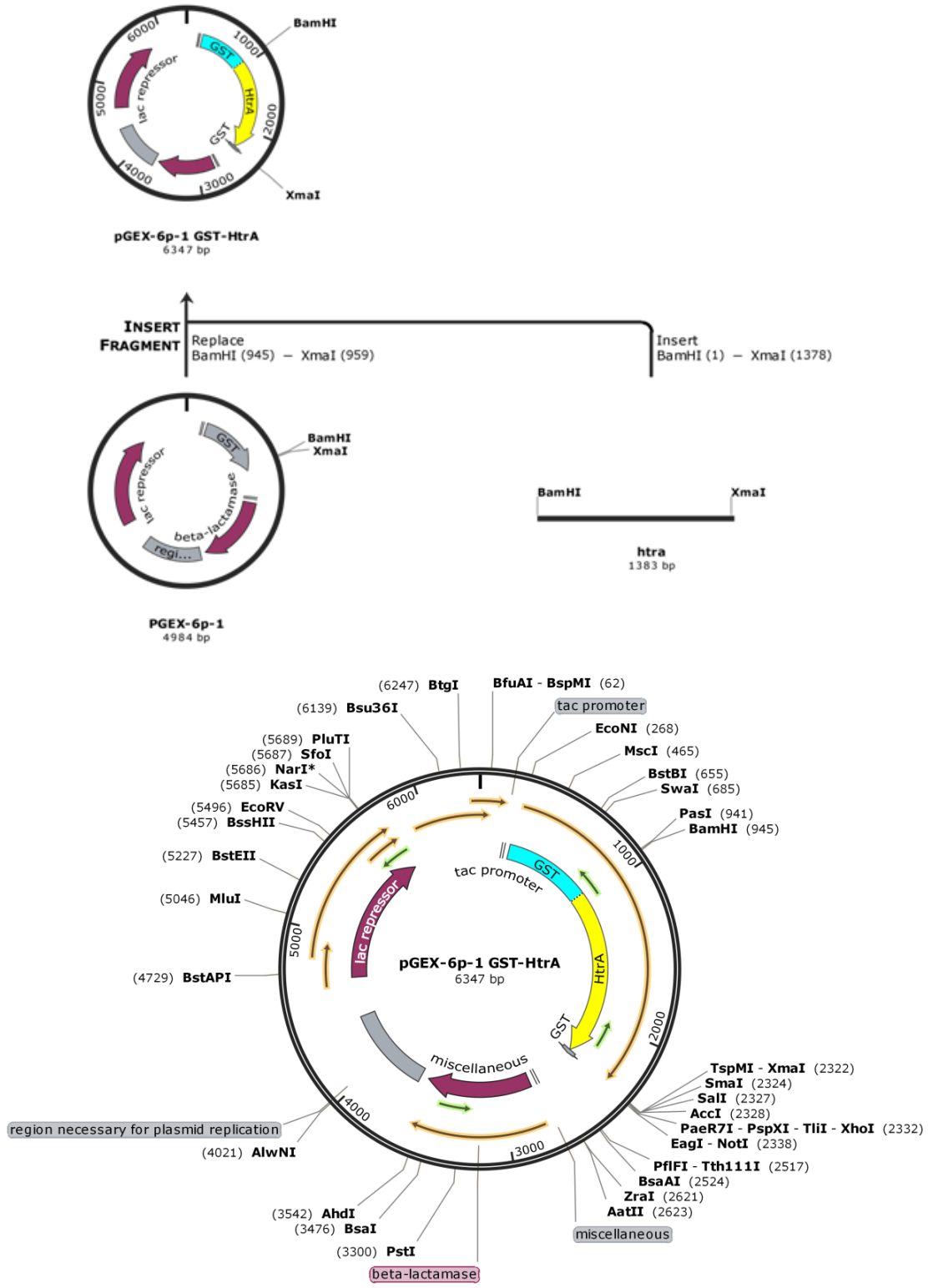

Figure 2.5: *At the top* of the figure, schematic representation of the cloning of the gene of interest (*htra* gene) into the MCS of the pGEX-6P-1 plasmid vector, between restriction sites BamHI and XmaI. *At the bottom*, representation of the final gene construct (6347bp) with the *htra* gene and other main components (GST gene, tac promoter, the lac operon system and the restriction sites).

2.2.2 HtrA Over-expression and Standard Purification

2.2.2.1 Purification Principles

The standard purification protocol adopted provides the use of a Glutathione Sepharose medium: indeed, GST-tagged proteins are easily purified from bacterial lysates by affinity chromatography using glutathione immobilized to a matrix such as Sepharose (see Fig. 2.6). When applied to the affinity medium at low flow rate, the tagged proteins bind to the ligand, and impurities are removed by washing with binding buffer. Tagged proteins are then eluted from the Glutathione Sepharose under mild, non-denaturing conditions using reduced glutathione, to preserve both protein structure and function. Eventually, if separation of the cloned protein from the GST-tag is desired, the tagged protein can be treated with an appropriate site-specific protease (Paragraphs 2.2.2.3 and 2.2.2.4).

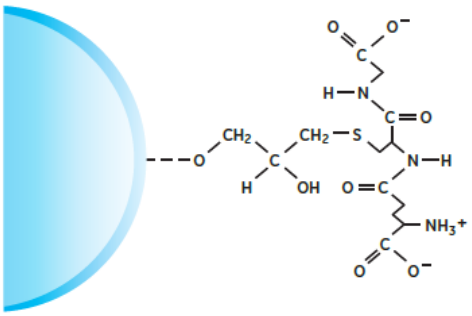

Figure 2.6: Terminal structure of Glutathion Sepharose. Glutathione is specifically and stably coupled to Sepharose by reaction of the SH-group with oxirane groups obtained by epoxy-activation of the Sepharose matrix. The structure of Glutathione is complementary to the binding site of Glutathione-S-transferase.

2.2.2.2 HtrA over-expression and purification

E.coli cells transformation protocol used provides the addition of 1µL of the plasmid vector into 20-50µL of competent cells in a microcentrifuge tube, gently mixing by flicking the bottom of the tube. Competent cells were thaw on ice and, after the addition of the plasmid, were still maintained at 4°C for 30 min. Subsequently, the cells were placed in a water bath at 42°C for 45s allowing the heat shock happening. At the end, 800µL of LB or TB were added and the mixture was incubated for 1h at 37°C, under mild shaking. Cells were plated onto LB agar containing the appropriate antibiotic and incubated at 37°C overnight to allow the growth.

A small quantities of that cells harbouring pGEX-6P-1·*HtrA* were dispersed (pre-inoculated) in 50mL of LB or TB supplemented with the appropriate antibiotic (Ampicillin to a final concentration of 50µg/mL; Chloramphenicol to a final concentration of 34µg/mL) and allowed to grow overnight at 37°C under mild shaking.

Subsequently, this aliquot was added to 1L of LB or TB (1:20 ratio), with the proper antibiotic and place, under agitation, in the appropriate conditions of temperature and time (depending on the specific trial) until 0.6 OD_{600}. A small volume (1mL) has been kept aside, treated with SB[1] 1X at 100°C for 10 min (hereinafter referred to as "uninduced" sample). Protein expression was induced by adding isopropyl-β-D-1-thiogalactopyranoside (IPTG) 1M, to a final concentration of 0.5mM, and incubating the bacterial cells at the appropriate conditions of temperature and time. At the end, OD_{600} was measured and, as before, 1mL of the culture was treated with SB 1X (hererinafter referred to as the "induced" sample) and the remaining cells were harvested by centrifugation at 6000rpm for 15 min at 4°C and suspended in 10mL of PBS 1X with PMSF 100mM at a final concentration of 1mM and in the presence of the 3 protease inhibitors E64, Aprotinin and Leupeptin 1000X, to 1X as final concentration. Resuspended cells were lysate with the Constant Cell Disruption System (Constant Systems Ltd; pressure set to 1.35kbar): after centrifugation at 15000rpm for 30 min at 4°C, 20µL of the supernatant were treated with SB 2X and a small quantity of the pellet was treated with SB 5X. Then, the set up for the affinity column, necessary to subsequent purification of the protein, was prepared equilibrating 500µL of Glutathione Sepharose 4B with PBS 1X. The soluble fraction was loaded onto the resin and incubated by rotation at 4°C overnight. Then, for the second time, the suspension was loaded onto the affinity column, the Flow-Through (FT) was collected and the subsequent solutions were added, in order: PBS 1X and Tris 50mM/Tween 0.1% pH 7.5. A Tris 50mM/GSH 10mM pH 8.0 freshly prepared solution was added at the end, in order to recover the protein from the resin: to do this, three aliquot of 1mL were added (the first two aliquot were eluted after a 30 min incubation at ambient temperature, whereas the third aliquot was immediately eluted from the column). All the fractions eluted from the column were treated with SB 2X and all the samples were submitted to SDS-PAGE (Gradient PreCast Gel 4-12%, Mes 1X, ΔV = 200V, current intensity: variable, P = 50W), after which the polyacrylamide gel was washed with water, stained with Coomassie Blue and destained using acetic acid 10%. The fractions containing the protein were combined and concentrated through centrifugation over a nitrocellulose membrane (Millipore Amicon Ultra; cut-off: 10kDa). The concentrated fraction was then analysed by Analytical Gel Filtration, FPLC, with a column for Size-Exclusion Chromatography (Superdex™ 200 Increase 10/300GL, GE Healthcare) equilibrated with Tris 50mM pH 7.5 as elution buffer. Molecular weights of the proteins or fragments associated with the different peaks were determined with the use of a calibration curve obtained from commercial protein standards.

During the purification steps, all the aliquots (protein, FT, washes with buffer) were constantly maintained at 4°C because of the suspected low stability of the HtrA protease (as common for most protein belonging to this class).

[1] A mixture of bromophenol blue, glycerol, 2-mercaptoethanol and SDS: together with the heat treatment, it favours the complete denaturation of all proteins in the sample necessary for the subsequent SDS-PAGE analysis.

2.2.2.3 HtrA Purification removing GST-tag with PreScission Protease: Principles of GST-tag removal

Principles underlying the method, as its practical aspects, can be found in the useful GE Healthcare Handbook "Recombinant Protein Purification" and the experimental work done is based on this exhaustive reference. In addition to the purification of the HtrA protease with the GST-tag, purification of the protein without the fusion tag was also performed, using the PreScission Protease whose recognition sequence has been inserted in the pGEX vector for this purpose. For the removal of the GST moiety (a naturally occurring protein with MW of 26kDa), the tagged protein can be digested with PreScission Protease (or another appropriate site specific protease) while bound to Glutathione Sepharose or, alternatively, after elution. Cleavage of GST-tagged protein bound to the column/bulk medium eliminates the extra steps of separating the released protein from GST, since the GST-tag remains bound. The cleaved target is then eluted using binding buffer. Another important feature is that PreScission Protease itself has a GST-tag and therefore will bind to Glutathione Sepharose: it will thus not co-elute and contaminate the cleaved target protein. As a practical recommendation, cleavage with PreScission Protease is very specific, but the maximum cleavage is obtained in the cold (the protein is most active at 4°C), thus improving the stability of the target protein.

2.2.2.4 HtrA Purification removing GST-tag with PreScission Protease: Purification and Cleavage

Cleavage of GST-tag using PreScission protease can be done in two different ways, named on-column and off-column cleavage. In both cases, the cell lysate is added to Glutathione Sepharose but, in the off-column method, this step is followed by elution with reduced glutathione and, after, by the cleavage of the eluted tagged protein with PreScission Protease. Finally, by passing the solution through the column, only the cleaved protein is allowed to be collected. By contrast, in the on-column method the tagged protein is cleaved with PreScission Protease directly in the column and the Flow Through with the cloned protein without the GST-tag is collected. At the end of these methods, the protein is usually analyzed by means of SDS-PAGE or mass spectrometry. Following the protocols described in the GE Healthcare Handbook, either off-column and on-column method were performed: in both cases, 500µL of Glutathione Sepharose were used and the protease inhibitors PMSF, E64, Leupeptin and Aprotinin (to the same final concentration reported above) were added to the cell lysate.

Great care was used to keep all the samples, during all the steps, at 0°C or at 4°C during the incubation time. In addition, 50µL of PreScission Protease were added in both methods and the following composition characterized the Elution and Cleavage Buffer used:

Elution Buffer: 50mM Tris-HCl, 10mM reduced glutathione, pH 8.0
Cleavage Buffer: 50mM Tris-HCl, 150mM NaCl, 1mM EDTA, 1mM DTT, pH 7.0

After purification and cleavage, the samples were submitted to SDS-PAGE and the fractions with a detectable quantity of protein were combined, concentrated and analysed through Analytical Gel Filtration, FPLC, with column for Size-Exclusion Chromatography (Superdex™ 200 Increase 10/300GL, GE Healthcare) equilibrated with Tris 50mM pH 7.5 as elution buffer.

2.2.3 Western Blot Analysis

In order to investigate the possible HtrA degradation pathway, part of the samples obtained from the previous expression and purification steps were used to carry out a Western Blot Analysis. To do this, proteins of the samples were separated using gel electrophoresis: in order to make the proteins accessible to antibody detection, they were moved from within the gel onto a nitrocellulose membrane made through electroblotting (30V, 1h) using the Transfer Buffer. Since the membrane has been chosen for its ability to bind protein and as both antibodies and the target are proteins, steps must be taken to prevent the interactions between the membrane and the antibody used for detection of the target protein. Blocking of non-specific binding were achieved by placing the membrane in BSA 3% in TBS 1X for one hour under gentle agitation. After blocking, three washes with TTBS for 15 min were done and 10mL of the primary monoclonal mouse antibody IgG_1 anti-GST (1:100 in TTBS; stock solution at 200µg/ml purchased from Santa Cruiz Biotechnology) were added to the membrane, maintaining it under gentle agitation for 2 hours. Then, three washes with TTBS for 15 min were done and 10mL of the anti-mouse IgG secondary antibody-peroxidase (1:10000 in TTBS; stock solution purchased from Sigma) were incubated with the membrane under gentle agitation. Finally, three washes with TTBS for 15 min were done and the membrane was submitted for chemiluminescent detection adding to it a freshly prepared luminol/hydrogen peroxide solution and using as Chemiluminescent Imaging System the instrument Kodak Image Station 4000MM Pro with the Carestream Molecular Imaging Software.

2.3 RESULTS & DISCUSSION

In this section, results obtained after several attempts of expression and purification of the HtrA protease will be illustrated and critically analyzed. Some Bioinformatics tools were also exploited to understand how to solve its structure and that of the same protein in *Helicobacter pylori*.

2.3.1 HtrA Bioinformatic analysis

2.3.1.1 Bioinformatic analysis

Crystal structure of HtrA from *Cj* could be solved either using SeMet isomorphous derivatives with the SAD/MAD techniques or, more likely, through Molecular Replacement (MR), owing to the high sequence and structural homology with other known proteins. Indeed, a similarity analysis using BLASTp software (www.blast.ncbi.nlm.nih.gov/Blast.cgi) with amino acid sequence of HtrA of *Cj* (GenBank: EAQ72966.1) as input sequence, identified high homology (41%) with Chain A in DegP24 of *E. coli* (PDB ID: 3CS0 A). The two sequences have been compared using ClustalW software (www.ebi.ac.uk/Tools/msa/clustalw2/). The homology is higher in the central portion and lower at the N- and C-terminus. The program also identified some putative conserved domains, in particular the Trypsin like domain and the PDZ domain of trypsin-like serine proteases, as expected.

```
HtrA            MKKIFLSLSLASALFAASINFNESTATANRVNPAAGNAVLSYHDSIKDAKKSVVNISTSK 60
DegP24          ----------------------AETSSATTAQQXPSLAPXLEKVXPSVVS-----INVEGST 35
                                       : *:**: :  *: .  : .   *: .     :*:. *.

HtrA            TITRANRPSPLDDFFND--PYFKQ---FFDFDFPQR----KGKNDKEVVSSLGSGVIISK 111
DegP24          TVNTPRXPRNFQQFFGDDSPFCQEGSPFQSSPFCQGGQGGNGGGQQQKFXALGSGVIIDA 95
                *:. .. *  :::**.*  *: ::   * .  * *     :* .::: . :*******.

HtrA            D-GYIVTNNHVVDDADTITVNLPGSDIEYKAKLIGKDPKTDLAVIKIEAN-NLSAITFTN 169
DegP24          DKGYVVTNNHVVDNATVIKVQLS-DGRKFDAKXVGKDPRSDIALIQIQNPKNLTAIKXAD 154
                * **:********:* .*.*:*. .. ::.** :****::*:*:*:*:   **:**. ::

HtrA            SDDLMEGDVVFALGNPFGVGFSVTSGIISALNKDNIGLNQYENFIQTDASINPGNSGGAL 229
DegP24          SDALRVGDYTVAIGNPFGLGETVTSGIVSALGRSGLNAENYENFIQTDAAINRGNSGGAL 214
                ** *  ** ..*:*****:* :*****:***.:..:. ::*********:** *******

HtrA            VDSRGYLVGINSAILSRGGGNNGIGFAIPSNMVKDIAKKLIEKGKIDRGFLGVTILALQG 289
DegP24          VNLNGELIGINTAILAPDGGNIGIGFAIPSNXVKNLTSQXVEYGQVKRGELGIXGTELNS 274
                *: .* *:***:***: .*** ********* **:::.: :* *::.** **:    *:.

HtrA            DTKKAYKN--QEGALITDVQKGSSADEAGLKRGDLVTKVNNKVIKSPIDLKNYIGTLEIG 347
DegP24          ELAKAXKVDAQRGAFVSQVLPNSSAAKAGIKAGDVITSLNGKPISSFAALRAQVGTXPVG 334
                :  ** *   *.**::::*  .*** :**:* **::*.:*.* *.*   *:  :**  :*

HtrA            QKISLSYERDGENKQASFILKGEKENPKGVQSDLIDGLSLRNLDPRLKDRLQIPKDVNGV 407
DegP24          SKLTLGLLRDGKQVNVNLELQQSSQN-QVDSSSIFNGIEGAEXSNKGKD--------QGV 385
                .*::*.  ***:: :..: *: ..:* :  .*.:::*:.  : . : **        :**

HtrA            LVDSVKEKSKGKNSGFQEGDIIIGVGQSEIKNLKDLEQALKQVNKKEFTKVWVYRNGFAT 467
DegP24          VVNNVKTGTPAAQIGLKKGDVIIGANQQAVKNIAELRKVLD--SKPSVLALNIQRGDSTI 443
                :*:.**  : . : *:::**:***..*. :**: :*.:.*.  .* ..  : : *.. :

HtrA            LLVLK 472
DegP24          YLLXQ 448
                 *: :
```

Figure 2.7: Comparison of amino acids sequence of HtrA from *Cj* and DegP24 from *E. coli* (***** for identical residues, **:** for conserved residues and **.** for semiconserved residues)

Structural homology was confirmed using two different protein structure homology-modelling server, SWISS-MODEL (swissmodel.expasy.org/) and Phyre2 (www.sbg.bio.ic.ac.uk/phyre2/html/page.cgi?id=index): homology modelling is currently the most accurate method to generate reliable three-dimensional protein

structure models. The methods predict the three-dimensional structure of a protein sequence using the principles and technique of homology modelling. Since the 3D structure of a protein is more conserved in evolution than its amino acid sequence, a protein sequence of interest (the target) can be modelled with reasonable accuracy on a very distantly related sequence of known structure (the template), provided that the relationship between target and template can be discerned through sequence alignment. The results obtained from these two independent modelling, based on the same principles, converge toward the same structure of the *E. coli* DegP (PDB ID: 2ZLE). The degree of structural homology (template identity) was 41.6% and 44% from SWISS-MODEL and Phyre2, respectively, confirming not only a sequence homology but, also, a good similarity in the three-dimensional folding. In addition, Phyre2 report a secondary structure and disorder prediction, in which it appears that the percentages of disordered regions, α-helix and β-strand are, respectively, 28%, 19% and 35%. Through bioinformatics tools it is possible to say that there is a good chance to solve the structure of HtrA from *Cj* using MR, thanks to some hopeful templates.

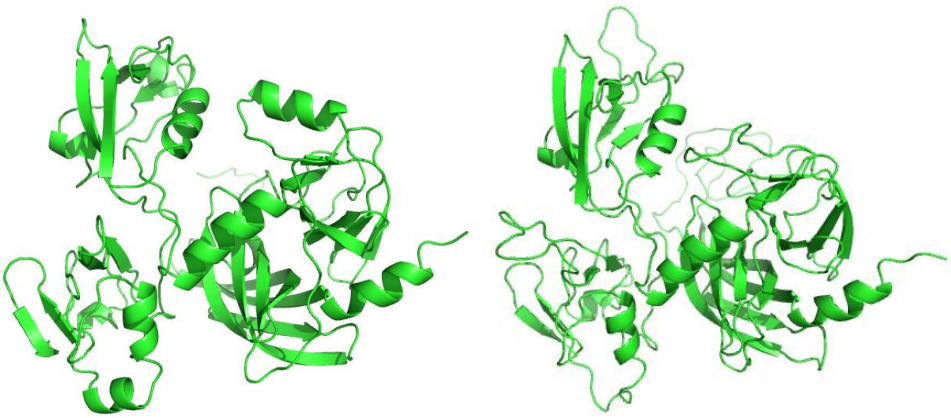

Figure 2.8: *On the left*, cartoon representation of the three-dimensional model generated by Phyre2 and, *on the right*, the structure obtained from SWISS-MODEL.

However, it is more interesting to see if there is sequence homology with some HtrA from *Helicobacter pylori*: if so, the structure of the HtrA from *Hp* could be solved using *ab initio* or Molecular Dynamics methods. Once obtained the structure of HtrA from *Cj*, it cannot be used as a reference structure for the determination, via MR, of the three-dimensional model of *Hp*-HtrA because MR requires the knowledge of diffracted intensities, structure factors for each reflections *etc*. However, this is not the case because obtaining the crystal of the HtrA from *Hp* is hard, owing to its instability (without the crystal, it is impossible to obtain the experimental data required for resolution via MR). Effectively, by aligning the amino acid sequence of HtrA in *Cj* against the sequence of the HtrA from a common strain of *Hp* (GenBank: EJC53984.1) proves that there is a high degree of homology (46%).

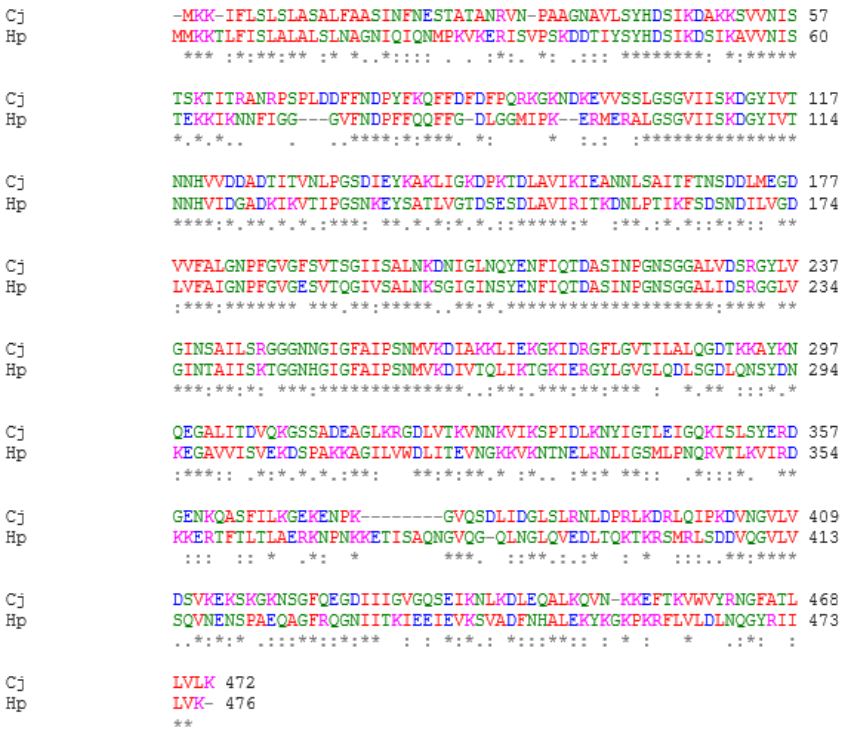

Figure 2.9: Comparison of amino acids sequence of HtrA from *Cj* and HtrA from *Hp* P-41 (***** for identical residues, **:** for conserved residues and **.** for semiconserved residues)

2.3.2 Over-expression and purification

Several attempts have been made in order to obtain a sufficient amount of *Cj* HtrA pure protein: the main variables include the type of *E. coli* strain, culture medium, temperature and time. The HtrA expression was evaluated in the course of several tests in which these conditions were varied but, in all cases, only a small quantity of the protein was obtained, preventing the possibility of crystallizing it. Moreover, the purification protocols failed to provide the protein in a very pure form, required for any crystallization trials. Results are summarized and, together with them, also possible explanations are given.

First Attempt

In the first attempt, *E. coli* BL21(DE3) competent cells were transformed with the plasmid vector and used for pre-inoculation and inoculation at 30°C for 3h, with LB as growth medium. The protocol reported in the experimental section was followed and the result of HtrA expression was evaluated from SDS-PAGE and from the size-exclusion chromatography-FPLC analysis. No purification with PreScission Protease was done.

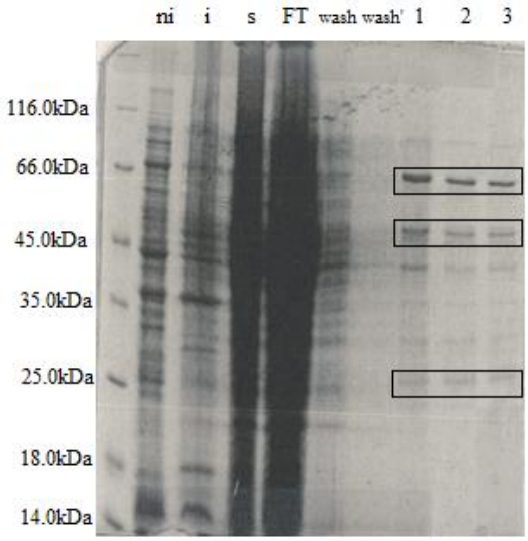

Figure 2.10: SDS-PAGE gel corresponding to the uninduced sample (**ni**), induced sample (**i**), the supernatant (**s**), the Flow Through (**FT**), the washes with Buffer (**wash** and **wash'**) and the three eluted fractions with Glutathione Buffer, in order (**1**, **2**, **3**). On the left, molecular weights of the protein markers.

Owing to its cytoplasmic localization, HtrA is a soluble protein and, as a consequence, it is expected in the supernatant. As the gel shows, only a weak expression of the tagged protein was obtained: slightly above the signal of the protein marker at 66kDa, near the molecular weight of HtrA with the GST-tag (79kDa), three bands with decreasing intensity could be identified in the eluted fractions.

However, other bands at lower molecular weights appear in the gel, particularly near the signal of the protein marker at 45kDa, and compatible with HtrA without GST-tag (53kDa) and, although less easily visible, near 25kDa and relative to the free GST moiety (26kDa). Unfortunately, other bands appear in the gel and this poses into question the efficacy of the purification protocol and/or suggests susceptibility to degradation of the HtrA protease. These suspects are confirmed also after gel filtration experiment: as can be seen in Fig. 2.11, at least six different peaks are visible. Given the known molecular weight of HtrA·GST, one would expect a peak around 13.5ml: at this elution volume there is a relative intense peak that can be attributed to the HtrA·GST complex. The same can be said for the peak relative to HtrA, which should elute roughly at 14.3ml. However, HtrA is not a monomer in its native/inactive form but, as demonstrated, a homotrimer[2]; furthermore it could result in the formation of oligomers with higher molecular weights and this is more likely when the protein solution is concentrated. Assuming that HtrA and HtrA·GST are present as homotrimers, they should elute with two peaks at 12.2ml and 11.4ml, but none is visible in this region of the gel filtration curve. In any case, due to the low absorbance of the putative peak, only a low amount of protein (free or in complex with GST) was probably obtained. Finally, free GST should elute at about 15.7ml: however, no peak is observed. This could be due to aggregation of free GST to give oligomers with greater molecular weights. Another possible explanation for the unsatisfactory protein yield concerns the formation of the so-called inclusion bodies: recombinant protein over-expression in bacterial hosts often results in insoluble and misfolded proteins directed to inclusion bodies. These aggregates are deleterious, because they sequester the protein reducing the yield of the process; furthermore, attempts to prevent protein aggregation are in general unsuccessful and when inclusion bodies are formed, (partial) recovery of the native and correctly folded protein are difficult and time-consuming.

[2] Protein expression in an heterologous system can result in a monomeric form as well as in one or more different oligomeric forms. The oligomeric form with which the protein is expressed does not necessarily coincide with that present in physiological conditions within the organism. Not necessarily HtrA is expressed in its native/inactive form as homotrimer but may be secreted in the form of higher oligomeric species or as a monomer. The aggregation state that can be deduced from gel filtration experiments depends on the pH and chemical composition of the buffer in which the protein is eluted, the protein concentration in solution and not only.

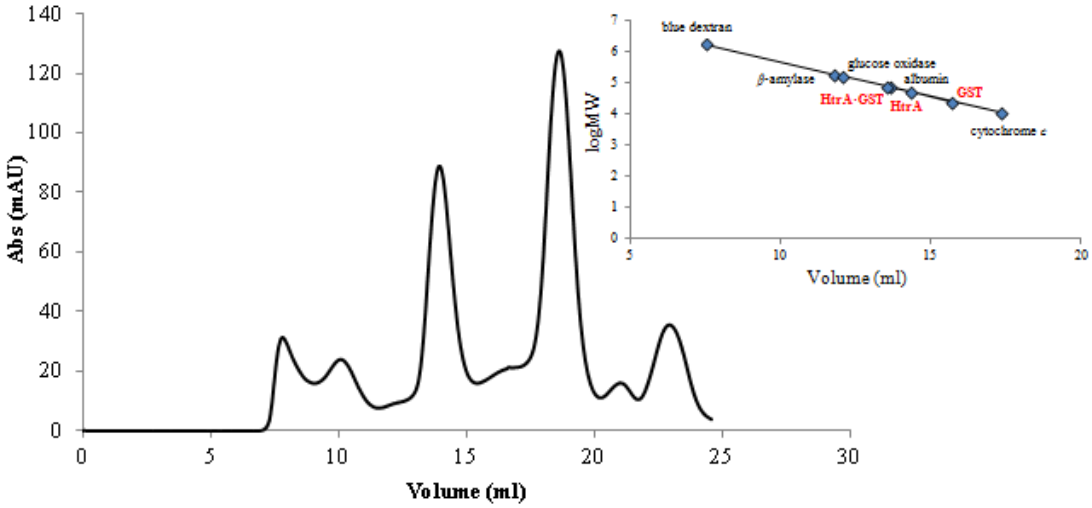

Figure 2.11: Analytical gel filtration after purification and concentration (absorbance measured at λ=280nm). The upper-right panel shows the calibration curve obtained with five protein standards of known MW (note that the graph was created having a logarithmic scale for the y-axis).

Looking better to the SDS-PAGE gel, it is possible to see a band compatible with the presence of tagged HtrA also in the non induced sample: this may seem strange but, in some expression systems, this is quite common. Indeed, a basal level of expression is possible, especially for some kind of bacterial strains, as is the case of *E. coli* BL21(DE3) cells. In addition, if the protein being expressed is toxic for cells, this can explain the low amount of protein detected both in SDS-PAGE and in the chromatogram. A basal level of expression before the addition of IPTG is expected, but after the induction the cells started to produce the protein and its toxic effects are manifested from the beginning: this causes cell death and prevents protein expression.

Other growth conditions have been tested but, even in these cases, expression was not as satisfactory as expected. Also using a more nutrient culture medium as the Terrific Broth (TB), instead of the Luria-Bertani (LB), provides the same results.

Second Attempt

To overcome a possible toxic effect of the protein already prior to induction, a different commercial available *E. coli* strain has been used: BL21(DE3)pLysS cells carry both the DE3 lysogen and the plasmid pLysS. pLysS constitutively expresses low levels of T7 lysozyme, which reduces basal expression of recombinant genes by inhibiting basal levels of T7 RNA polymerase (T7 lysozyme is a natural inhibitor of T7 RNA polymerase). This strain was tested in different conditions of expression, *i.e.* by varying temperature and time during the inoculation step. However, as seen from Fig. 2.12, a basal level of expression is still present and, due to the minimum difference between band intensity, it is difficult to judge if there was or not

expression after induction. As in the first attempt, other bands are present, not only associated with HtrA and free GST but relative to other proteins or fragments, part of which probably derived from HtrA degradation.

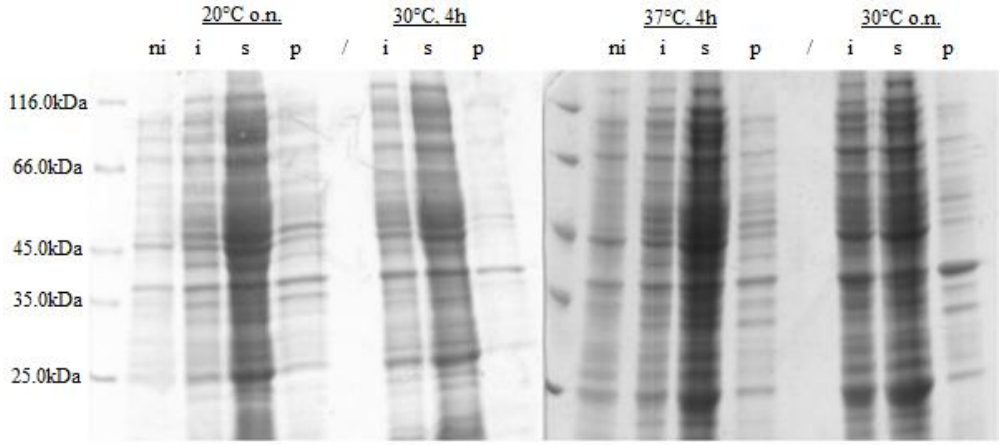

Figure 2.12: SDS-PAGE gel corresponding to expression trials at various conditions of time and temperature (in this case, **p** represents the pellet sample).

Third Attempt

In the third attempt a different *E. coli* strain was used, in particular *E. coli* BL21 cells. In addition, purification protocol based on the removal of the GST-tag with PreScission Protease was implemented, either with the off-column and on-column cleavage. Remove the GST-tag has the advantage of allowing the crystallization and structure determination of the protein itself: without the tag, the protein more likely adopts the native conformation, and the structure so obtained reflects the real three-dimensional conformation of the protein. This is particularly true in the case in which the tag have a considerable molecular weight, as it is for GST: the main drawback is probably this, meaning that the protein of interest is attached to GST, altering its native state. However, GST-tag at the N-terminus of recombinant proteins have different advantages: because GST rapidly folds into a stable and highly soluble protein upon translation, inclusion of the GST-tag often promotes greater expression and solubility of recombinant proteins than expression without the tag. In addition, as discussed in precedence, GST-tagged fusion proteins can be purified or detected based on the ability of GST to bind its substrate, glutathione. Unfortunately, the use of *E. coli* BL21 cells and the cleavage of the tagged HtrA with PreScission Protease does not produce enhancements because numerous bands and peaks are still visible either in SDS-PAGE and in the chromatogram relative to the size-exclusion chromatography-FPLC.

Among the various difficulties inherent with the cleavage method, it is possible to identify some of it that have a prominent role and are, probably, largely responsible for the failure of the cleavage. When GST-tagged proteins are not cleaved completely, there are different possible critical points in the procedure: first, it is possible that the ratio of PreScission Protease to GST-tagged protein is not optimal. This requires a preliminary quantification of the protein before the cleavage, but the estimate of the amount of protein from a gel is not an easy task; in any case, the optimal amount must be determined empirically. Second, there is the possibility that the incubation time and/or enzyme concentration is not sufficient for complete cleavage of the protein from the GST-tag: in this case, the advice is to increase the incubation time for the cleavage reaction. Increasing the reaction time to 20 hours or more should improve cleavage as long as the tagged protein is not degraded by the extended incubation period. Alternatively, increasing the amount of the enzyme used for cleavage can represents a valid solution. Third, it is also possible that the specific cleavage site for the protease has been altered during cloning of the tagged protein or, fourth, the presence of cleavage enzyme inhibitors is interfering with the cleavage reaction. When multiple bands are observed after electrophoresis/Western Blotting analysis (see *Fourth Attempt*) of the cleaved target protein, possible causes are the occurrence of proteolysis in the host bacteria prior to the cleavage reaction or the presence, in the target protein itself, of recognition sequences for PreScission Protease or other cleavage proteases. With respect to the former cause, the determination when the extra bands appear is needed, as it is also necessary to verify that additional bands are not present prior to PreScission cleavage. In regard to the latter cause, it is necessary to check the sequence of the tagged protein to determine if it contains recognition sequences for the cleavage enzymes. Last but not least, it is of great importance to find the correct amount of resin (Glutathione Sepharose), because an excess of beads results in unspecific protein binding and too few beads result in a low protein yield: owing to these considerations, it is necessary to check that the amount of tagged protein does not exceed the capacity of the Glutathione Sepharose media (in most purification, however, the medium is not saturated with tagged protein). Despite all these suggestions have been taken into account during the experimental optimization of the cleavage protocol, no improvements were observed.

Fourth Attempt

To investigate further the presence of several bands observed after electrophoresis, a Western-Blot Analysis has been made using anti-GST primary antibody and a secondary antibody carrying the horseradish peroxidase enzyme that, upon addition of its substrate (luminol in the presence of hydrogen peroxide) cleaved it, generating a chemiluminescent reaction product which luminescence is proportional to the amount of protein. The result is shown in Fig. 2.13, in which the dark signals are due to the presence of GST free or bound to HtrA (or to possible fragments).

Among the different samples analysed, it is of relevance the discussion of some of it, particularly samples 5, 7, 8, 9, 10 and 11. Sample 5 represents the first eluted fraction with the Glutathione Buffer during the purification procedure without the use of PreScission Protease and the bands clearly visible represent different intermediate products derived from the degradation of the tagged HtrA. The number, intensity and heights of these bands confirm the existence of a degradation pathway of the tagged protein, probably due to its autoproteolytic activity. Samples from 7 to 11 are relative to fractions 2, 5, 6, 7 and 8 in the chromatogram of Fig. 2.14. Also in this case it was obtained a not clean chromatogram with several peaks. HtrA·GST should elute roughly at 14.2ml, but at this elution volume there is a shoulder in the curve. The shoulder in the curve probably cover the HtrA·GST peak: however, it is also possible that HtrA elute not as a monomer but in an higher oligomeric form, visible at a lower volume. Differently, HtrA should elute near 15.2ml but, also in this case, at this point is present a shoulder in the curve, even if with a very low absorbance. Assuming that HtrA and HtrA·GST are present as homotrimers, they should elute with two peaks at 12.4ml and 11.4ml: these elution volumes matches with the fractions 6 and 5. Lastly, free GST should elute at about 16.9ml but no peaks are visible.

It is clear that HtrA undergo rapid degradation, probably due to its autoproteolytic activity, in which a series of different intermediate products, with also attached GST, are generated. This happens despite the continuous control of the temperature, constantly maintained at 0°C, and despite the presence of different serine protease inhibitors. These protease inhibitors are essential because when cells are lysed some proteases, many of which are contained within lysosomes, are released. These proteases, if freely present in the lysate, would destroy any protein or any other component of interest. However, in the present case they do not appear sufficient to prevent HtrA degradation. This is the reason why it was decided to continue the study on a HtrA mutant characterized from the substitution, in the active site, of one amino acid: in particular, the critical serine in the catalytic triad was mutated to alanine in order to prevent autoproteolysis. It is expected that this substitution makes the protein more stable, facilitating in this way its purification and crystallization.

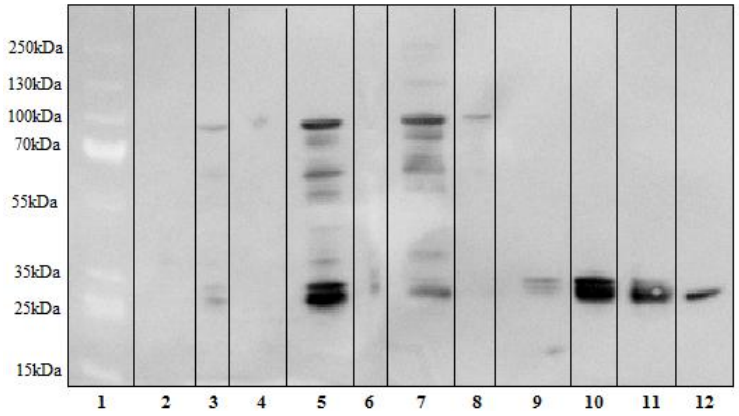

Figure 2.13: Western-Blot Analysis of Prestained Protein Molecular Weight Markers (**1**), ni (**2**), i (**3**), s (**4**), first eluted fraction (**5**), FT (**6**), Fraction 2 (**7**), Fraction 5 (**8**), Fraction 6 (**9**), Fraction 7 (**10**), Fraction 8 (**11**), Fraction after incubation with PreScission Protease (**12**). Fractions 2, 5, 6, 7 and 8 are relative to purification without PreScission Protease (see chromatogram in Fig. A.14).

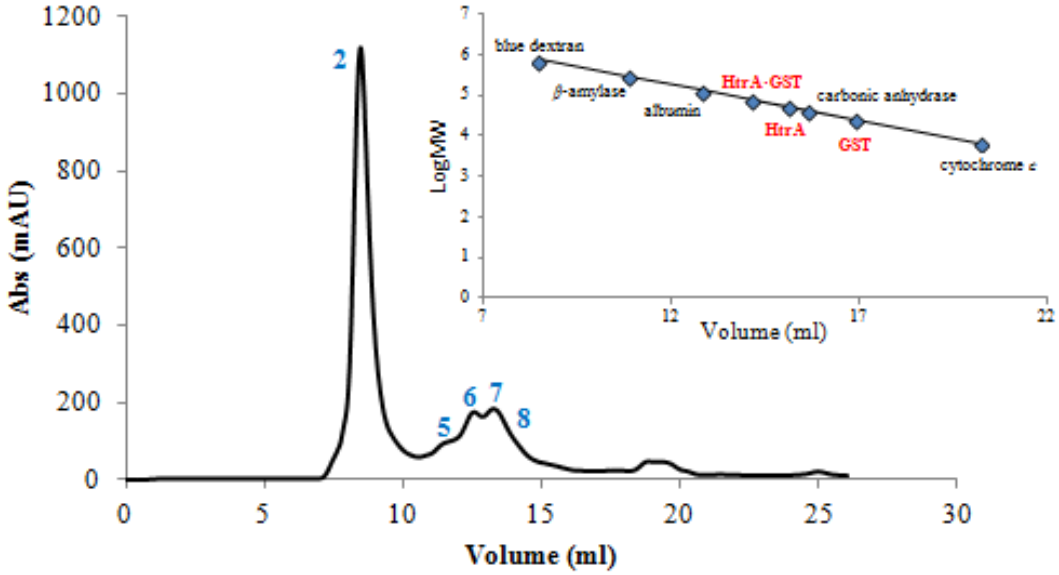

Figure 2.14: Analytical gel filtration after purification, cleavage with PreScission Protease and concentration; fractions of major interest are indicated in bold blue. The upper-right panel shows the calibration curve obtained with five protein standards of known MW (note that the graph was created having a logarithmic scale for the y-axis).

Fifth Attempt

Competent *E. coli* BL21 cells were transformed in the presence of the pGEX-6P-1 vector plasmid carrying the mutated *htra* gene; after inoculation and induction with IPTG, pellet were harvested and resuspended in PBS 1X in the presence of PMSF 1mM. After lysis the supernatant was incubated over night at 4°C with Glutathione Sepharose 4B. FT was collected and the resin washed with 10mL of Cleavage Buffer; 70µL of PreScission Protease were added directly on-column and the mixture was placed under agitation over night at 4°C. The next day, FT was collected and the resin was washed with the Cleavage Buffer; at the end, a single wash with the Elution Buffer was done. All the fractions were submitted to SDS-PAGE and, after analyzing the gel obtained, fractions containing the cleaved protein (1, wash and wash' in Fig. 2.15) were combined and concentrated. The concentrated protein was analyzed in a gel filtration experiment (Fig. 2.16), after which some fractions were run in a SDS-PAGE.

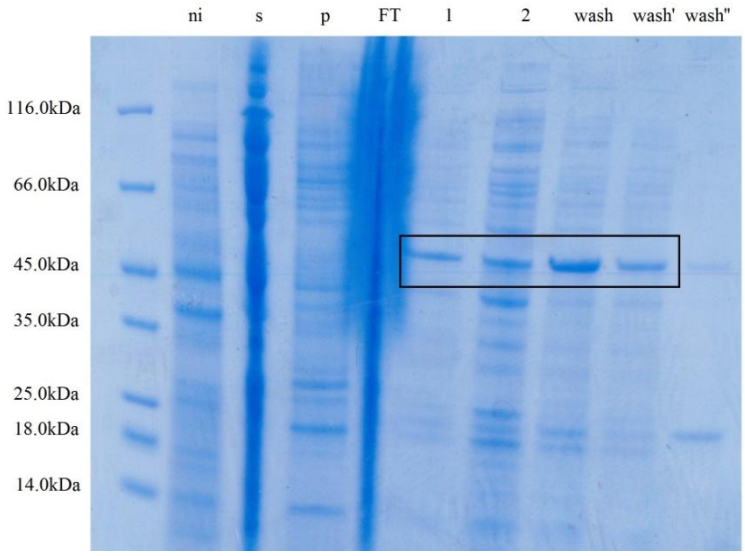

Figure 2.15: SDS-PAGE gel after expression and purification with PreScission protease; **1** and **2** represent the FT after incubation over night of Glutathione Sepharose 4B with the site-specific protease, **wash** and **wash'** were obtained after washing of the column with Cleavage Buffer and **wash''** after the same procedure but using Elution Buffer.

SDS-PAGE of fractions indicated in Fig. 2.16 reveals the presence of the cleaved protein only in fraction 4, which appears as a principal band in the gel; however, bare visible bands at different molecular weights were detected. Although fraction 4 is more clean than those obtained in precedent attempts, it is not yet enough to proceed with crystallization trials.

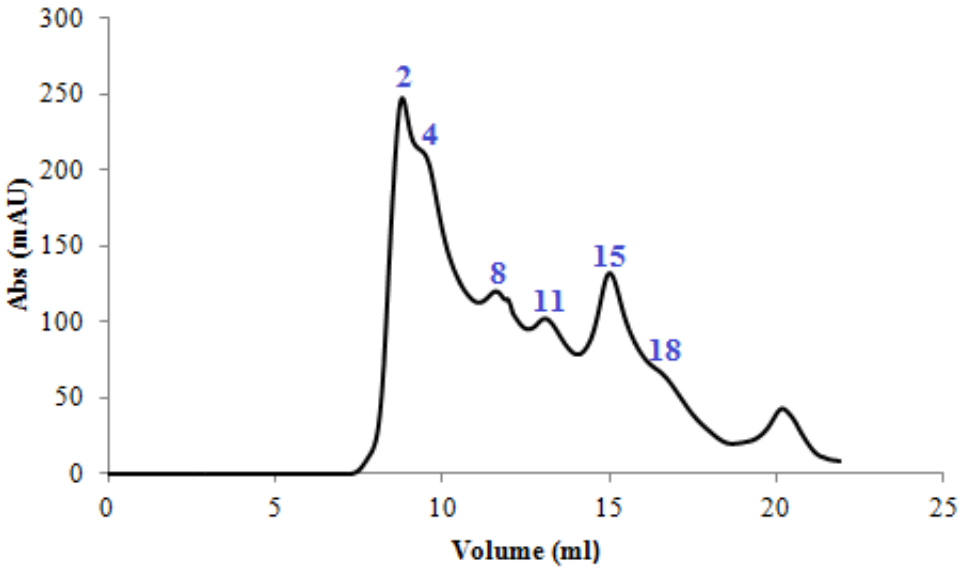

Figure 2.16: Analytical gel filtration after purification, cleavage with PreScission Protease and concentration. Fractions of major interest are indicated in bold blue.

After gel filtration experiment, it was decided to investigate the stability of the HtrA mutant with the aim to understand its stability relative to that of *Cj*-HtrA. Fig. 2.17 reported the result after Western-Blot analysis of significant fractions collected in the previous expression and purification steps:

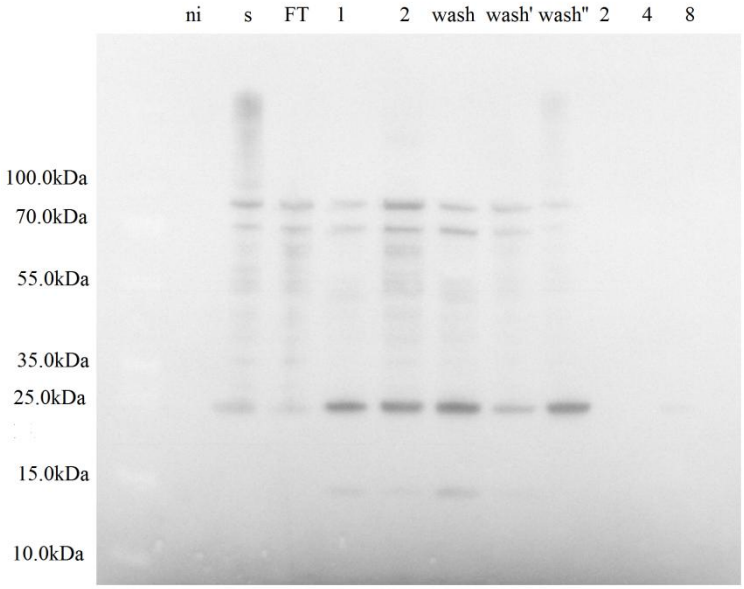

Figure 2.17: Western-Blot Analysis of Prestained Protein Molecular Weight Markers (leftmost) and various samples which significance is discussed above in the text.

The presence of the bands relative to HtrA·GST in supernatant and FT is expected because these samples were obtained before the PreScission cleavage. Conversely, the presence of the bands relative to HtrA·GST in samples 1, 2, wash and wash' looks suspicious as they were collected after incubation overnight with the site-specific protease. However, is to be considered that the same bands are quite weak in SDS-PAGE gel and that the Western-Blot analysis is extremely sensitive. The band at 25kDa in wash'' is expected because it derives from the washing with GSH (competitive ligand) which determines the release of GST moiety bound to the resin. It is also expected the absence of any bands in fractions derived from gel filtration (only a merely detectable band is present in fraction 8, more likely due to eluted GST). This also confirm that the band in fraction 4 (seen from SDS-PAGE) is relative to cleaved HtrA. In light of this, the cleaved protein in fraction 4 was concentrated (Millipore Amicon Ultra cellulose membrane; cut-off: 10kDa) to 7 mg/ml for crystallization purposes: the effective protein concentration was determined by UV/Vis Spectroscopy (280nm, Thermo Scientific NanoDrop 2000/2000c UV-Vis spectrophotometer). Crystallization conditions were identified using vapour diffusion technique performed in sitting drop variant and Oryx8 crystallization robot (Douglas Instruments). General conditions trials were performed mixing 0.30 µl of protein solution with 0.30 µl of precipitant on 96-well plates (Douglas Instruments), containing 75 µl of precipitant in every well, allowing the crystallization at the constant temperature of 20°C. For the first crystallization trial the Structure Screen 1+2 HT-96 kit (Molecular Dimensions) was used.

2.3.3 Conclusions

Attempts to obtain *Cj*-HtrA protease in a pure form making use of heterologous over-expression in a bacterial host and successive purification was difficult to reach. Further investigations are required in order to understand more in depth the protein instability and to perform a better protocol. Although preliminary, the results obtained for mutant HtrA are not satisfactory: despite the HtrA mutant seems to be less prone to autodegradation, as seen from Western-Blot analysis, the protein yield is low as in the case of wt-HtrA and even after purification steps the fractions are not sufficiently pure for crystallization purposes.

About the instability of HtrA from *Cj*, there are at least two possible explanations: first, instability can be dictated merely by the primary amino acid sequence of the protein, without particular biological reasons. Second, and more interestingly, behind the instability of the HtrA protease there may be physiological and biological implications. In 2008, Sacchettini *et al*. [150] have determined the structure of HtrA from *Mycobacterium tubercolosis* (*Mtb*): the crystal structure revealed tetrapeptides bound to the protease active site and to PDZ domains. These peptides most likely derived from autoproteolytic processing of HtrA. Based on this and other observations, they speculated that the protease might regulate itself by its autoproteolytic products; furthermore, the binding of tetrapeptides should have an effect on the substrate specificity, might regulate the activity of the protease domain and might have significant importance in HtrA-associated virulence of *Mtb*. In addition, other studies reported on the instability of HtrA: in 2011 it was observed autodegradation both *in vivo* and *in vitro* (with purified wt-HtrA) for HtrA from *Cj* [193]. However, it was noted that HtrA from *E. coli* was less prone to autodegradation and this was explained on the basis of disulfide bridges, absent in *Cj*-HtrA but present in HtrA from *E. coli*. Other authors have focused on a possible biological role of different HtrA [172] [198] but, nowadays, the physiological consequences of the observed autocleavage remain unclear.

The presence of multiple bands in SDS-PAGE gels even after purification with or without PreScission Protease suggests a residual autoproteolytic activity and possible aspecific binding to the resin (this can be inferred from bands at higher molecular weights with respect to that of HtrA bound to GST) from proteins derived from lysis of *E. coli* cells. These proteins were co-eluted with the cleaved HtrA and hinder crystallization trials, together with the fragments generated by autocatalytic cleavage. In addition, it seems strange the presence, evidenced from Western-Blot analysis, of the band relative to HtrA·GST in the fractions after site-specific cleavage: this shows that not all the HtrA bound to GST was cleaved during the 24h incubation. It can be speculated a possible alteration of the overall structure of the protease caused by the GST moiety: GST is a non-small protein that can alter the protein conformation in a manner such that it is incorporated in a non exposed region. This, in turn, can be

responsible for the incapacity of PreScission Protease to cleave correctly the recombinant protein.

To further increase the stability of HtrA a double or triple mutant may be necessary. With a more stable protein, both expression and purification procedures should benefit from this; reducing the induction/expression time can also counteract certain propensity of the protein to degrade itself. In addition to the problem of instability, there are other weakness in the procedure such as the protein tag: the GST-tag are useful because it often promotes greater expression and solubility of recombinant proteins. However, HtrA is a cytoplasmic protein: owing to this, it is likely that it is a soluble protein and the GST-tag appears probably not necessary. An His_6-tag is smaller and, thanks to this, it can be maintained attached to the protein even during the crystallization step. Another possible improvements could include growth in a more acidic pH medium, in order to resemble the environment in which *Cj*-HtrA is secreted.

However, the crystal structure, combined with other experimental evidences, can provide clues about the physiological and pathological role of HtrA protease in *Cj* and, by inference, even in *Hp*: this underlines the importance of proceeding in attempts to express and purify HtrA protein or its mutants.

Appendix A[3]

In this Appendix, the space group of crystals analyzed in the thesis are reported, in order to highlight the geometrical features.

$P2_12_12$ $P\,2_1\,2_1\,2$ 222 No. 18

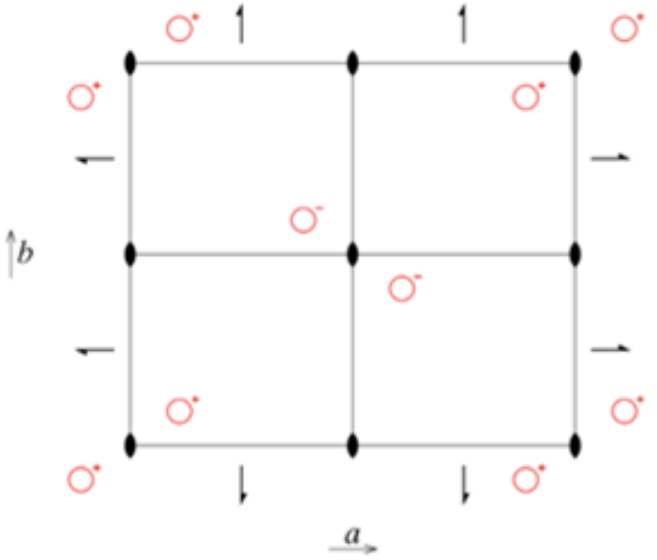

1 x, y, z
2 $\frac{1}{2}+x, \frac{1}{2}-y, \bar{z}$
3 $\frac{1}{2}-x, \frac{1}{2}+y, \bar{z}$
4 $\bar{x}, \bar{y}, z$

Symmetry Operators		Reflection Conditions
1 x, y, z	1	(general)
2 $\frac{1}{2}+x, \frac{1}{2}-y, z$	2_1 $(x, \frac{1}{4}, 0)$ $[\frac{1}{2}, 0, 0]$	$h00: h = 2n$
3 $\frac{1}{2}-x, \frac{1}{2}+y, z$	2_1 $(\frac{1}{4}, y, 0)$ $[0, \frac{1}{2}, 0]$	$0k0: k = 2n$
4 $\bar{x}, \bar{y}, z$	2 $(0, 0, z)$	

[3] This Appendix is taken referring to *International Tables for Crystallography* (2006) Vol. A, Ch. 7.1, pp.112-717.

Appendix B

Amino acids

Alanine	Ala	A
Arginine	Arg	R
Aspartic acid	Asp	D
Asparagine	Asn	N
Cysteine	Cys	C
Glycine	Gly	G
Glutamine	Gln	Q
Glutamic acid	Glu	E
Histidine	His	H
Isoleucine	Ile	I
Leucine	Leu	L
Lysine	Lys	K
Methionine	Met	M
Phenylalanine	Phe	F
Proline	Pro	P
Serine	Ser	S
Threonine	Thr	T
Tyrosine	Tyr	Y
Tryptophan	Trp	W
Valine	Val	V

BIBLIOGRAPHY

[1] E. A. Kabat, D. H. Moore and H. Landow, "An Electrophoretic Study of the Protein Components in Cerebrospinal Fluid and Their Relationship To the Serum Proteins", *J. Clin. Invest.*, vol. 21, no. 5, pp. 571–577, 1942.

[2] C. C. Blake, M. J. Geisow, S. J. Oatley, B. Rérat and C. Rérat, "Structure of prealbumin: secondary, tertiary and quaternary interactions determined by Fourier refinement at 1.8 Å", *J. Mol. Biol.*, vol. 121, no. 3, pp. 339–356, 1978.

[3] A. Wojtczak, "Crystal structure of rat transthyretin at 2.5 Å resolution: First report on a unique tetrameric structure", *Acta Biochimica Polonica*, vol. 44, no. 3. pp. 505–518, 1997.

[4] A. Hörnberg, T. Eneqvist, A. Olofsson, E. Lundgren and A. E. Sauer-Eriksson, "A comparative analysis of 23 structures of the amyloidogenic protein transthyretin", *J. Mol. Biol.*, vol. 302, no. 3, pp. 649–669, 2000.

[5] M. Sunde, S. J. Richardson, L. Chang, T. M. Pettersson, G. Schreiber and C. C. Blake, "The crystal structure of transthyretin from chicken", *Eur. J. Biochem.*, vol. 236, no. 2, pp. 491–499, 1996.

[6] C. Folli, N. Pasquato, I. Ramazzina, R. Battistutta, G. Zanotti and R. Berni, "Distinctive binding and structural properties of piscine transthyretin", *FEBS Lett.*, vol. 555, no. 2, pp. 279–284, 2003.

[7] T. Eneqvist, E. Lundberg, A. Karlsson, S. Huang, C. R. A. Santos, D. M. Power and A. E. Sauer-Eriksson, "High resolution crystal structures of piscine transthyretin reveal different binding modes for triiodothyronine and thyroxine", *J. Biol. Chem.*, vol. 279, no. 25, pp. 26411–26416, 2004.

[8] D. R. Soprano, J. Herbert, K. J. Soprano, E. A. Schon and D. S. Goodman, "Demonstration of transthyretin mRNA in the brain and other extrahepatic tissues in the rat", *J. Biol. Chem.*, vol. 260, no. 21, pp. 11793–11798, 1985.

[9] P. W. Dickson, A. R. Aldred, P. D. Marley, D. Bannister and G. Schreiber, "Rat choroid plexus specializes in the synthesis and the secretion of transthyretin (Prealbumin). Regulation of transthyretin synthesis in choroid plexus is independent from that in liver", *J. Biol. Chem.*, vol. 261, no. 8, pp. 3475–3478, 1986.

[10] J. Herbert, J. N. Wilcox, K. T. Pham, R. T. Fremeau, M. Zeviani, A. Dwork, D. R. Soprano, A. Makover, D. S. Goodman and E. A. Zimmerman, "Transthyretin: a choroid plexus-specific transport protein in human brain. The 1986 S. Weir Mitchell award", *Neurology*, vol. 36, no. 7, pp. 900–911, 1986.

[11] Y. Kanda, D. S. Goodman, R. E. Canfield and F. J. Morgan, “The Amino Acid Sequence of Human Plasma Prealbumin”, *J. Biol. Chem.*, vol. 249, no. 21, pp. 6796–6805, Nov. 1974.

[12] C. C. Blake and S. J. Oatley, “Protein-DNA and protein-hormone interactions in prealbumin: a model of the thyroid hormone nuclear receptor?”, *Nature*, vol. 268, no. 5616, pp. 115–120, 1977.

[13] C. C. F. Blake, M. J. Geisow, I. D. A. Swan, C. Rerat and B. Rerat, “Structure of human plasma prealbumin at 2.5 Å resolution”, *J. Mol. Biol.*, vol. 88, no. 1, pp. 1–12, Sep. 1974.

[14] J. A. Hamilton, L. K. Steinrauf, B. C. Braden, J. Liepnieks, M. D. Benson, G. Holmgren, O. Sandgren and L. Steen, “The x-ray crystal structure refinements of normal human transthyretin and the amyloidogenic Val-30-->Met variant to 1.7Å resolution”, *J. Biol. Chem.*, vol. 268, no. 4, pp. 2416–2424, 1993.

[15] S. K. Palaninathan, “Nearly 200 X-Ray Crystal Structures of Transthyretin: What Do They Tell Us About This Protein and the Design of Drugs for TTR Amyloidoses?”, *Current Medicinal Chemistry*, vol. 19, no. 15. pp. 2324–2342, 2012.

[16] P. Prapunpoj, K. Yamauchi, N. Nishiyama, S. J. Richardson and G. Schreiber, “Evolution of structure, ontogeny of gene expression, and function of *Xenopus laevis* transthyretin”, *Am. J. Physiol. Regul. Integr. Comp. Physiol.*, vol. 279, no. 6, pp. R2026–R2041, 2000.

[17] S. J. Richardson, “The evolution of transthyretin synthesis in vertebrate liver, in primitive eukaryotes and in bacteria”, *Clinical Chemistry and Laboratory Medicine*, vol. 40, no. 12. pp. 1191–1199, 2002.

[18] I. Ramazzina, C. Folli, A. Secchi, R. Berni and R. Percudani, “Completing the uric acid degradation pathway through phylogenetic comparison of whole genomes”, *Nat. Chem. Biol.*, vol. 2, no. 3, pp. 144–148, 2006.

[19] S. C. Hennebry, R. H. P. Law, S. J. Richardson, A. M. Buckle and J. C. Whisstock, “The Crystal Structure of the Transthyretin-like Protein from *Salmonella dublin*, a Prokaryote 5-Hydroxyisourate Hydrolase”, *J. Mol. Biol.*, vol. 359, no. 5, pp. 1389–1399, 2006.

[20] D. K. Jung, Y. Lee, S. G. Park, B. C. Park, G. H. Kim, and S. Rhee, “Structural and functional analysis of PucM, a hydrolase in the ureide pathway and a member of the transthyretin-related protein family”, *Proc. Natl. Acad. Sci. U. S. A.*, vol. 103, no. 26, pp. 9790–9795, 2006.

[21] G. Zanotti, L. Cendron, I. Ramazzina, C. Folli, R. Percudani and R. Berni, “Structure of Zebra fish HIUase: Insights into Evolution of an Enzyme to a Hormone Transporter”, *J. Mol. Biol.*, vol. 363, no. 1, pp. 1–9, 2006.

[22] E. Lundberg, S. Bäckström, U. H. Sauer and A. E. Sauer-Eriksson, "The transthyretin-related protein: Structural investigation of a novel protein family", *J. Struct. Biol.*, vol. 155, no. 3, pp. 445–457, 2006.

[23] Y. Lee, B. C. Park, D. H. Lee, K. H. Bae, S. Cho, C. H. Lee, J. S. Lee, P. K. Myung and S. G. Park, "Mouse transthyretin-related protein is a hydrolase which degrades 5-hydroxyisourate, the end product of the uricase reaction", *Mol. Cells*, vol. 22, no. 2, pp. 141–145, 2006.

[24] Y. Lee, H. L. Do, W. K. Chang, Y. L. Ah, M. Jang, S. Cho, H. L. Choong, S. L. Jong, K. M. Pyung, B. C. Park and S. G. Park, "Transthyretin-related proteins function to facilitate the hydrolysis of 5-hydroxyisourate, the end product of the uricase reaction", *FEBS Lett.*, vol. 579, no. 21, pp. 4769–4774, 2005.

[25] T. Eneqvist, E. Lundberg, L. Nilsson, R. Abagyan and A. E. Sauer-Eriksson, "The transthyretin-related protein family", *Eur. J. Biochem.*, vol. 270, no. 3, pp. 518–532, 2003.

[26] L. Cendron, I. Ramazzina, R. Percudani, C. Rasore, G. Zanotti and R. Berni, "Probing the evolution of hydroxyisourate hydrolase into transthyretin through active-site redesign", *J. Mol. Biol.*, vol. 409, no. 4, pp. 504–512, 2011.

[27] A. Raz and D. S. Goodman, "The interaction of thyroxine with human plasma prealbumin and with the prealbumin-retinal-binding protein complex", *J. Biol. Chem.*, vol. 244, no. 12, pp. 3230–3237, 1969.

[28] S. J. Richardson, J. A. Monk, C. A. Shepherdley, L. O. E. Ebbesson, F. Sin, D. M. Power, P. B. Frappell, J. Köhrle and M. B. Renfree, "Developmentally regulated thyroid hormone distributor proteins in marsupials, a reptile, and fish", *Am. J. Physiol. Regul. Integr. Comp. Physiol.*, vol. 288, no. 5, pp. R1264–R1272, 2005.

[29] S. F. Nilsson, L. Rask and P. A. Peterson, "Studies on thyroid hormone binding proteins. II. Binding of thyroid hormones, retinol binding protein, and fluorescent probes to prealbumin and effects of thyroxine on prealbumin subunit self association", *J. Biol. Chem.*, vol. 250, no. 21, pp. 8554–8563, 1975.

[30] H. L. Monaco, M. Rizzi and A. Coda, "Structure of a complex of two plasma proteins: transthyretin and retinol-binding protein", *Science*, vol. 268, no. 5213, pp. 1039–1041, 1995.

[31] H. M. Naylor and M. E. Newcomer, "The structure of human retinol-binding protein (RBP) with its carrier protein transthyretin reveals an interaction with the carboxy terminus of RBP", *Biochemistry*, vol. 38, no. 9, pp. 2647–2653, 1999.

[32] J. A. Hamilton and M. D. Benson, "Cellular and Molecular Life Sciences Transthyretin: a review from a structural perspective", *Cell. Mol. Life Sci.*, vol. 58, no. 10, pp. 1491– 1521, 2001.

[33] V. Episkopou, S. Maeda, S. Nishiguchi, K. Shimada, G. A. Gaitanaris, M. E. Gottesman and E. J. Robertson, "Disruption of the transthyretin gene results in mice with depressed levels of plasma retinol and thyroid hormone", *Proc. Natl. Acad. Sci. U. S. A.*, vol. 90, no. 6, pp. 2375–2379, 1993.

[34] A. F. Nunes, M. J. Saraiva and M. M. Sousa, "Transthyretin knockouts are a new mouse model for increased neuropeptide Y", *FASEB J.*, vol. 20, no. 1, pp. 166–168, 2006.

[35] C. E. Fleming, M. J. Saraiva and M. M. Sousa, "Transthyretin enhances nerve regeneration", *J. Neurochem.*, vol. 103, no. 2, pp. 831–839, 2007.

[36] M. A. Liz, F. M. Mar, F. Franquinho and M. M. Sousa, "Aboard transthyretin: From transport to cleavage", *IUBMB Life*, vol. 62, no. 6, pp. 429–435, 2010.

[37] J. Carlos Sousa, C. Grandela, J. Fernández-Ruiz, R. De Miguel, L. De Sousa, A. I. Magalhães, M. João Saraiva, N. Sousa and J. A. Palha, "Transthyretin is involved in depression-like behaviour and exploratory activity", *J. Neurochem.*, vol. 88, no. 5, pp. 1052–1058, 2004.

[38] J. N. Buxbaum, Z. Ye, N. Reixach, L. Friske, C. Levy, P. Das, T. Golde, E. Masliah, A. R. Roberts and T. Bartfai, "Transthyretin protects Alzheimer's mice from the behavioral and biochemical effects of Abeta toxicity", *Proc. Natl. Acad. Sci. U. S. A.*, vol. 105, no. 7, pp. 2681–2686, 2008.

[39] R. Costa, A. Gonçalves, M. J. Saraiva, and I. Cardoso, "Transthyretin binding to A-Beta peptide - Impact on A-Beta fibrillogenesis and toxicity", *FEBS Lett.*, vol. 582, no. 6, pp. 936–942, 2008.

[40] M. A. Liz, C. J. Faro, M. J. Saraiva and M. M. Sousa, "Transthyretin, a new cryptic protease", *J. Biol. Chem.*, vol. 279, no. 20, pp. 21431–21438, 2004.

[41] P. P. Costa, A. S. Figueira, and F. R. Bravo, "Amyloid fibril protein related to prealbumin in familial amyloidotic polyneuropathy", *Proc. Natl. Acad. Sci. U. S. A.*, vol. 75, no. 9, pp. 4499–4503, 1978.

[42] J. N. Buxbaum and C. E. Tagoe, "The genetics of the amyloidoses", *Annu. Rev. Med.*, vol. 51, pp. 543–569, 2000.

[43] J. Hardy and D. J. Selkoe, "The amyloid hypothesis of Alzheimer's disease: progress and problems on the road to therapeutics", *Science*, vol. 297, no. 5580, pp. 353–356, 2002.

[44] R. E. Tanzi and L. Bertram, "Twenty years of the Alzheimer's disease amyloid hypothesis: A genetic perspective", *Cell*, vol. 120, no. 4, pp. 545–555, 2005.

[45] J. Hardy, “The amyloid hypothesis for Alzheimer’s disease: A critical reappraisal”, *J. Neurochem.*, vol. 110, no. 4, pp. 1129–1134, 2009.

[46] M. Jobo, M. Saraiva, P. P. Costa and D. S. Goodman, “Biochemical Marker in Familial Amyloidotic Polyneuropathy, Portuguese Type”, pp. 2171–2177.

[47] P. Westermark, K. Sletten, B. Johansson and G. G. Cornwell, “Fibril in senile systemic amyloidosis is derived from normal transthyretin”, *Proc. Natl. Acad. Sci. U. S. A.*, vol. 87, no. 7, pp. 2843–2845, 1990.

[48] D. R. Jacobson, R. D. Pastore, R. Yaghoubian, I. Kane, G. Gallo, F. S. Buck and J. N. Buxbaum, “Variant-sequence transthyretin (isoleucine 122) in late-onset cardiac amyloidosis in black Americans”, *N. Engl. J. Med.*, vol. 336, no. 7, pp. 466–473, 1997.

[49] A. R. Hurshman, J. T. White, E. T. Powers and J. W. Kelly, “Transthyretin aggregation under partially denaturing conditions is a downhill polymerization”, *Biochemistry*, vol. 43, no. 23, pp. 7365–7381, 2004.

[50] A. Quintas, D. C. Vaz, I. Cardoso, M. J. M. Saraiva and R. M. M. Brito, “Tetramer Dissociation and Monomer Partial Unfolding Precedes Protofibril Formation in Amyloidogenic Transthyretin Variants”, *J. Biol. Chem.*, vol. 276, no. 29, pp. 27207–27213, 2001.

[51] S. M. Johnson, R. L. Wiseman, Y. Sekijima, N. S. Green, S. L. Adamski-Werner and J. W. Kelly, “Native state kinetic stabilization as a strategy to ameliorate protein misfolding diseases: A focus on the transthyretin amyloidoses”, *Acc. Chem. Res.*, vol. 38, no. 12, pp. 911–921, 2005.

[52] W. Colon and J. W. Kelly, “Partial denaturation of transthyretin is sufficient for amyloid fibril formation in vitro”, *Biochemistry*, vol. 31, no. 36, pp. 8654–8660, 1992.

[53] S. L. McCutchen, W. Colon and J. W. Kelly, “Transthyretin mutation Leu-55-Pro significantly alters tetramer stability and increases amyloidogenicity”, *Biochemistry*, vol. 32, no. 45, pp. 12119–12127, 1993.

[54] T. R. Foss, R. L. Wiseman and J. W. Kelly, “The pathway by which the tetrameric protein transthyretin dissociates”, *Biochemistry*, vol. 44, no. 47, pp. 15525–15533, 2005.

[55] S. L. McCutchen, Z. Lai, G. J. Miroy, J. W. Kelly and W. Colon, “Comparison of lethal and nonlethal transthyretin variants and their relationship to amyloid disease”, *Biochemistry*, vol. 34, no. 41, pp. 13527–13536, 1995.

[56] H. A. Lashuel, C. Wurth, L. Woo and J. W. Kelly, “The most pathogenic transthyretin variant, L55P, forms amyloid fibrils under acidic conditions and protofilaments under physiological conditions”, *Biochemistry*, vol. 38, no. 41, pp. 13560–13573, 1999.

[57] H. A. Lashuel, Z. Lai and J. W. Kelly, "Characterization of the transthyretin acid denaturation pathways by analytical ultracentrifugation: Implications for wild-type, V30M, and L55P amyloid fibril formation", *Biochemistry*, vol. 37, no. 51, pp. 17851–17864, 1998.

[58] Z. Lai, W. Colón and J. W. Kelly, "The acid-mediated denaturation pathway of transthyretin yields a conformational intermediate that can self-assemble into amyloid", *Biochemistry*, vol. 35, no. 20, pp. 6470–6482, 1996.

[59] M. J. Bonifácio, Y. Sakaki and M. J. Saraiva, "*In vitro* amyloid fibril formation from transthyretin: The influence of ions and the amyloidogenicity of TTR variants", *Biochim. Biophys. Acta - Mol. Basis Dis.*, vol. 1316, no. 1, pp. 35–42, 1996.

[60] L. C. De Palmieri, L. M. T. R. Lima, J. B. B. Freire, L. Bleicher, I. Polikarpov, F. C. L. Almeida and D. Foguel, "Novel Zn^{2+}-binding sites in human transthyretin: Implications for amyloidogenesis and retinol-binding protein recognition", *J. Biol. Chem.*, vol. 285, no. 41, pp. 31731–31741, 2010.

[61] L. E. Wilkinson-White and S. B. Easterbrook-Smith, "Characterization of the Binding of Cu(II) and Zn(II) to Transthyretin: Effects on Amyloid Formation,", *Biochemistry*, pp. 9123–9132, 2007.

[62] C. C. F. Blake, I. D. A. Swan, C. Rerat, J. Berthou, A. Laurent and B. Rerat, "An X-ray study of the subunit structure of prealbumin", *J. Mol. Biol.*, vol. 61, no. 1, pp. 217–224, 1971.

[63] S. K. Palaninathan, "Nearly 200 X-Ray Crystal Structures of Transthyretin: What Do They Tell Us About This Protein and the Design of Drugs for TTR Amyloidoses?", *Current Medicinal Chemistry*, vol. 19, no. 15. pp. 2324–2342, 2012.

[64] R. A. Pages, J. Robbins and H. Edelhoch, "Binding of thyroxine and thyroxine analogs to human serum prealbumin", *Biochemistry*, vol. 12, no. 14, pp. 2773–2779, 1973.

[65] S. Y. Cheng, R. A. Pages, H. A. Saroff, H. Edelhoch and J. Robbins, "Analysis of thyroid hormone binding to human serum prealbumin by 8-anilinonaphthalene-1-sulfonate fluorescence", *Biochemistry*, vol. 16, no. 16, pp. 3707–3713, 1977.

[66] R. N. Ferguson, H. Edelhoch, H. A. Saroff, J. Robbins and H. J. Cahnmann, "Negative cooperativity in the binding of thyroxine to human serum prealbumin. Preparation of tritium-labeled 8-anilino-1-naphthalenesulfonic acid", *Biochemistry*, vol. 14, no. 2, pp. 282–289, 1975.

[67] S. K. Palaninathan, N. N. Mohamedmohaideen, E. Orlandini, G. Ortore, S. Nencetti, A. Lapucci, A. Rossello, J. S. Freundlich and J. C. Sacchettini, "Novel Transthyretin amyloid fibril formation inhibitors: Synthesis, biological evaluation, and X-ray structural analysis", *PLoS One*, vol. 4, no. 7, 2009.

[68] P. Neumann, V. Cody and A. Wojtczak, “Structural basis of negative cooperativity in transthyretin”, *Acta Biochim. Pol.*, vol. 48, no. 4, pp. 867–875, 2001.

[69] M. Cianci, C. Folli, R. Berni and G. Zanotti, "Structural evidence for asymmetric ligand binding to Transthyretin", *Acta Cryst. D*, 2015 (*under publication*).

[70] M. Haupt, M. P. Blakeley, S. J. Fisher, S. A. Mason, J. B. Cooper, E. P. Mitchell and V. T. Forsyth, “Binding site asymmetry in human transthyretin: insights from a joint neutron and X-ray crystallographic analysis using perdeuterated protein”, *IUCrJ*, vol. 1, no. 6, pp. 429–438, 2014.

[71] N. Pasquato, R. Berni, C. Folli, B. Alfieri, L. Cendron and G. Zanotti, “Acidic pH-induced Conformational Changes in Amyloidogenic Mutant Transthyretin”, *J. Mol. Biol.*, vol. 366, no. 3, pp. 711–719, 2007.

[72] S. K. Palaninathan, N. N. Mohamedmohaideen, W. C. Snee, J. W. Kelly and J. C. Sacchettini, “Structural Insight into pH-Induced Conformational Changes within the Native Human Transthyretin Tetramer”, *J. Mol. Biol.*, vol. 382, no. 5, pp. 1157–1167, 2008.

[73] T. Eneqvist, K. Andersson, A. Olofsson, E. Lundgren and A. E. Sauer-Eriksson, “The beta-slip: a novel concept in transthyretin amyloidosis”, *Mol. Cell*, vol. 6, no. 5, pp. 1207–1218, 2000.

[74] Y. Sekijima, J. W. Kelly and S. Ikeda, “Pathogenesis of and therapeutic strategies to ameliorate the transthyretin amyloidoses”, *Curr. Pharm. Des.*, vol. 14, no. 30, pp. 3219–3230, 2008.

[75] A. M. Damas and M. J. Saraiva, “Review: TTR amyloidosis-structural features leading to protein aggregation and their implications on therapeutic strategies”, *J. Struct. Biol.*, vol. 130, no. 2–3, pp. 290–299, 2000.

[76] M. J. Pröpsting, M. Blaschke, R. E. Haas, J. Genschel, H. J. Hedrich, M. P. Manns and H. H. Schmidt, “Inosine(15.1) hammerhead ribozymes for targeting the transthyretin-30 mutation”, *Biochem. Biophys. Res. Commun.*, vol. 260, no. 2, pp. 313–317, 1999.

[77] K. Tanaka, T. Yamada, Y. Ohyagi, H. Asahara, I. Horiuchi and J. I. Kira, “Suppression of transthyretin expression by ribozymes: A possible therapy for familial amyloidotic polyneuropathy”, *J. Neurol. Sci.*, vol. 183, no. 1, pp. 79–84, 2001.

[78] M. D. Benson, B. Kluve-Beckerman, S. R. Zeldenrust, A. M. Siesky, D. M. Bodenmiller, A. D. Showalter and K. W. Sloop, “Targeted suppression of an amyloidogenic transthyretin with antisense oligonucleotides”, *Muscle and Nerve*, vol. 33, no. 5, pp. 609–618, 2006.

[79] M. Nakamura, Y. Ando, S. Nagahara, A. Sano, T. Ochiya, S. Maeda, T. Kawaji, M. Ogawa, A. Hirata, H. Terazaki, K. Haraoka, H. Tanihara, M. Ueda, M. Uchino and K. Yamamura, "Targeted conversion of the transthyretin gene in vitro and in vivo", *Gene Ther.*, vol. 11, no. 10, pp. 838–846, 2004.

[80] T. Kurosawa, S. Igarashi, M. Nishizawa and O. Onodera, "Selective silencing of a mutant transthyretin allele by small interfering RNAs", *Biochem. Biophys. Res. Commun.*, vol. 337, no. 3, pp. 1012–1018, 2005.

[81] P. Hammarström, F. Schneider and J. W. Kelly, "Trans-suppression of misfolding in an amyloid disease", *Science*, vol. 293, no. 5539, pp. 2459–2462, 2001.

[82] J. C. Sacchettini and J. W. Kelly, "Therapeutic strategies for human amyloid diseases", *Nat. Rev. Drug Discov.*, vol. 1, no. 4, pp. 267–275, 2002.

[83] H. Terazaki, Y. Ando, R. Fernandes, K. Yamamura, S. Maeda and M. J. Saraiva, "Immunization in familial amyloidotic polyneuropathy: counteracting deposition by immunization with a Y78F TTR mutant", *Lab. Invest.*, vol. 86, no. 1, pp. 23–31, 2006.

[84] S. S. Ray, R. J. Nowak, R. H. Brown and P. T. Lansbury, "Small-molecule-mediated stabilization of familial amyotrophic lateral sclerosis-linked superoxide dismutase mutants against unfolding and aggregation", *Proc. Natl. Acad. Sci. U. S. A.*, vol. 102, no. 10, pp. 3639–3644, 2005.

[85] D. R. Booth, M. Sunde, V. Bellotti, C. V Robinson, W. L. Hutchinson, P. E. Fraser, P. N. Hawkins, C. M. Dobson, S. E. Radford, C. C. Blake and M. B. Pepys, "Instability, unfolding and aggregation of human lysozyme variants underlying amyloid fibrillogenesis", *Nature*, vol. 385, no. 6619, pp. 787–793, 1997.

[86] M. Dumoulin, A. M. Last, A. Desmyter, K. Decanniere, D. Canet, G. Larsson, A. Spencer, D. B. Archer, J. Sasse, S. Muyldermans, L. Wyns, C. Redfield, A. Matagne, C. V Robinson and C. M. Dobson, "A camelid antibody fragment inhibits the formation of amyloid fibrils by human lysozyme", *Nature*, vol. 424, no. 6950, pp. 783–788, 2003.

[87] G. J. Miroy, Z. Lai, H. A. Lashuel, S. A. Peterson, C. Strang and J. W. Kelly, "Inhibiting transthyretin amyloid fibril formation via protein stabilization", *Proc. Natl. Acad. Sci. U. S. A.*, vol. 93, no. 26, pp. 15051–15056, 1996.

[88] T. Klabunde, H. M. Petrassi, V. B. Oza, P. Raman, J. W. Kelly and J. C. Sacchettini, "Rational design of potent human transthyretin amyloid disease inhibitors", *Nat. Struct. Biol.*, vol. 7, no. 4, pp. 312–321, 2000.

[89] S. L. Adamski-Werner, S. K. Palaninathan, J. C. Sacchettini and J. W. Kelly, "Diflunisal Analogues Stabilize the Native State of Transthyretin. Potent Inhibition of Amyloidogenesis", *J. Med. Chem.*, vol. 47, no. 2, pp. 355–374, 2004.

[90] S. A. Peterson, T. Klabunde, H. A. Lashuel, H. Purkey, J. C. Sacchettini and J. W. Kelly, "Inhibiting transthyretin conformational changes that lead to amyloid fibril formation", *Proc. Natl. Acad. Sci. U. S. A.*, vol. 95, no. 22, pp. 12956–12960, 1998.

[91] T. Mairal, J. Nieto, M. Pinto, M. R. Almeida, L. Gales, A. Ballesteros, J. Barluenga, J. J. Pérez, J. T. Vázquez, N. B. Centeno, M. J. Saraiva, A. M. Damas, A. Planas, G. Arsequell and G. Valencia, "Iodine atoms: A new molecular feature for the design of potent transthyretin fibrillogenesis inhibitors", *PLoS One*, vol. 4, no. 1, 2009.

[92] S. M. Johnson, S. Connelly, C. Fearns, E. T. Powers and J. W. Kelly, "The transthyretin amyloidoses: From delineating the molecular mechanism of aggregation linked to pathology to a regulatory-agency-approved drug", *Journal of Molecular Biology*, vol. 421, no. 2–3. pp. 185–203, 2012.

[93] A. Wojtczak, V. Cody, J. R. Luft and W. Pangborn, "Structures of human transthyretin complexed with thyroxine at 2.0 Å resolution and 3',5'-dinitro-N-acetyl-L-thyronine at 2.2 Å resolution", *Acta Crystallogr. D. Biol. Crystallogr.*, vol. 52, no. 4, pp. 758–765, 1996.

[94] G. Fex, P. A. Albertsson, and B. Hansson, "Interaction between prealbumin and retinol-binding protein studied by affinity chromatography, gel filtration and two-phase partition", *Eur. J. Biochem.*, vol. 99, no. 2, pp. 353–360, 1979.

[95] G. Malpeli, C. Folli and R. Berni, "Retinoid binding to retinol-binding protein and the interference with the interaction with transthyretin", *Biochim. Biophys. Acta - Protein Struct. Mol. Enzymol.*, vol. 1294, no. 1, pp. 48–54, 1996.

[96] G. Zanotti, C. Folli, L. Cendron, B. Alfieri, S. K. Nishida, F. Gliubich, N. Pasquato, A. Negro and R. Berni, "Structural and mutational analyses of protein-protein interactions between transthyretin and retinol-binding protein", *FEBS J.*, vol. 275, no. 23, pp. 5841–5854, 2008.

[97] G. Zanotti and R. Berni, "Plasma Retinol-Binding Protein: Structure and Interactions with Retinol, Retinoids, and Transthyretin", *Vitam. Horm.*, vol. 69, pp. 271–295, 2004.

[98] C. E. Bulawa, S. Connelly, M. DeVit, L. Wang, C. Weigel, J. A. Fleming, J. Packman, E. T. Powers, R. L. Wiseman, T. R. Foss, I. A. Wilson, J. W. Kelly and R. Labaudiniere, "Tafamidis, a potent and selective transthyretin kinetic stabilizer that inhibits the amyloid cascade", *Proceedings of the National Academy of Sciences*, vol. 109, no. 24. pp. 9629–9634, 2012.

[99] G. Zanotti, L. Cendron, C. Folli, P. Florio, B. Pietro Imbimbo and R. Berni, "Structural evidence for native state stabilization of a conformationally labile amyloidogenic transthyretin variant by fibrillogenesis inhibitors", *FEBS Lett.*, vol. 587, no. 15, pp. 2325–2331, 2013.

[100] B. P. Imbimbo, E. Del Giudice, D. Colavito, A. D. Arrigo, M. D. Carbonare, G. Villetti, F. Facchinetti, R. Volta, V. Pietrini, M. F. Baroc, L. Serneels, B. De Strooper and A. Leon, "Cyclopropanecarboxylic Acid (CHF5074), a Novel γ-Secretase Modulator, Reduces Brain β-Amyloid Pathology in a Transgenic Mouse Model of Alzheimer's Disease without Causing Peripheral Toxicity", *Pharmacology*, vol. 323, no. 3, pp. 822–830, 2007.

[101] B. P. Imbimbo, B. Hutter-Paier, G. Villetti, F. Facchinetti, V. Cenacchi, R. Volta, A. Lanzillotta, M. Pizzi and M. Windisch, "CHF5074, a novel γ-secretase modulator, attenuates brain β-amyloid pathology and learning deficit in a mouse model of Alzheimer's disease", *Br. J. Pharmacol.*, vol. 156, no. 6, pp. 982–993, 2009.

[102] Y. Mu, S. Jin, J. Shen, A. Sugano, Y. Takaoka, L. Qiang, B. P. Imbimbo, K. Yamamura and Z. Li, "CHF5074 (CSP-1103) stabilizes human transthyretin in mice humanized at the transthyretin and retinol-binding protein loci", *FEBS Lett.*, vol. 589, no. 7, pp. 849–856, 2015.

[103] I. Peretto, S. Radaelli, C. Parini, M. Zandi, L. F. Raveglia, G. Dondio, L. Fontanella, P. Misiano, C. Bigogno, A. Rizzi, B. Riccardi, M. Biscaioli, S. Marchetti, P. Puccini, S. Catinella, I. Rondelli, V. Cenacchi, P. T. Bolzoni, P. Caruso, G. Villetti, F. Facchinetti, E. Del Giudice, N. Moretto and B. P. Imbimbo, "Synthesis and biological activity of flurbiprofen analogues as selective inhibitors of beta-amyloid42 secretion", *J. Med. Chem.*, vol. 48, no. 18, pp. 5705–20, 2005.

[104] W. Kabsch, "Xds", *Acta Crystallogr. Sect. D Biol. Crystallogr.*, vol. 66, no. 2, pp. 125–132, 2010.

[105] P. Evans, "Scaling and assessment of data quality", *Acta Crystallogr. Sect. D Biol. Crystallogr.*, vol. 62, no. 1, pp. 72–82, 2006.

[106] M. D. Winn, C. C. Ballard, K. D. Cowtan, E. J. Dodson, P. Emsley, P. R. Evans, R. M. Keegan, E. B. Krissinel, A. G. W. Leslie, A. McCoy, S. J. McNicholas, G. N. Murshudov, N. S. Pannu, E. A. Potterton, H. R. Powell, R. J. Read, A. Vagin and K. S. Wilson, "Overview of the CCP4 suite and current developments", *Acta Crystallogr. Sect. D Biol. Crystallogr.*, vol. 67, no. 4, pp. 235–242, 2011.

[107] J. Painter and E. A. Merritt, "Optimal description of a protein structure in terms of multiple groups undergoing TLS motion", *Acta Crystallogr. Sect. D Biol. Crystallogr.*, vol. 62, no. 4, pp. 439–450, 2006.

[108] A. W. Schüttelkopf and D. M. F. Van Aalten, "PRODRG: A tool for high-throughput crystallography of protein-ligand complexes", *Acta Crystallogr. Sect. D Biol. Crystallogr.*, vol. 60, no. 8, pp. 1355–1363, 2004.

[109] P. D. Adams, P. V. Afonine, G. Bunkóczi, V. B. Chen, I. W. Davis, N. Echols, J. J. Headd, L. W. Hung, G. J. Kapral, R. W. Grosse-Kunstleve, A. J. McCoy, N. W. Moriarty, R. Oeffner, R. J. Read, D. C. Richardson, J. S. Richardson, T.

C. Terwilliger, and P. H. Zwart, “PHENIX: A comprehensive Python-based system for macromolecular structure solution”, *Acta Crystallogr. Sect. D Biol. Crystallogr.*, vol. 66, no. 2, pp. 213–221, 2010.

[110] P. Emsley and K. Cowtan, “Coot: Model-building tools for molecular graphics”, *Acta Crystallogr. Sect. D Biol. Crystallogr.*, vol. 60, no. 12 I, pp. 2126–2132, 2004.

[111] S. M. Johnson, S. Connelly, I. A. Wilson and J. W. Kelly, “Biochemical and structural evaluation of highly selective 2-arylbenzoxazole-based transthyretin amyloidogenesis inhibitors”, *J. Med. Chem.*, vol. 51, no. 2, pp. 260–270, 2008.

[112] G. Said, S. Grippon and P. Kirkpatrick, “Tafamidis”, *Nat. Rev. Drug Discov.*, vol. 11, no. 3, pp. 185–186, 2012.

[113] C. Montecucco and R. Rappuoli, “Living dangerously: how *Helicobacter pylori* survives in the human stomach”, *Nat. Rev. Mol. Cell Biol.*, vol. 2, no. 6, pp. 457–466, 2001.

[114] H. Mobley, M. Island and R. Hausinger, “Molecular biology of microbial ureases”, *Microbiol. Rev.*, vol. 59, no. 3, pp. 451–480, 1995.

[115] F. Megraud, V. Neman-Simha and D. Brugmann, “Further evidence of the toxic effect of ammonia produced by *Helicobacter pylori* urease on human epithelial cells”, *Infect. Immun.*, vol. 60, no. 5, pp. 1858–1863, 1992.

[116] K. A. Eaton, C. L. Brooks, D. R. Morgan and S. Krakowka, “Essential role of urease in pathogenesis of gastritis induced by *Helicobacter pylori* in gnotobiotic piglets”, *Infect. Immun.*, vol. 59, no. 7, pp. 2470–2475, 1991.

[117] P. W. O’ Toole, M. C. Lane and S. Porwollik, “*Helicobacter pylori* motility”, *Microbes Infect.*, vol. 2, no. 10, pp. 1207–1214, 2000.

[118] K. A. Eaton, D. R. Morgan and S. Krakowka, “*Campylobacter pylori* virulence factors in gnotobiotic piglets”, *Infect. Immun.*, vol. 57, no. 4, pp. 1119–1125, 1989.

[119] Y. Yamaoka, “Mechanisms of disease: *Helicobacter pylori* virulence factors”, *Nat. Rev. Gastroenterol. Hepatol.*, vol. 7, no. 11, pp. 629–641, 2011.

[120] J. G. Kusters, A. H. M. Van Vliet and E. J. Kuipers, “Pathogenesis of *Helicobacter pylori* infection”, *Clin. Microbiol. Rev.*, vol. 19, no. 3, pp. 449–490, 2006.

[121] S. Backert, E. Ziska, V. Brinkmann, U. Zimny-Arndt, A. Fauconnier, P. R. Jungblut, M. Naumann and T. F. Meyer, “Translocation of the *Helicobacter pylori* CagA protein in gastric epithelial cells by a type IV secretion apparatus”, *Cell. Microbiol.*, vol. 2, no. 2, pp. 155–164, 2000.

[122] K. M. Bourzac and K. Guillemin, "*Helicobacter pylori*-host cell interactions mediated by type IV secretion", *Cell. Microbiol.*, vol. 7, no. 7, pp. 911–919, 2005.

[123] E. J. Kuipers, "*Helicobacter pylori* and the risk and management of associated diseases: gastritis, ulcer disease, atrophic gastritis and gastric cancer", *Aliment. Pharmacol. Ther.*, vol. 11 Suppl 1, pp. 71–88, 1997.

[124] T. L. Cover and M. J. Blaser, "Purification and characterization of the vacuolating cytotoxin from *Helicobacter pylori*", *J.Biol.Chem.*, vol. 267, no. 15, pp. 10570–10575, 1992.

[125] T. L. Cover, C. P. Dooley, and M. J. Blaser, "Characterization of and human serologic response to proteins in *Helicobacter pylori* broth culture supernatants with vacuolizing cytotoxin activity", *Infect. Immun.*, vol. 58, no. 3, pp. 603–610, 1990.

[126] T. L. Cover and S. R. Blanke, "*Helicobacter pylori* VacA, a paradigm for toxin multifunctionality", *Nat. Rev. Microbiol.*, vol. 3, no. 4, pp. 320–332, 2005.

[127] J. M. Ketley, "Pathogenesis of enteric infection by *Campylobacter*", *Microbiology*, vol. 143, no. 1 997, pp. 5–21, 1997.

[128] M. J. Blaser, "Epidemiologic and clinical features of *Campylobacter jejuni* infections", *J. Infect. Dis.*, vol. 176 Suppl , no. Suppl 2, pp. S103–S105, 1997.

[129] S. F. Altekruse, N. J. Stern, P. I. Fields and D. L. Swerdlow, "*Campylobacter jejuni* - An emerging foodborne pathogen", *Emerg. Infect. Dis.*, vol. 5, no. 1, pp. 28–35, 1999.

[130] M. C. Peterson, "Clinical aspects of *Campylobacter jejuni* infections in adults", *West. J. Med.*, vol. 161, no. 2, pp. 148–152, 1994.

[131] B. M. Allos, "*Campylobacter jejuni* Infections: update on emerging issues and trends", *Clin. Infect. Dis.*, vol. 32, no. 8, pp. 1201–1206, 2001.

[132] B. M. Allos, "Association between *Campylobacter* infection and Guillain-Barré syndrome", *J. Infect. Dis.*, vol. 176 Suppl , no. Suppl 2, pp. S125–S128, 1997.

[133] I. Nachamkin, B. M. Allos and T. Ho, "*Campylobacter* Species and Guillain-Barré Syndrome", *Clin. Microbiol. Rev.*, vol. 11, no. 3, pp. 555–567, 1998.

[134] A. Elmi, E. Watson, P. Sandu, O. Gundogdu, D. C. Mills, N. F. Inglis, E. Manson, L. Imrie, M. Bajaj-Elliott, B. W. Wren, D. G. E. Smith and N. Dorrell, "*Campylobacter jejuni* outer membrane vesicles play an important role in bacterial interactions with human intestinal epithelial cells", *Infect. Immun.*, vol. 80, no. 12, pp. 4089–4098, 2012.

[135] B. Lindmark, P. K. Rompikuntal, K. Vaitkevicius, T. Song, Y. Mizunoe, B. E. Uhlin, P. Guerry and S. N. Wai, "Outer membrane vesicle-mediated release of cytolethal distending toxin (CDT) from *Campylobacter jejuni*", *BMC Microbiol.*, vol. 9, p. 220, 2009.

[136] J. Parkhill, B. W. Wren, K. Mungall, J. M. Ketley, C. Churcher, D. Basham, T. Chillingworth, R. M. Davies, T. Feltwell, S. Holroyd, K. Jagels, A. V Karlyshev, S. Moule, M. J. Pallen, C. W. Penn, M. A. Quail, M. A. Rajandream, K. M. Rutherford, A. H. van Vliet, S. Whitehead and B. G. Barrell, "The genome sequence of the food-borne pathogen *Campylobacter jejuni* reveals hypervariable sequences", *Nature*, vol. 403, no. 6770, pp. 665–668, 2000.

[137] T. Clausen, M. Kaiser, R. Huber and M. Ehrmann, "HTRA proteases: regulated proteolysis in protein quality control", *Nat. Rev. Mol. Cell Biol.*, vol. 12, no. 3, pp. 152–162, 2011.

[138] T. Clausen, C. Southan and M. Ehrmann, "The HtrA Family of Proteases: Implications for Protein Composition and Cell Fate", *Mol. Cell*, vol. 10, no. 3, pp. 443–455, 2002.

[139] B. Lipinska, O. Fayet, L. Baird and C. Georgopoulos, "Identification, Characterization, and Mapping of the *Escherichia coli* HtrA Gene, whose Product is Essential for Bacterial-Growth Only at Elevated-Temperatures", *J. Bacteriol.*, vol. 171, no. 3, pp. 1574–1584, 1989.

[140] K. L. Strauch and J. Beckwith, "An *Escherichia coli* mutation preventing degradation of abnormal periplasmic proteins", *Proc. Natl. Acad. Sci. U. S. A.*, vol. 85, no. 5, pp. 1576–1580, 1988.

[141] M. J. Page and E. Di Cera, "Evolution of peptidase diversity", *J. Biol. Chem.*, vol. 283, no. 44, pp. 30010–30014, 2008.

[142] P. F. Huesgen, H. Schuhmann and I. Adamska, "Deg/HtrA proteases as components of a network for photosystem II quality control in chloroplasts and cyanobacteria", *Res. Microbiol.*, vol. 160, no. 9, pp. 726–732, 2009.

[143] M. García-Lorenzo, A. Sjödin, S. Jansson and C. Funk, "Protease gene families in *Populus* and *Arabidopsis*", *BMC Plant Biol.*, vol. 6, p. 30, 2006.

[144] H. Kolmar, P. R. H. Waller and R. T. Sauer, "The DegP and DegQ periplasmic endoproteases of *Escherichia coli*: Specificity for cleavage sites and substrate conformation", *J. Bacteriol.*, vol. 178, no. 20, pp. 5925–5929, 1996.

[145] T. Krojer, J. Sawa, E. Schäfer, H. R. Saibil, M. Ehrmann, and T. Clausen, "Structural basis for the regulated protease and chaperone function of DegP", *Nature*, vol. 453, no. 7197, pp. 885–890, 2008.

[146] Q. T. Shen, X. C. Bai, L. F. Chang, Y. Wu, H. W. Wang, and S. F. Sui, "Bowl-shaped oligomeric structures on membranes as DegP's new functional forms in protein quality control", *Proc. Natl. Acad. Sci. U. S. A.*, vol. 106, no. 12, pp. 4858–4863, 2009.

[147] R. Wrase, H. Scott, R. Hilgenfeld and G. Hansen, "The *Legionella* HtrA homologue DegQ is a self-compartmentizing protease that forms large 12-meric assemblies" *Proc. Natl. Acad. Sci. U. S. A.*, vol. 108, no. 26, pp. 10490–10495, 2011.

[148] J. Jiang, X. Zhang, Y. Chen, Y. Wu, Z. H. Zhou, Z. Chang and S. F. Sui, "Activation of DegP chaperone-protease via formation of large cage-like oligomers upon binding to substrate proteins", *Proc. Natl. Acad. Sci. U. S. A.*, vol. 105, no. 33, pp. 11939–11944, 2008.

[149] C. Wilken, K. Kitzing, R. Kurzbauer, M. Ehrmann and T. Clausen, "Crystal structure of the DegS stress sensor: How a PDZ domain recognizes misfolded protein and activates a protease", *Cell*, vol. 117, no. 4, pp. 483–494, 2004.

[150] N. N. MohamedMohaideen, S. K. Palaninathan, P. M. Morin, B. J. Williams, M. Braunstein, S. E. Tichy, J. Locker, D. H. Russell, W. R. Jacobs and J. C. Sacchettini, "Structure and function of the virulence-associated high-temperature requirement A of *Mycobacterium tuberculosis*", *Biochemistry*, vol. 47, no. 23, pp. 6092–6102, 2008.

[151] C. Spiess, A. Beil and M. Ehrmann, "A temperature-dependent switch from chaperone to protease in a widely conserved heat shock protein", *Cell*, vol. 97, no. 3, pp. 339–347, 1999.

[152] J. Skórko-Glonek, D. Zurawa, E. Kuczwara, M. Wozniak, Z. Wypych and B. Lipinska, "The *Escherichia coli* heat shock protease HtrA participates in defense against oxidative stress", *Mol. Gen. Genet.*, vol. 262, no. 2, pp. 342–350, 1999.

[153] O. Onder, S. Turkarslan, D. Sun and F. Daldal, "Overproduction or absence of the periplasmic protease DegP severely compromises bacterial growth in the absence of the dithiol: disulfide oxidoreductase DsbA", *Mol. Cell. Proteomics*, vol. 7, no. 5, pp. 875–890, 2008.

[154] J. Skórko-Glonek, A. Wawrzynow, K. Krzewski, K. Kurpierz, B. Lipinska and A. Wawrzynw, "Site-directed mutagenesis of the HtrA (DegP) serine-protease, whose proteolytic activity is indispensable for *Escherichia coli* survival at elevated-temperatures", *Gene*, vol. 163, no. 1, pp. 47–52, 1995.

[155] B. M. Alba and C. A. Gross, "Regulation of the *Escherichia coli* sigma-dependent envelope stress response", *Mol. Microbiol.*, vol. 52, no. 3, pp. 613–619, 2004.

[156] C. Foucaud-Scheunemann and I. Poquet, “HtrA is a key factor in the response to specific stress conditions in *Lactococcus lactis*”, *FEMS Microbiol. Lett.*, vol. 224, no. 1, pp. 53–59, 2003.

[157] S. Biswas, S. Biswas, I. Biswas and I. Biswas, “Role of HtrA in Surface Protein Expression and BioFilm Formation by *Streptococcus mutans*”, *Microbiology*, vol. 73, no. 10, pp. 6923–6934, 2005.

[158] C. Baud, H. Hodak, E. Willery, H. Drobecq, C. Locht, M. Jamin and F. Jacob-Dubuisson, “Role of DegP for two-partner secretion in *Bordetella*”, *Mol. Microbiol.*, vol. 74, no. 2, pp. 315–329, 2009.

[159] B. Hoy, M. Löwer, C. Weydig, G. Carra, N. Tegtmeyer, T. Geppert, P. Schröder, N. Sewald, S. Backert, G. Schneider and S. Wessler, “*Helicobacter pylori* HtrA is a new secreted virulence factor that cleaves E-cadherin to disrupt intercellular adhesion”, *EMBO Rep.*, vol. 11, no. 10, pp. 798–804, 2010.

[160] W. M. Huston, “Bacterial proteases from the intracellular vacuole niche; Protease conservation and adaptation for pathogenic advantage”, *FEMS Immunol. Med. Microbiol.*, vol. 59, no. 1, pp. 1–10, 2010.

[161] H. Ingmer and L. Brøndsted, “Proteases in bacterial pathogenesis”, *Res. Microbiol.*, vol. 160, no. 9, pp. 704–710, 2009.

[162] R. L. Wilson, L. L. Brown, D. Kirkwood-Watts, T. K. Warren, S. A. Lund, D. S. King, K. F. Jones, and D. E. Hruby, “*Listeria monocytogenes* 10403S HtrA is necessary for resistance to cellular stress and virulence”, *Infect. Immun.*, vol. 74, no. 1, pp. 765–768, 2006.

[163] H. M. Stack, R. D. Sleator, M. Bowers, C. Hill, and C. G. M. Gahan, “Role for HtrA in Stress Induction and Virulence Potential in *Listeria monocytogenes*”, vol. 71, no. 8, pp. 4241–4247, 2005.

[164] G. Rowley, A. Stevenson, J. Kormanec and M. Roberts, “Effect of inactivation of degS on *Salmonella enterica serovar typhimurium in vitro* and *in vivo*”, *Infect. Immun.*, vol. 73, no. 1, pp. 459–463, 2005.

[165] R. S. Flannagan, D. Aubert, C. Kooi, P. A. Sokol and M. A. Valvano, “*Burkholderia cenocepacia* requires a periplasmic HtrA protease for growth under thermal and osmotic stress and for survival *in vivo*”, *Infect. Immun.*, vol. 75, no. 4, pp. 1679–1689, 2007.

[166] J. Farn and M. Roberts, “Effect of inactivation of the HtrA-like serine protease DegQ on the virulence of *Salmonella enterica serovar Typhimurium* in mice”, *Infect. Immun.*, vol. 72, no. 12, pp. 7357–7359, 2004.

[167] T. Chitlaru, G. Zaide, S. Ehrlich, I. Inbar, O. Cohen and A. Shafferman, “HtrA is a major virulence determinant of *Bacillus anthracis*”, *Mol. Microbiol.*, vol. 81, no. 6, pp. 1542–1559, 2011.

[168] T. L. Raivio, "Envelope stress responses and Gram-negative bacterial pathogenesis," *Mol. Microbiol.*, vol. 56, no. 5, pp. 1119–1128, 2005.

[169] S. Humphreys, A. Stevenson, A. Bacon, A. B. Weinhardt and M. Roberts, "The alternative sigma factor, σ(E), is critically important for the virulence of *Salmonella typhimurium*", *Infect. Immun.*, vol. 67, no. 4, pp. 1560–1568, 1999.

[170] G. Cortés, B. De Astorza, V. J. Benedí and S. Albertí, "Role of the htrA gene in *Klebsiella pneumoniae* virulence", *Infect. Immun.*, vol. 70, no. 9, pp. 4772–4776, 2002.

[171] S. R. Li, N. Dorrell, P. H. Everest, G. Dougan and B. W. Wren, "Construction and characterization of a *Yersinia enterocolitica* O:8 high-temperature requirement (htrA) isogenic mutant", *Infect. Immun.*, vol. 64, no. 6, pp. 2088–2094, 1996.

[172] G. Hansen and R. Hilgenfeld, "Architecture and regulation of HtrA-family proteins involved in protein quality control and stress response", *Cell. Mol. Life Sci.*, vol. 70, no. 5, pp. 761–775, 2013.

[173] H. Itzhaki, L. Naveh, M. Lindahl, M. Cook and Z. Adam, "Identification and characterization of DegP, a serine protease associated with the luminal side of the thylakoid membrane", *J. Biol. Chem.*, vol. 273, no. 12, pp. 7094–7096, 1998.

[174] E. Kapri-Pardes, L. Naveh and Z. Adam, "The thylakoid lumen protease Deg1 is involved in the repair of photosystem II from photoinhibition in *Arabidopsis*", *Plant Cell*, vol. 19, no. 3, pp. 1039–1047, 2007.

[175] X. Sun, M. Ouyang, J. Guo, J. Ma, C. Lu, Z. Adam and L. Zhang, "The thylakoid protease Deg1 is involved in photosystem-II assembly in *Arabidopsis thaliana*", *Plant J.*, vol. 62, no. 2, pp. 240–249, 2010.

[176] M. Edelman and A. K. Mattoo, "D1-protein dynamics in photosystem II: The lingering enigma", *Photosynth. Res.*, vol. 98, no. 1–3, pp. 609–620, 2008.

[177] S. Grau, A. Baldi, R. Bussani, X. Tian, R. Stefanescu, M. Przybylski, P. Richards, S. A. Jones, V. Shridhar, T. Clausen and M. Ehrmann, "Implications of the serine protease HtrA1 in amyloid precursor protein processing", *Proc. Natl. Acad. Sci. U. S. A.*, vol. 102, no. 17, pp. 6021–6026, 2005.

[178] J. Chien and M. Campioni, "HtrA serine proteases as potential therapeutic targets in cancer", *Cancer Drug Targets*, vol. 9, no. 4, pp. 451–468, 2009.

[179] H. R. Coleman, C. C. Chan, F. L. Ferris and E. Y. Chew, "Age-related macular degeneration", *Lancet*, vol. 372, no. 9652, pp. 1835–1845, 2008.

[180] K. Hara, A. Shiga, T. Fukutake, H. Nozaki, A. Miyashita, A. Yokoseki, H. Kawata, A. Koyama, K. Arima, T. Takahashi, M. Ikeda, H. Shiota, M.

Tamura, Y. Shimoe, M. Hirayama, T. Arisato, S. Yanagawa, A. Tanaka, I. Nakano, S. Ikeda, Y. Yoshida, T. Yamamoto, T. Ikeuchi, R. Kuwano, M. Nishizawa, S. Tsuji and O. Onodera, "Association of HTRA1 mutations and familial ischemic cerebral small-vessel disease", *N. Engl. J. Med.*, vol. 360, no. 17, pp. 1729–1739, 2009.

[181] J. M. Milner, A. Patel and A. D. Rowan, "Emerging roles of serine proteinases in tissue turnover in arthritis", *Arthritis Rheum.*, vol. 58, no. 12, pp. 3644–3656, 2008.

[182] J. Chien, T. Ota, G. Aletti, R. Shridhar, M. Boccellino, L. Quagliuolo, A. Baldi and V. Shridhar, "Serine protease HtrA1 associates with microtubules and inhibits cell migration", *Mol. Cell. Biol.*, vol. 29, no. 15, pp. 4177–4187, 2009.

[183] J. Chien, G. Aletti, A. Baldi, V. Catalano, P. Muretto, G. L. Keeney, K. R. Kalli, J. Staub, M. Ehrmann, W. A. Cliby, Y. K. Lee, K. C. Bible, L. C. Hartmann, S. H. Kaufmann and V. Shridhar, "Serine protease HtrA1 modulates chemotherapy-induced cytotoxicity", *J. Clin. Invest.*, vol. 116, no. 7, pp. 1994–2004, 2006.

[184] A. Baldi, A. De Luca, M. Morini, T. Battista, A. Felsani, F. Baldi, C. Catricalà, A. Amantea, D. M. Noonan, A. Albini, P. G. Natali, D. Lombardi and M. G. Paggi, "The HtrA1 serine protease is down-regulated during human melanoma progression and represses growth of metastatic melanoma cells", *Oncogene*, vol. 21, no. 43, pp. 6684–6688, 2002.

[185] L. M. Martins, A. Morrison, K. Klupsch, V. Fedele, N. Moisoi, P. Teismann, A. Abuin, E. Grau, M. Geppert, P. George, C. L. Creasy, A. Martin, I. Hargreaves, S. J. Heales, H. Okada, S. Brandner, B. Schulz, T. Mak, J. Downward and G. P. Livi, "Neuroprotective Role of the Reaper-Related Serine Protease HtrA2/Omi Revealed by Targeted Deletion in Mice", *Mol. Cell. Biol.*, vol. 24, no. 22, pp. 9848–9862, 2004.

[186] N. Singh, R. R. Kuppili and K. Bose, "The structural basis of mode of activation and functional diversity: A case study with HtrA family of serine proteases", *Arch. Biochem. Biophys.*, vol. 516, no. 2, pp. 85–96, 2011.

[187] F. Jeleń, A. Oleksy, K. Śmietana and J. Otlewski, "PDZ domains - Common players in the cell signaling", *Acta Biochim. Pol.*, vol. 50, no. 4, pp. 985–1017, 2003.

[188] A. S. Fanning and J. M. Anderson, "Protein–protein interactions: PDZ domain networks", pp. 1385–1388, 1996.

[189] P. Jemth and S. Gianni, "PDZ domains: Folding and binding", *Biochemistry*, vol. 46, no. 30, pp. 8701–8708, 2007.

[190] H. J. Lee and J. J. Zheng, "PDZ domains and their binding partners: structure, specificity, and modification", *Cell Commun. Signal.*, vol. 8, p. 8, 2010.

[191] C. Southan, "A genomic perspective on human proteases as drug targets", *Drug Discov. Today*, vol. 6, no. 13, pp. 681–688, Jul. 2001.

[192] L. Brøndsted, M. T. Andersen, M. Parker, K. Jørgensen and H. Ingmer, "The HtrA protease of *Campylobacter jejuni* is required for heat and oxygen tolerance and for optimal interaction with human epithelial cells", *Appl. Environ. Microbiol.*, vol. 71, no. 6, pp. 3205–3212, 2005.

[193] K. T. Bæk, C. S. Vegge, J. Skórko-Glonek, and L. Brøndsted, "Different contributions of HtrA protease and chaperone activities to *Campylobacter jejuni* stress tolerance and physiology", *Appl. Environ. Microbiol.*, vol. 77, no. 1, pp. 57–66, 2011.

[194] K. T. Bæk, C. S. Vegge and L. Brøndsted, "HtrA chaperone activity contributes to host cell binding in *Campylobacter jejuni*", *Gut Pathog.*, vol. 3, no. 1, p. 13, 2011.

[195] B. Hoy, T. Geppert, M. Boehm, F. Reisen, P. Plattner, G. Gadermaier, N. Sewald, F. Ferreira, P. Briza, G. Schneider, S. Backert and S. Wessler, "Distinct roles of secreted HtrA proteases from gram-negative pathogens in cleaving the junctional protein and tumor suppressor E-cadherin", *J. Biol. Chem.*, vol. 287, no. 13, pp. 10115–10120, 2012.

[196] M. Boehm, B. Hoy, M. Rohde, N. Tegtmeyer, K. T. Bæk, O. A. Oyarzabal, L. Brøndsted, S. Wessler and S. Backert, "Rapid paracellular transmigration of *Campylobacter jejuni* across polarized epithelial cells without affecting TER: role of proteolytic-active HtrA cleaving E-cadherin but not fibronectin", *Gut Pathog.*, vol. 4, no. 1, p. 3, 2012.

[197] K. T. Young, L. M. Davis and V. J. Dirita, "*Campylobacter jejuni*: molecular biology and pathogenesis", *Nat. Rev. Microbiol.*, vol. 5, no. 9, pp. 665–679, 2007.

[198] M. J. Pallen and B. W. Wren, "The HtrA family of serine proteases", *Mol. Microbiol.*, vol. 26, no. 2, pp. 209–221, 1997.

Acknowledgements

First and foremost, I wish to express my sincere gratitude to my academic advisor, Professor Giuseppe Zanotti, for accepting me into his group: I appreciate his vast knowledge and skills in many areas, as well as his assistance throughout the Thesis work. I am indebted to him for sharing his expertise and for his willingness to discuss different themes: despite his numerous commitments, he was always available and he has devoted much of his time to answer my doubts and questions. I will never forget the interesting discussions undertaken with him; he shared with passion his knowledge and I've always tried to get as much as possible from discussions with him. I thank Prof. Zanotti for scientific guidance not only about the Thesis work but also because he supporting my attendance at various Conferences, Schools and Seminars. In addition, he gave me useful suggestions for my fate, particularly about a future Ph.D. experience: he has always shown interest, frequently asking news about the contacts that I have taken with Prof. JC Sacchettini at Texas A&M University.

I am also grateful to Professor Roberto Battistutta: he has always been available and has always devoted his time to ask about the project and the problems encountered along the Thesis work. Through his useful criticisms I could improve the present work; also, he instilled in me the importance of rigor and precision in all aspects of a scientific project.

I owe intellectual and personal debts also to many other people: first of all, I thanks Dr. Paola Berto, Dr. Francesca Vallese and Dr. Valentina Loconte: they have been an extremely reliable source of practical scientific knowledge and I am thankful for their patience and assistance. They always answered all my questions and doubts and they have always participated with interest in discussions about the most diverse scientific issues, introduced by me after the reading of novel papers. I was lucky to have the chance to work with them, who patiently taught me the basis of Molecular Biology; in addition, they provided a friendly and cooperative atmosphere in laboratory and also useful feedbacks and insightful comments on my work.

I must also acknowledge Professor Rodolfo Berni and Professor Steffen Backert who provides, respectively, the co-crystals between TTR and different ligands and the wt- and mutant-HtrA from *Cj*. Without their samples, this work would not have been possible.

Finally, I would like to acknowledge friends and family who supported me in the last year, for their constant love, encouragements and moral support and for their willingness, especially in the most difficult and intense periods.